

Techniques for the calculation of electroweak radiative corrections at the one-loop level and results for W -physics at LEP200

A. DENNER

*Physikalisches Institut, Universität Würzburg
8700 Würzburg, Germany*

Abstract:

We review the techniques necessary for the calculation of virtual electroweak and soft photonic corrections at the one-loop level. In particular we describe renormalization, calculation of one-loop integrals and evaluation of one-loop Feynman amplitudes. We summarize many explicit results of general relevance. We give the Feynman rules and the explicit form of the counter terms of the electroweak standard model, we list analytical expressions for scalar one-loop integrals and reduction of tensor integrals, we present the decomposition of the invariant matrix element for processes with two external fermions and we give the analytic form of soft photonic corrections. These techniques are applied to physical processes with external W -bosons. We present the full set of analytical formulae and the corresponding numerical results for the decay width of the W -boson and the top quark. We discuss the cross section for the production of W -bosons in e^+e^- -annihilation including all $O(\alpha)$ radiative corrections and finite width effects. Improved Born approximations for these processes are given.

Contents

1	Introduction	1
2	The Glashow-Salam-Weinberg Model	4
2.1	The Yang-Mills-part	4
2.2	The Higgs part	5
2.3	Fermionic Part	5
2.4	Physical fields and parameters	6
2.5	Quantization	8
3	Renormalization	9
3.1	Renormalization constants and counterterms	10
3.2	Renormalization conditions	11
3.3	Explicit form of renormalization constants	15
4	One-loop integrals	19
4.1	Definitions	19
4.2	Reduction of tensor integrals to scalar integrals	22
4.3	Scalar one-loop integrals for $N \leq 4$	24
4.3.1	Scalar one-point function	25
4.3.2	Scalar two-point function	25
4.3.3	Scalar three-point function	26
4.3.4	Scalar four-point function	27
4.4	Reduction of scalar and tensor integrals for vanishing Gram determinant	29
4.4.1	Reduction of scalar five-point functions	29
4.4.2	Reduction of N-point functions for zero Gram determinant	31
4.5	UV-divergent parts of tensor integrals	32
5	Standard matrix elements	33
5.1	Definition	33
5.2	Standard matrix elements for processes with two external fermions	35
5.2.1	$S \rightarrow F\bar{F}$	35
5.2.2	$V \rightarrow F\bar{F}$	35
5.2.3	$F\bar{F} \rightarrow SS$	36
5.2.4	$F\bar{F} \rightarrow SV$	36
5.2.5	$F\bar{F} \rightarrow VV$	36
5.3	Calculation of standard matrix elements	37
6	Calculation of one-loop amplitudes	40
6.1	Algebraic reduction of Feynman diagrams	40
6.2	Generic Feynman diagrams	43
6.3	The decay $W \rightarrow f_i \bar{f}'_j$ for massless fermions	43
6.4	Computeralgebraic calculation of one-loop diagrams	46

7	Soft photon bremsstrahlung	47
7.1	Soft photon approximation	47
7.2	Soft photon cross section	49
8	Input parameters and leading higher order contributions	51
8.1	Input parameters	51
8.2	Leading higher order contributions	54
8.2.1	Leading logarithms from light fermion masses	54
8.2.2	Leading m_t^2 contributions	55
8.2.3	Recipes for leading universal corrections	56
9	The width of the W-boson	57
9.1	Lowest order	57
9.2	Electroweak virtual corrections	58
9.3	Photon bremsstrahlung	62
9.4	QCD corrections	64
9.5	Results and Discussion	64
10	The top width	70
10.1	Notation and lowest order decay width	70
10.2	Virtual corrections	71
10.3	Bremsstrahlung	71
10.4	Results and discussion	72
11	W-pair production	76
11.1	Notation and amplitudes	76
11.2	Born cross section	77
11.3	Virtual and soft photonic corrections	82
11.3.1	Virtual corrections	82
11.3.2	Soft photonic corrections	83
11.3.3	Leading weak corrections	84
11.3.4	Numerical results for the virtual and soft photonic corrections . . .	85
11.4	Hard photon bremsstrahlung	87
11.4.1	Complete calculations	87
11.4.2	Leading logarithmic approximation	89
11.4.3	Numerical results	90
11.5	Finite widths effects	90
12	Conclusion	95
A	Feynman rules	97
B	Self energies	105
C	Vertex formfactors	109
D	Bremsstrahlung integrals	113

1 Introduction

All known experimental facts about the electroweak interaction are in agreement with the Glashow-Salam-Weinberg (GSW) model [1, 2, 3, 4]. Therefore, this theory is called the standard model (SM) of electroweak physics. Despite its extraordinary experimental success it is by no means tested in its full scope. Many more experimental and theoretical efforts are needed for its further confirmation.

An important step in this direction is provided by the e^+e^- colliders SLC and LEP100 which started a new era of precision experiments. The first important results from these experiments were the determination of the number of light neutrinos and the precise measurement of the mass of the neutral weak gauge boson, the Z -boson [5]. Furthermore the total and partial widths of the Z -boson and various on-resonance asymmetries have been determined and will be measured with increasing accuracy. These experiments will uniquely allow to study in great detail all the properties of the Z -boson and its couplings to fermions.

There are, however, ingredients of the electroweak SM, which are not directly accessible at SLC and LEP100. The most important one is probably the gauge boson self-interaction which is crucial for the nonabelian structure of the GSW model. It will be directly tested for the first time at LEP200, the upgraded version of LEP. There the center of mass energy will be high enough to produce pairs of charged weak gauge bosons, the W -bosons, such that one can study the reaction $e^+e^- \rightarrow W^+W^-$ in great detail. It will allow the investigation of the nonabelian three-gauge boson interactions γW^+W^- and ZW^+W^- at the classical level of the theory. Moreover, all the properties of the W -boson, like its mass and its total and partial widths can be measured directly there. The statistics will not be as good as on the Z -peak. One expects of the order of 10^4 W -pairs and thus an accuracy at the percent level. The examination of several independent methods indicates that an error of about 0.1% for the W -mass determination can be reached [6].

Theoretical predictions should have an accuracy comparable to or even better than the experimental errors. If the experimental precision is of the order of one percent the classical level of the theory is no longer sufficient. One is forced to take into account quantum corrections: the radiative corrections. In the case of the electroweak SM these can reach several percent. For the high precision experiments at LEP100 even the first order corrections are inadequate, one has to take into account leading higher order corrections, too.

Radiative corrections are not only compelling for the precise comparison between the theoretical predictions and the experimental results, but offer the possibility to get informations about sectors of the theory that are not directly observable. While the direct investigation of certain objects may not be possible because the available energy is too small to produce them they may affect the radiative corrections noticeably.

In the electroweak SM there are at least two such objects. The top quark, the still undiscovered constituent of the third fermion generation, and the Higgs boson, the physical remnant of the Higgs-Kibble mechanism of spontaneous symmetry breaking. Both particles seem to be too massive to be produced directly in the existing colliders. However, the high precision experiments performed so far together with the precise knowledge of the radiative corrections of the electroweak SM already allow to derive limits on the mass of the top quark within the SM [7, 5]. Since the sensitivity of radiative corrections

to the mass of the Higgs boson is weaker, the restrictions on this parameter are at present only marginal [8]. The situation may improve with increasing experimental accuracy. While direct determinations of physical parameters are in general to a large extent model independent, the information extracted from radiative corrections depends on the entire structure of the underlying theory.

Finally there is a third important issue concerning radiative corrections. It is likely that the electroweak SM, despite its experimental success, is only an effective theory, the low-energy approximation of a more general structure. This would manifest itself typically in small deviations from the SM predictions. Furthermore most of the presently discussed new physics is connected with scales bigger than the experimentally accessible energies. Therefore new phenomena will show up predominantly via indirect effects rather than via direct production of new particles. In order to disentangle these small effects one has to know once again the predictions of the SM accurately and thus needs radiative corrections.

The actual evaluation of the radiative corrections is a tedious and time consuming task. It requires extensive calculations involving many different techniques, like renormalization, evaluation of loop integrals, Dirac algebra calculations, phase space integrations and so on. Fortunately the whole procedure can be organized into different independent steps. Furthermore many steps can be facilitated with the help of computer algebra [9, 10, 11, 12].

For the interesting processes at LEP100 radiative corrections have been calculated by many authors [13]. Their structure is relatively simple since the masses of the external fermions can be neglected. Calculations for gauge boson production processes at LEP200 are already more complicated because the masses of the external gauge bosons are non-negligible. Such calculations have been performed by several groups and we will give the most important results in the second part of this review. The whole complexity of one-loop corrections will show up when considering reactions where all external particles are massive like e.g. gauge boson scattering processes which may be investigated at the LHC or SSC. The calculation of radiative corrections to these processes has just started.

In the first part of this review we collect the relevant formulae and techniques necessary for the calculation of electroweak one-loop radiative corrections. Although we discuss everything in the context of the SM the presented material is – apart from the explicit form of the renormalization constants – applicable to extended models as well. In the second part these methods are applied to physical processes with external W -bosons. This part not only gives examples for the calculation of one-loop electroweak corrections, but also provides a survey on the status of radiative corrections for the production and the decay of W -pairs in e^+e^- annihilation. The corresponding experiments will be carried through in a few years at LEP200.

The general techniques described in this paper are restricted to the virtual part of the electroweak corrections and soft photon bremsstrahlung. We do not consider the methods appropriate for hard photon bremsstrahlung. This can be efficiently treated using spinor techniques [14] and Monte Carlo simulations [15]. Furthermore we do not touch the methods developed for calculating higher order QCD corrections.

This paper is organized as follows:

In chapter 2 we specify the Lagrangian of the electroweak SM. Chapter 3 outlines the on-shell renormalization for the physical sector of the electroweak SM and provides explicit expressions for the counter terms. All relevant formulae for the calculation of one-

loop Feynman integrals are collected in chapter 4. In chapter 5 we introduce the standard matrix elements, a concept which allows to represent the results for one-loop diagrams in a systematic and simple way. In chapter 6 we show how everything is put together in the actual calculation of one-loop amplitudes and provide first simple examples. The relevant formulae for the calculation of the soft photon corrections are summarized in chapter 7. Chapter 8 serves to define our input parameters and the way of resumming higher order corrections.

The remaining chapters are devoted to applications. In chapter 9 we give results for the width of the W -boson, in chapter 10 for the width of the top quark. Finally the radiative corrections to the production of W -pairs in e^+e^- annihilation are discussed in chapter 11.

The appendices contain the Feynman rules of the electroweak SM, the explicit expressions for the self energies of the physical particles and the vertex functions as well as the bremsstrahlung integrals relevant for the W -boson and top quark decay width.

2 The Glashow-Salam-Weinberg Model

The Glashow-Salam-Weinberg (GSW) model of the electroweak interaction has been proposed by Glashow [1], Weinberg [2], and Salam [3] for leptons and extended to the hadronic degrees of freedom by Glashow, Iliopoulos and Maiani [4]. It is the presently most comprehensive formulation of a theory of the unified electroweak interaction: theoretically consistent and in agreement with all experimentally known phenomena of electroweak origin. For energies that are small compared to the electroweak scale it reproduces quantum electrodynamics and the Fermi model, which already accomplished a good description of the electromagnetic and weak interactions at low energies. It is minimal in the sense that it contains the smallest number of degrees of freedom necessary to describe the known experimental facts.

The electroweak standard model (SM) is a nonabelian gauge theory based on the non-simple group $SU(2)_W \times U(1)_Y$. From experiment we know that three out of the four associated gauge bosons have to be massive. This is implemented via the Higgs-Kibble mechanism [16]. By introducing a scalar field with nonvanishing vacuum expectation value the $SU(2)_W \times U(1)_Y$ gauge symmetry is spontaneously broken in such a way that invariance under the electromagnetic subgroup $U(1)_{em}$ is preserved. The SM is chiral since right- and left-handed fermions transform according to different representations of the gauge group. Consequently fermion masses are forbidden in the symmetric theory. They are generated through spontaneous symmetry breaking from the Yukawa couplings. Diagonalization of the fermion mass matrices introduces the quark mixing matrix in the quark sector. This can give rise to CP-violation. Fermions appear in generations. The model does not fix their number, but from experiment we know that there are exactly three with light neutrinos [5].

The SM is a consistent quantum field theory. It is renormalizable, as was proven by 't Hooft [17], and free of anomalies. Therefore it allows to calculate unique quantum corrections. Given a finite set of input parameters measurable quantities can be predicted order by order in perturbation theory.

The classical Lagrangian \mathcal{L}_C of the SM is composed of a Yang-Mills, a Higgs and a fermion part

$$\mathcal{L}_C = \mathcal{L}_{YM} + \mathcal{L}_H + \mathcal{L}_F . \quad (2.1)$$

Each of them is separately gauge invariant. They are specified as follows:

2.1 The Yang-Mills-part

The gauge fields are four vector fields transforming according to the adjoint representation of the gauge group $SU(2)_W \times U(1)_Y$. The isotriplet W_μ^a , $a = 1, 2, 3$ is associated with the generators I_W^a of the weak isospin group $SU(2)_W$, the isosinglet B_μ with the weak hypercharge Y_W of the group $U(1)_Y$. The pure gauge field Lagrangian reads

$$\mathcal{L}_{YM} = -\frac{1}{4} \left(\partial_\mu W_\nu^a - \partial_\nu W_\mu^a + g_2 \varepsilon^{abc} W_\mu^b W_\nu^c \right)^2 - \frac{1}{4} (\partial_\mu B_\nu - \partial_\nu B_\mu)^2 , \quad (2.2)$$

where ε^{abc} are the totally antisymmetric structure constants of $SU(2)$. Since the gauge group is non-simple there are two gauge coupling constants, the $SU(2)_W$ gauge coupling g_2 and the $U(1)_Y$ gauge coupling g_1 . The covariant derivative is given by

$$D_\mu = \partial_\mu - ig_2 I_W^a W_\mu^a + ig_1 \frac{Y_W}{2} B_\mu. \quad (2.3)$$

The electric charge operator Q is composed of the weak isospin generator I_W^3 and the weak hypercharge according to the Gell-Mann Nishijima relation

$$Q = I_W^3 + \frac{Y_W}{2}. \quad (2.4)$$

2.2 The Higgs part

The minimal Higgs sector consists of a single complex scalar $SU(2)_W$ doublet field with hypercharge $Y_W = 1$

$$\Phi(x) = \begin{pmatrix} \phi^+(x) \\ \phi^0(x) \end{pmatrix}. \quad (2.5)$$

It is coupled to the gauge fields with the covariant derivative (2.3) and has a self coupling resulting in the Lagrangian

$$\mathcal{L}_H = (D_\mu \Phi)^\dagger (D^\mu \Phi) - V(\Phi). \quad (2.6)$$

The Higgs potential

$$V(\Phi) = \frac{\lambda}{4} (\Phi^\dagger \Phi)^2 - \mu^2 \Phi^\dagger \Phi \quad (2.7)$$

is constructed in such a way that it gives rise to spontaneous symmetry breaking. This means that the parameters λ and μ are chosen such that the potential $V(\Phi)$ takes its minimum for a nonvanishing Higgs field, i.e. the vacuum expectation value $\langle \Phi \rangle$ of the Higgs field is nonzero.

2.3 Fermionic Part

The left-handed fermions of each lepton (L) and quark (Q) generation are grouped into $SU(2)_W$ doublets (we suppress the colour index)

$$L_j^L = \omega_- L'_j = \begin{pmatrix} \nu_j^L \\ l_j^L \end{pmatrix}, \quad Q_j^L = \omega_- Q'_j = \begin{pmatrix} u_j^L \\ d_j^L \end{pmatrix}, \quad (2.8)$$

the right-handed fermions into singlets

$$l_j^R = \omega_+ l'_j, \quad u_j^R = \omega_+ u'_j, \quad d_j^R = \omega_+ d'_j, \quad (2.9)$$

where $\omega_\pm = \frac{1 \pm \gamma_5}{2}$ is the projector on right- and left-handed fields, respectively, j is the generation index and ν , l , u and d stand for neutrinos, charged leptons, up-type quarks and down-type quarks, respectively. The weak hypercharge of the right- and left-handed multiplets is chosen such that the known electromagnetic charges of the fermions are

reproduced by the Gell-Mann-Nishijima relation (2.4). There are no right-handed neutrinos. These could be easily added, but they would induce nonvanishing neutrino masses, which have not been observed experimentally so far.

The fermionic part of the Lagrangian reads

$$\begin{aligned}
\mathcal{L}_F = & \sum_i \left(\overline{L}_i^L i\gamma^\mu D_\mu L_i^L + \overline{Q}_i^L i\gamma^\mu D_\mu Q_i^L \right) \\
& + \sum_i \left(\overline{l}_i^R i\gamma^\mu D_\mu l_i^R + \overline{u}_i^R i\gamma^\mu D_\mu u_i^R + \overline{d}_i^R i\gamma^\mu D_\mu d_i^R \right) \\
& - \sum_{ij} \left(\overline{L}_i^L G_{ij}^l l_j^R \Phi + \overline{Q}_i^L G_{ij}^u u_j^R \tilde{\Phi} + \overline{Q}_i^L G_{ij}^d d_j^R \Phi + h.c. \right).
\end{aligned} \tag{2.10}$$

Note that in the covariant derivative D_μ acting on right-handed fermions the term involving g_2 is absent, since they are $SU(2)_W$ singlets. The primed fermion fields are by definition eigenstates of the electroweak gauge interaction, i.e. the covariant derivatives are diagonal in this basis with respect to the generation indices. G_{ij}^l , G_{ij}^u and G_{ij}^d are the Yukawa coupling matrices, $\tilde{\Phi} = (\phi^{0*}, -\phi^-)^T$ is the charge conjugated Higgs field and $\phi^- = (\phi^+)^*$. The $SU(2)_W \times U(1)_Y$ symmetry forbids explicit mass terms for the fermions. The masses of the fermions are generated through the Yukawa couplings via spontaneous symmetry breaking.

2.4 Physical fields and parameters

The theory is constructed such that the classical ground state of the scalar field satisfies

$$|\langle \Phi \rangle|^2 = \frac{2\mu^2}{\lambda} = \frac{v^2}{2} \neq 0. \tag{2.11}$$

In perturbation theory one has to expand around the ground state. Its phase is chosen such that the electromagnetic gauge invariance $U(1)_{em}$ is preserved and the Higgs field is written as

$$\Phi(x) = \begin{pmatrix} \phi^+(x) \\ \frac{1}{\sqrt{2}}(v + H(x) + i\chi(x)) \end{pmatrix}, \tag{2.12}$$

where the components ϕ^+ , H and χ have zero vacuum expectation values. ϕ^+ , ϕ^- and χ are unphysical degrees of freedom and can be eliminated by a suitable gauge transformation. The gauge in which they are absent is called unitary. The field H is the physical Higgs field with mass

$$M_H = \sqrt{2}\mu. \tag{2.13}$$

Inserting (2.12) into \mathcal{L}_C the vacuum expectation value v introduces couplings with mass dimension and mass terms for the gauge bosons and fermions.

The physical gauge boson and fermion fields are obtained by diagonalizing the corresponding mass matrices

$$\begin{aligned}
W_\mu^\pm &= \frac{1}{\sqrt{2}} (W_\mu^1 \mp iW_\mu^2), \\
\begin{pmatrix} Z_\mu \\ A_\mu \end{pmatrix} &= \begin{pmatrix} c_W & s_W \\ -s_W & c_W \end{pmatrix} \begin{pmatrix} W_\mu^3 \\ B_\mu \end{pmatrix},
\end{aligned} \tag{2.14}$$

$$f_i^L = U_{ik}^{f,L} f_k^L,$$

$$f_i^R = U_{ik}^{f,R} f_k^R,$$

where

$$c_W = \cos \theta_W = \frac{g_2}{\sqrt{g_2^2 + g_1^2}}, \quad s_W = \sin \theta_W, \tag{2.15}$$

with the weak mixing angle θ_W and f stands for ν , l , u or d . The resulting masses are

$$\begin{aligned}
M_W &= \frac{1}{2} g_2 v, & M_Z &= \frac{1}{2} \sqrt{g_1^2 + g_2^2} v, \\
M_\gamma &= 0, & m_{f,i} &= U_{ik}^{f,L} G_{km}^f U_{mi}^{f,R\dagger} \frac{v}{\sqrt{2}}.
\end{aligned} \tag{2.16}$$

The neutrinos remain massless since the absence of the right-handed neutrinos forbids the Yukawa couplings which would generate their masses. With (2.16) we find for the weak mixing angle

$$c_W = \frac{M_W}{M_Z}. \tag{2.17}$$

Identifying the coupling of the photon field A_μ to the electron with the electrical charge $e = \sqrt{4\pi\alpha}$ yields

$$e = \frac{g_1 g_2}{\sqrt{g_1^2 + g_2^2}}, \tag{2.18}$$

or

$$g_1 = \frac{e}{c_W}, \quad g_2 = \frac{e}{s_W}. \tag{2.19}$$

The diagonalization of the fermion mass matrices introduces a matrix into the quark-W-boson couplings, the unitary quark mixing matrix

$$V_{ij} = U_{ik}^{u,L} U_{kj}^{d,L\dagger}. \tag{2.20}$$

There is no corresponding matrix in the lepton sector. Since there is no neutrino mass matrix, $U^{\nu,L}$ is completely arbitrary and can be chosen such that it cancels $U^{l,L}$ in the lepton-W-boson couplings. The same would also be true for the quark sector if all up-type or down-type quarks would be degenerate in masses. For degenerate masses one can choose $U^L = U^{R\dagger}$ arbitrary without destroying the diagonality of the corresponding mass matrix and thus eliminate V_{ij} .

The above relations (2.13, 2.16, 2.18, 2.20) allow to replace the original set of parameters

$$g_1, g_2, \lambda, \mu^2, G^l, G^u, G^d \tag{2.21}$$

by the parameters

$$e, M_W, M_Z, M_H, m_{f,i}, V_{ij} \quad (2.22)$$

which have a direct physical meaning. Thus we can express the Lagrangian (2.1) in terms of physical parameters and fields.

Inserting (2.12) into \mathcal{L}_C generates a term linear in the Higgs field H which we denote by $tH(x)$ with

$$t = v(\mu^2 - \frac{\lambda}{4}v^2). \quad (2.23)$$

The tadpole t vanishes at lowest order due to the choice of v . We use t instead of v in the following. Choosing v as the correct vacuum expectation value of the Higgs field Φ is equivalent to the vanishing of t .

2.5 Quantization

Quantization of \mathcal{L}_C and higher order calculations require the specification of a gauge. We choose a renormalizable 't Hooft gauge with the following linear gauge fixings

$$\begin{aligned} F^\pm &= (\xi_1^W)^{-\frac{1}{2}} \partial^\mu W_\mu^\pm \mp iM_W(\xi_2^W)^{\frac{1}{2}} \phi^\pm, \\ F^Z &= (\xi_1^Z)^{-\frac{1}{2}} \partial^\mu Z_\mu - M_Z(\xi_2^Z)^{\frac{1}{2}} \chi, \\ F^\gamma &= (\xi_1^\gamma)^{-\frac{1}{2}} \partial^\mu A_\mu, \end{aligned} \quad (2.24)$$

leading to the following gauge fixing Lagrangian

$$\mathcal{L}_{fix} = -\frac{1}{2} [(F^\gamma)^2 + (F^Z)^2 + 2F^+ F^-]. \quad (2.25)$$

\mathcal{L}_{fix} involves the unphysical components of the gauge fields. In order to compensate their effects one introduces Faddeev Popov ghosts $u^\alpha(x)$, $\bar{u}^\alpha(x)$ ($\alpha = \pm, \gamma, Z$) with the Lagrangian

$$\mathcal{L}_{FP} = \bar{u}^\alpha(x) \frac{\delta F^\alpha}{\delta \theta^\beta(x)} u^\beta(x). \quad (2.26)$$

$\frac{\delta F^\alpha}{\delta \theta^\beta(x)}$ is the variation of the gauge fixing operators F^α under infinitesimal gauge transformations characterized by $\theta^\beta(x)$.

The 't Hooft Feynman gauge $\xi^\alpha = 1$ is particularly simple. At lowest order the poles of the ghost fields, unphysical Higgs fields and longitudinal gauge fields coincide with the poles of the corresponding transverse gauge fields. Furthermore no gauge-field-Higgs mixing occurs.

With \mathcal{L}_{fix} and \mathcal{L}_{FP} the complete renormalizable Lagrangian for the electroweak SM reads

$$\mathcal{L}_{GSW} = \mathcal{L}_C + \mathcal{L}_{fix} + \mathcal{L}_{FP}. \quad (2.27)$$

The corresponding Feynman rules are given in App. A.

3 Renormalization

The Lagrangian (2.1) of the minimal $SU(2)_W \times U(1)_Y$ model involves a certain number of free parameters (2.22) which have to be determined experimentally. These are chosen such that they have an intuitive physical meaning at tree level (physical masses, couplings), i.e. they are directly related to experimental quantities. This direct relation is destroyed through higher order corrections. Moreover the parameters of the original Lagrangian, the so-called bare parameters, differ from the corresponding physical quantities by UV-divergent contributions. However, in renormalizable theories these divergencies cancel in relations between physical quantities, thus allowing meaningful predictions. The renormalizability of nonabelian gauge theories with spontaneous symmetry breaking and thus of the SM was proven by 't Hooft [17].

One possibility to evaluate predictions of a renormalizable model is the following:

- Calculate physical quantities in terms of the bare parameters.
- Use as many of the resulting relations as bare parameters exist to express these in terms of physical observables.
- Insert the resulting expressions into the remaining relations.

Thus one arrives at predictions for physical observables in terms of other physical quantities, which have to be determined from experiment. In these predictions all UV-divergencies cancel in any order of perturbation theory. The predictions obtained from different input parameters differ in finite orders of perturbation theory by higher order contributions. This treatment of renormalization has been pioneered by Passarino, Veltman and Consoli [18] and is the basis of the so-called 'star' scheme of Kennedy and Lynn [19].

We use the counterterm approach. Here the UV-divergent bare parameters are expressed by finite renormalized parameters and divergent renormalization constants (counterterms). In addition the bare fields may be replaced by renormalized fields. The counterterms are fixed through renormalization conditions. These can be chosen arbitrarily, but determine the relation between renormalized and physical parameters. Further evaluation proceeds like described above. The results depend in finite orders of perturbation theory not only on the choice of the input parameters but also on the choice of the renormalized parameters. Clearly the physical results are unambiguous up to the orders which have been taken into account completely. The renormalization procedure can be summarized as follows:

- Choose a set of independent parameters (e.g. (2.22) in the SM).
- Separate the bare parameters (and fields) into renormalized parameters (fields) and renormalization constants (see Sect. 3.1).
- Choose renormalization conditions to fix the counterterms (see Sect. 3.2).
- Express physical quantities in terms of the renormalized parameters.
- Choose input data in order to fix the values of the renormalized parameters.
- Evaluate predictions for physical quantities as functions of the input data.

The first three items in this list specify a renormalization scheme.

Putting the counterterms equal to zero, the renormalized parameters equal the bare parameters and we recover the first approach.

However, we can choose the counterterms such that the finite renormalized parameters are equal to physical parameters in all orders of perturbation theory. This is the so-called on-shell renormalization scheme. In the SM one uses the masses of the physical particles M_W, M_Z, M_H, m_f , the charge of the electron e and the quark mixing matrix V_{ij} as renormalized parameters. This scheme was proposed by Ross and Taylor [20] and is widely used in the electroweak theory. The advantage of the on-shell scheme is that all parameters have a clear physical meaning and can be measured directly in suitable experiments¹. Furthermore the Thomson cross section from which e is obtained is exact to all orders of perturbation theory. However, not all of the particle masses are known experimentally with good accuracy. Therefore other schemes may sometimes be advantageous.

Renormalization of the parameters is sufficient to obtain finite S-matrix elements, but it leaves Green functions divergent. This is due to the fact that radiative corrections change the normalization of the fields by an infinite amount. In order to get finite propagators and vertex functions the fields have to be renormalized, too. Furthermore radiative corrections provide nondiagonal corrections to the mass matrices so that the bare fields are no longer mass eigenstates. In order to rediagonalize the mass matrices one has to introduce matrix valued field renormalization constants. These allow to define the renormalized fields in such a way that they are the correct physical mass eigenstates in all orders of perturbation theory. If one does not renormalize the fields in this way, one needs a nontrivial wave function renormalization for the external particles. This is required in going from Green functions to S-matrix elements in order to obtain a properly normalized S-matrix.

The results for physical S-matrix elements are independent of the specific choice of field renormalization. There exist many different treatments in the literature [21, 22, 23, 24, 25]. Calculations without field renormalization were performed by [26].

3.1 Renormalization constants and counterterms

In the following we specify the on-shell renormalization scheme for the electroweak SM quantitatively. As independent parameters we choose the physical parameters specified in (2.22). The renormalized quantities and renormalization constants are defined as follows (we denote bare quantities by an index 0)

$$\begin{aligned}
 e_0 &= Z_e e = (1 + \delta Z_e) e, \\
 M_{W,0}^2 &= M_W^2 + \delta M_W^2, \\
 M_{Z,0}^2 &= M_Z^2 + \delta M_Z^2, \\
 M_{H,0}^2 &= M_H^2 + \delta M_H^2, \\
 m_{f,i,0} &= m_{f,i} + \delta m_{f,i},
 \end{aligned}
 \tag{3.1}$$

¹This is not the case for the quark masses, due to the presence of the strong interaction. In practice these are replaced by suitable experimental input parameters (see Sect. 8.1).

$$V_{ij,0} = (U_1 V U_2^\dagger)_{ij} = V_{ij} + \delta V_{ij}.$$

U_1 and U_2 are unitary matrices since $V_{ij,0}$ and V_{ij} are both unitary.

Radiative corrections affect the Higgs potential in such a way that its minimum is shifted. In order to correct for this shift one introduces a counterterm to the vacuum expectation value of the Higgs field, which is determined such that the renormalized v is given by the actual minimum of the effective Higgs potential. Since we have replaced v by t (2.23) we must introduce a counterterm δt . This is fixed such that it cancels all tadpole diagrams, i.e. that the effective potential contains no term linear in the Higgs field H .

The counterterms defined above are sufficient to render all S-matrix elements finite. In order to have finite Green functions we must renormalize the fields, too. As explained above we need field renormalization matrices in order to be able to define renormalized fields which are mass eigenstates

$$\begin{aligned} W_0^\pm &= Z_W^{1/2} W^\pm = (1 + \frac{1}{2}\delta Z_W) W^\pm, \\ \begin{pmatrix} Z_0 \\ A_0 \end{pmatrix} &= \begin{pmatrix} Z_{ZZ}^{1/2} & Z_{ZA}^{1/2} \\ Z_{AZ}^{1/2} & Z_{AA}^{1/2} \end{pmatrix} \begin{pmatrix} Z \\ A \end{pmatrix} = \begin{pmatrix} 1 + \frac{1}{2}\delta Z_{ZZ} & \frac{1}{2}\delta Z_{ZA} \\ \frac{1}{2}\delta Z_{AZ} & 1 + \frac{1}{2}\delta Z_{AA} \end{pmatrix} \begin{pmatrix} Z \\ A \end{pmatrix}, \\ H_0 &= Z_H^{1/2} H = (1 + \frac{1}{2}\delta Z_H) H, \\ f_{i,0}^L &= Z_{ij}^{1/2,f,L} f_j^L = (\delta_{ij} + \frac{1}{2}\delta Z_{ij}^{f,L}) f_j^L, \\ f_{i,0}^R &= Z_{ij}^{1/2,f,R} f_j^R = (\delta_{ij} + \frac{1}{2}\delta Z_{ij}^{f,R}) f_j^R. \end{aligned} \tag{3.2}$$

We do not discuss the renormalization constants of the unphysical ghost and Higgs fields. They do not affect Green functions of physical particles and are not relevant for the calculation of physical one-loop amplitudes. Furthermore the renormalization of the unphysical sector decouples from the one of the physical sector. It is governed by the Slavnov-Taylor identities. A discussion of this subject can be found e.g. in [24, 25].

In writing $Z = 1 + \delta Z$ for the multiplicative renormalization constants (matrices) we can split the bare Lagrangian \mathcal{L}_0 into the basic Lagrangian \mathcal{L} and the counterterm Lagrangian $\delta\mathcal{L}$

$$\mathcal{L}_0 = \mathcal{L} + \delta\mathcal{L}. \tag{3.3}$$

\mathcal{L} has the same form as \mathcal{L}_0 but depends on renormalized parameters and fields instead of unrenormalized ones. $\delta\mathcal{L}$ yields the counterterms. The corresponding Feynman rules are listed in App. A. They give rise to counterterm diagrams which have to be added to the loop graphs. Since we are only interested in one-loop corrections, we neglect terms of order $(\delta Z)^2$ everywhere.

3.2 Renormalization conditions

The renormalization constants introduced in the previous section are fixed by imposing renormalization conditions. These decompose into two sets. The conditions which define the renormalized parameters and the ones which define the renormalized fields. While the choice of the first affects physical predictions to finite orders of perturbation theory,

$$\frac{f_j}{p} \rightarrow \text{circle with diagonal lines} \rightarrow f_i = \hat{\Gamma}_{ij}^f(p)$$

$$= i\delta_{ij}(\not{p} - m_i) + i \left[\not{p}\omega_- \hat{\Sigma}_{ij}^{f,L}(p^2) + \not{p}\omega_+ \hat{\Sigma}_{ij}^{f,R}(p^2) + (m_{f,i}\omega_- + m_{f,j}\omega_+) \hat{\Sigma}_{ij}^{f,S}(p^2) \right].$$

The corresponding propagators are obtained as the inverse of these two-point functions. Note that we have to invert matrices for the neutral gauge bosons and for the fermions.

The renormalized mass parameters of the physical particles are fixed by the requirement that they are equal to the physical masses, i.e. to the real parts of the poles of the corresponding propagators which are equivalent to the zeros of the one-particle irreducible two-point functions. In case of mass matrices these conditions have to be fulfilled by the corresponding eigenvalues resulting in complicated expressions. These can be considerably simplified by requiring simultaneously the on-shell conditions for the field renormalization matrices. These state that the renormalized one-particle irreducible two-point functions are diagonal if the external lines are on their mass shell. This determines the nondiagonal elements of the field renormalization matrices. The diagonal elements are fixed such that the renormalized fields are properly normalized, i.e. that the residues of the renormalized propagators are equal to one. This choice of field renormalization implies that the renormalization conditions for the mass parameters (in all orders of perturbation theory) involve only the corresponding diagonal self energies. Thus we arrive at the following renormalization conditions for the two-point functions for on-shell external physical fields

$$\begin{aligned} \widetilde{\text{Re}} \hat{\Gamma}_{\mu\nu}^W(k) \varepsilon^\nu(k) \Big|_{k^2=M_W^2} &= 0, \\ \text{Re} \hat{\Gamma}_{\mu\nu}^{ZZ}(k) \varepsilon^\nu(k) \Big|_{k^2=M_Z^2} &= 0, & \text{Re} \hat{\Gamma}_{\mu\nu}^{AZ}(k) \varepsilon^\nu(k) \Big|_{k^2=M_Z^2} &= 0, \\ \hat{\Gamma}_{\mu\nu}^{AZ}(k) \varepsilon^\nu(k) \Big|_{k^2=0} &= 0, & \hat{\Gamma}_{\mu\nu}^{AA}(k) \varepsilon^\nu(k) \Big|_{k^2=0} &= 0, \\ \lim_{k^2 \rightarrow M_W^2} \frac{1}{k^2 - M_W^2} \widetilde{\text{Re}} \hat{\Gamma}_{\mu\nu}^W(k) \varepsilon^\nu(k) &= -i\varepsilon_\mu(k), \\ \lim_{k^2 \rightarrow M_Z^2} \frac{1}{k^2 - M_Z^2} \text{Re} \hat{\Gamma}_{\mu\nu}^{ZZ}(k) \varepsilon^\nu(k) &= -i\varepsilon_\mu(k), & \lim_{k^2 \rightarrow 0} \frac{1}{k^2} \text{Re} \hat{\Gamma}_{\mu\nu}^{AA}(k) \varepsilon^\nu(k) &= -i\varepsilon_\mu(k), \\ \text{Re} \hat{\Gamma}^H(k) \Big|_{k^2=M_H^2} &= 0, & \lim_{k^2 \rightarrow M_H^2} \frac{1}{k^2 - M_H^2} \text{Re} \hat{\Gamma}^H(k) &= i, \\ \widetilde{\text{Re}} \hat{\Gamma}_{ij}^f(p) u_j(p) \Big|_{p^2=m_{f,i}^2} &= 0, & \widetilde{\text{Re}} \bar{u}_i(p') \hat{\Gamma}_{ij}^f(p') \Big|_{p'^2=m_{f,i}^2} &= 0, \\ \lim_{p^2 \rightarrow m_{f,i}^2} \frac{\not{p} + m_{f,i}}{p^2 - m_{f,i}^2} \widetilde{\text{Re}} \hat{\Gamma}_{ii}^f(p) u_i(p) &= iu_i(p), & \lim_{p'^2 \rightarrow m_{f,i}^2} \bar{u}_i(p') \widetilde{\text{Re}} \hat{\Gamma}_{ii}^f(p') \frac{\not{p}' + m_{f,i}}{p'^2 - m_{f,i}^2} &= i\bar{u}_i(p'). \end{aligned} \tag{3.7}$$

$\varepsilon(k)$, $u(p)$ and $\bar{u}(p')$ are the polarization vectors and spinors of the external fields. $\widetilde{\text{Re}}$ takes the real part of the loop integrals appearing in the self energies but not of the quark mixing matrix elements appearing there. Since we restrict ourselves to the one-loop order we apply it only to those quantities which depend on the quark mixing matrix at one loop.

In higher orders Re must be replaced by $\widetilde{\text{Re}}$ everywhere. Re and $\widetilde{\text{Re}}$ are only relevant above thresholds and have no effect for the two-point functions of on-shell stable particles. If the quark mixing matrix is real $\widetilde{\text{Re}}$ can be replaced by Re. This holds in particular for a unit quark mixing matrix which is often used.

From the above equations we obtain the conditions for the self energy functions.

$$\begin{aligned}\widetilde{\text{Re}} \hat{\Sigma}_T^W(M_W^2) &= 0, \\ \text{Re} \hat{\Sigma}_T^{ZZ}(M_Z^2) &= 0, & \text{Re} \hat{\Sigma}_T^{AZ}(M_Z^2) &= 0, \\ \hat{\Sigma}_T^{AZ}(0) &= 0, & \hat{\Sigma}_T^{AA}(0) &= 0,^2\end{aligned}\tag{3.8}$$

$$\begin{aligned}\widetilde{\text{Re}} \left. \frac{\partial \hat{\Sigma}_T^W(k^2)}{\partial k^2} \right|_{k^2=M_W^2} &= 0, \\ \text{Re} \left. \frac{\partial \hat{\Sigma}_T^{ZZ}(k^2)}{\partial k^2} \right|_{k^2=M_Z^2} &= 0, & \text{Re} \left. \frac{\partial \hat{\Sigma}_T^{AA}(k^2)}{\partial k^2} \right|_{k^2=0} &= 0, \\ \text{Re} \hat{\Sigma}^H(M_H^2) &= 0, & \text{Re} \left. \frac{\partial \hat{\Sigma}^H(k^2)}{\partial k^2} \right|_{k^2=M_H^2} &= 0,\end{aligned}\tag{3.9}$$

$$\begin{aligned}m_{f,j} \widetilde{\text{Re}} \hat{\Sigma}_{ij}^{f,L}(m_{f,j}^2) + m_{f,j} \widetilde{\text{Re}} \hat{\Sigma}_{ij}^{f,S}(m_{f,j}^2) &= 0, \\ m_{f,j} \widetilde{\text{Re}} \hat{\Sigma}_{ij}^{f,R}(m_{f,j}^2) + m_{f,i} \widetilde{\text{Re}} \hat{\Sigma}_{ij}^{f,S}(m_{f,j}^2) &= 0, \\ \widetilde{\text{Re}} \hat{\Sigma}_{ii}^{f,R}(m_{f,i}^2) + \widetilde{\text{Re}} \hat{\Sigma}_{ii}^{f,L}(m_{f,i}^2) \\ + 2m_{f,i}^2 \frac{\partial}{\partial p^2} \left(\widetilde{\text{Re}} \hat{\Sigma}_{ii}^{f,R}(p^2) + \widetilde{\text{Re}} \hat{\Sigma}_{ii}^{f,L}(p^2) + 2\widetilde{\text{Re}} \hat{\Sigma}_{ii}^{f,S}(p^2) \right) \Big|_{p^2=m_{f,i}^2} &= 0.\end{aligned}\tag{3.10}$$

Note that the (unphysical) longitudinal part of the gauge boson self energies drops out for on-shell external gauge bosons.

Our choice for the renormalization condition of the quark mixing matrix V_{ij} can be motivated as follows. To lowest order V_{ij} is given by (see eq. 2.20)

$$V_{0,ij} = U_{ik}^{u,L} U_{kj}^{d,L\dagger},\tag{3.11}$$

where the matrices $U^{f,L}$ transform the weak interaction eigenstates f'_0 to the lowest order mass eigenstates f_0

$$U_{ij}^{f,L\dagger} f_{j,0}^L = f_{i,0}^L.\tag{3.12}$$

In the on-shell renormalization scheme the higher order mass eigenstates are related to the bare mass eigenstates through the field renormalization constants of the fermions

$$f_i^L = Z_{ij}^{1/2,f,L} f_{j,0}^L.\tag{3.13}$$

We define the renormalized quark mixing matrix in analogy to the unrenormalized one through the rotation from the weak interaction eigenstates to the renormalized mass

²This condition is automatically fulfilled due to a Ward identity.

eigenstates. In the one-loop approximation the rotation contained in the fermion wave function renormalization $1 + \frac{1}{2}\delta Z^L$ is simply given by the anti-Hermitian part δZ^{AH} of δZ^L

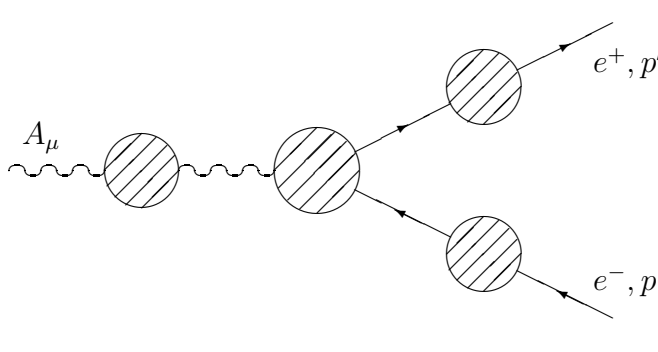
$$\delta Z_{ij}^{f,AH} = \frac{1}{2}(\delta Z_{ij}^{f,L} - \delta Z_{ij}^{f,L\dagger}). \quad (3.14)$$

Thus we are lead to define the renormalized quark mixing matrix as

$$\begin{aligned} V_{ij} &= (\delta_{ik} + \frac{1}{2}\delta Z_{ik}^{u,AH\dagger})U_{km}^{u,L}U_{mn}^{d,L\dagger}(\delta_{nj} + \frac{1}{2}\delta Z_{nj}^{d,AH}) \\ &= (\delta_{ik} + \frac{1}{2}\delta Z_{ik}^{u,AH\dagger})V_{0,kn}(\delta_{nj} + \frac{1}{2}\delta Z_{nj}^{d,AH}). \end{aligned} \quad (3.15)$$

It has been shown that this condition correctly cancels all one-loop divergencies and that $V_{ij} = V_{0,ij}$ in the limit of degenerate up- or down-type quark masses [27].

Finally the electrical charge is defined as the full $ee\gamma$ -coupling for on-shell external particles in the Thomson limit. This means that all corrections to this vertex vanish on-shell and for zero momentum transfer³

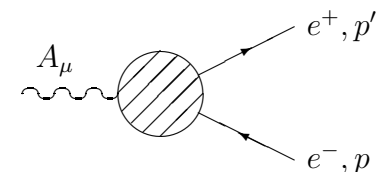


$$= ie\bar{u}(p)\gamma_\mu u(p). \quad (3.16)$$

The momenta p, p' flow in the direction of the fermion arrows. Due to our choice for the field renormalization the corrections in the external legs vanish and we obtain the condition

$$\bar{u}(p)\Gamma_\mu^{ee\gamma}(p, p)u(p)\Big|_{p^2=m_e^2} = ie\bar{u}(p)\gamma_\mu u(p), \quad (3.17)$$

for the (amputated) vertex function



$$\hat{\Gamma}_\mu^{ee\gamma}(p, p') = \quad (3.18)$$

3.3 Explicit form of renormalization constants

The renormalized quantities defined in Sect. 3.2 consist of the unrenormalized ones and the counterterms as specified by the Feynman rules in App. A. The renormalization conditions allow to express the counterterms by the unrenormalized self energies at special external momenta. This is evident for all renormalization constants apart from the one

³Due to the wave function renormalization of the external particles the self energy corrections in the external legs contribute only with a factor 1/2 to the S-matrix elements.

for the electrical charge. In this case, however, we can use a Ward identity to eliminate the vertex function.

From conditions (3.5, 3.8, 3.9) we obtain for the gauge boson and Higgs sector

$$\begin{aligned}
\delta t &= -T, \\
\delta M_W^2 &= \widetilde{\text{Re}} \Sigma_T^W(M_W^2), & \delta Z_W &= -\text{Re} \left. \frac{\partial \Sigma_T^W(k^2)}{\partial k^2} \right|_{k^2=M_W^2}, \\
\delta M_Z^2 &= \text{Re} \Sigma_T^{ZZ}(M_Z^2), & \delta Z_{ZZ} &= -\text{Re} \left. \frac{\partial \Sigma_T^{ZZ}(k^2)}{\partial k^2} \right|_{k^2=M_Z^2}, \\
\delta Z_{AZ} &= -2\text{Re} \frac{\Sigma_T^{AZ}(M_Z^2)}{M_Z^2}, & \delta Z_{ZA} &= 2 \frac{\Sigma_T^{AZ}(0)}{M_Z^2}, \\
\delta Z_{AA} &= -\left. \frac{\partial \Sigma_T^{AA}(k^2)}{\partial k^2} \right|_{k^2=0}, \\
\delta M_H^2 &= \text{Re} \Sigma^H(M_H^2), & \delta Z_H &= -\text{Re} \left. \frac{\partial \Sigma^H(k^2)}{\partial k^2} \right|_{k^2=M_H^2}.
\end{aligned} \tag{3.19}$$

In the fermion sector (3.10) yields

$$\begin{aligned}
\delta m_{f,i} &= \frac{m_{f,i}}{2} \widetilde{\text{Re}} \left(\Sigma_{ii}^{f,L}(m_{f,i}^2) + \Sigma_{ii}^{f,R}(m_{f,i}^2) + 2\Sigma_{ii}^{f,S}(m_{f,i}^2) \right), \\
\delta Z_{ij}^{f,L} &= \frac{2}{m_{f,i}^2 - m_{f,j}^2} \widetilde{\text{Re}} \left[m_{f,j}^2 \Sigma_{ij}^{f,L}(m_{f,j}^2) + m_{f,i} m_{f,j} \Sigma_{ij}^{f,R}(m_{f,j}^2) \right. \\
&\quad \left. + (m_{f,i}^2 + m_{f,j}^2) \Sigma_{ij}^{f,S}(m_{f,j}^2) \right], \quad i \neq j, \\
\delta Z_{ij}^{f,R} &= \frac{2}{m_{f,i}^2 - m_{f,j}^2} \widetilde{\text{Re}} \left[m_{f,j}^2 \Sigma_{ij}^{f,R}(m_{f,j}^2) + m_{f,i} m_{f,j} \Sigma_{ij}^{f,L}(m_{f,j}^2) \right. \\
&\quad \left. + 2m_{f,i} m_{f,j} \Sigma_{ij}^{f,S}(m_{f,j}^2) \right], \quad i \neq j, \\
\delta Z_{ii}^{f,L} &= -\widetilde{\text{Re}} \Sigma_{ii}^{f,L}(m_{f,i}^2) - m_{f,i}^2 \frac{\partial}{\partial p^2} \widetilde{\text{Re}} \left[\Sigma_{ii}^{f,L}(p^2) + \Sigma_{ii}^{f,R}(p^2) + 2\Sigma_{ii}^{f,S}(p^2) \right] \Big|_{p^2=m_{f,i}^2}, \\
\delta Z_{ii}^{f,R} &= -\widetilde{\text{Re}} \Sigma_{ii}^{f,R}(m_{f,i}^2) - m_{f,i}^2 \frac{\partial}{\partial p^2} \widetilde{\text{Re}} \left[\Sigma_{ii}^{f,L}(p^2) + \Sigma_{ii}^{f,R}(p^2) + 2\Sigma_{ii}^{f,S}(p^2) \right] \Big|_{p^2=m_{f,i}^2}.
\end{aligned} \tag{3.20}$$

The use of $\widetilde{\text{Re}}$ ensures reality of the renormalized Lagrangian. Furthermore it yields

$$\delta Z_{ij}^\dagger = \delta Z_{ij}(m_i^2 \leftrightarrow m_j^2), \tag{3.21}$$

and in particular

$$\delta Z_{ii}^\dagger = \delta Z_{ii}. \tag{3.22}$$

In the lepton sector we have $V_{ij} = \delta_{ij}$. Consequently all lepton self energies are diagonal and the off-diagonal lepton wave function renormalization constants are zero. The same holds for the quark sector if one replaces the quark mixing matrix by a unit matrix as is usually done in calculations of radiative corrections for high energy processes.

The renormalization constant for the quark mixing matrix V_{ij} can be directly read off from (3.15)

$$\delta V_{ij} = \frac{1}{4} [(\delta Z_{ik}^{u,L} - \delta Z_{ik}^{u,L\dagger}) V_{kj} - V_{ik} (\delta Z_{kj}^{d,L} - \delta Z_{kj}^{d,L\dagger})]. \quad (3.23)$$

Inserting the fermion field renormalization constants (3.20) yields

$$\begin{aligned} \delta V_{ij} = & \frac{1}{2} \widetilde{\text{Re}} \left\{ \frac{1}{m_{u,i}^2 - m_{u,k}^2} \left[m_{u,k}^2 \Sigma_{ik}^{u,L}(m_{u,k}^2) + m_{u,i}^2 \Sigma_{ik}^{u,L}(m_{u,i}^2) \right. \right. \\ & + m_{u,i} m_{u,k} \left(\Sigma_{ik}^{u,R}(m_{u,k}^2) + \Sigma_{ik}^{u,R}(m_{u,i}^2) \right) \\ & \left. \left. + (m_{u,k}^2 + m_{u,i}^2) \left(\Sigma_{ik}^{u,S}(m_{u,k}^2) + \Sigma_{ik}^{u,S}(m_{u,i}^2) \right) \right] V_{kj} \right. \\ & - V_{ik} \frac{1}{m_{d,k}^2 - m_{d,j}^2} \left[m_{d,j}^2 \Sigma_{kj}^{d,L}(m_{d,j}^2) + m_{d,k}^2 \Sigma_{kj}^{d,L}(m_{d,k}^2) \right. \\ & + m_{d,k} m_{d,j} \left(\Sigma_{kj}^{d,R}(m_{d,j}^2) + \Sigma_{kj}^{d,R}(m_{d,k}^2) \right) \\ & \left. \left. + (m_{d,k}^2 + m_{d,j}^2) \left(\Sigma_{kj}^{d,S}(m_{d,k}^2) + \Sigma_{kj}^{d,S}(m_{d,j}^2) \right) \right] \right\}. \end{aligned} \quad (3.24)$$

It remains to fix the charge renormalization constant δZ_e . This is determined from the $ee\gamma$ -vertex. To be more general we investigate the $ff\gamma$ -vertex for arbitrary fermions f . The renormalized vertex function reads

$$\hat{\Gamma}_{ij,\mu}^{\gamma ff}(p, p') = -ie Q_f \delta_{ij} \gamma_\mu + ie \hat{\Lambda}_{ij,\mu}^{\gamma ff}(p, p'). \quad (3.25)$$

For on-shell external fermions it can be decomposed as ($k = p' - p$)

$$\hat{\Lambda}_{ij,\mu}^{\gamma ff}(p, p') = \delta_{ij} \left(\gamma_\mu \hat{\Lambda}_V^f(k^2) - \gamma_\mu \gamma_5 \hat{\Lambda}_A^f(k^2) + \frac{(p+p')_\mu}{2m_f} \hat{\Lambda}_S^f(k^2) + \frac{(p'-p)_\mu}{2m_f} \gamma_5 \hat{\Lambda}_P^f(k^2) \right). \quad (3.26)$$

Expressing the renormalized quantities by the unrenormalized ones and the counterterms and inserting this in the analogue of the renormalization condition (3.17) for arbitrary fermions we find, using the Gordon identities,

$$\begin{aligned} 0 &= \bar{u}(p) \hat{\Lambda}_{ii,\mu}^{\gamma ff}(p, p) u(p) \\ &= \bar{u}(p) \gamma_\mu u(p) \left[-Q_f (\delta Z_e + \delta Z_{ii}^{f,V} + \frac{1}{2} \delta Z_{AA}) + \Lambda_V^f(0) + \Lambda_S^f(0) + v_f \frac{1}{2} \delta Z_{ZA} \right] \\ &\quad - \bar{u}(p) \gamma_\mu \gamma_5 u(p) \left[-Q_f \delta Z_{ii}^{f,A} + \Lambda_A^f(0) + a_f \frac{1}{2} \delta Z_{ZA} \right], \end{aligned} \quad (3.27)$$

where

$$\delta Z_{ii}^{f,V} = \frac{1}{2} (\delta Z_{ii}^{f,L} + \delta Z_{ii}^{f,R}), \quad \delta Z_{ii}^{f,A} = \frac{1}{2} (\delta Z_{ii}^{f,L} - \delta Z_{ii}^{f,R}), \quad (3.28)$$

and v_f, a_f are the vector and axialvector couplings of the Z -boson to the fermion f , given explicitly in (A.15). This yields in fact two conditions, namely

$$0 = -Q_f(\delta Z_e + \delta Z_{ii}^{f,V} + \frac{1}{2}\delta Z_{AA}) + \Lambda_V^f(0) + \Lambda_S^f(0) + v_f \frac{1}{2}\delta Z_{ZA}, \quad (3.29)$$

$$0 = -Q_f \delta Z_{ii}^{f,A} + \Lambda_A^f(0) + a_f \frac{1}{2}\delta Z_{ZA}. \quad (3.30)$$

The first one (3.29) for $f = e$ fixes the charge renormalization constant. The second (3.30) is automatically fulfilled due to a Ward identity which can be derived from the gauge invariance of the theory. The same Ward identity moreover yields

$$\Lambda_V^f(0) + \Lambda_S^f(0) - Q_f \delta Z_{ii}^{f,V} + a_f \frac{1}{2}\delta Z_{ZA} = 0. \quad (3.31)$$

Inserting this in (3.29) we finally find (using $v_f - a_f = -Q_f s_W/c_W$)

$$\delta Z_e = -\frac{1}{2}\delta Z_{AA} - \frac{s_W}{c_W} \frac{1}{2}\delta Z_{ZA} = \frac{1}{2} \frac{\partial \Sigma_T^{AA}(k^2)}{\partial k^2} \Big|_{k^2=0} - \frac{s_W}{c_W} \frac{\Sigma_T^{AZ}(0)}{M_Z^2}. \quad (3.32)$$

This result is independent of the fermion species, reflecting electric charge universality. Clearly it does not depend on a specific choice of field renormalization. Consequently the analogue of (3.17) holds for arbitrary fermions f .

In the on-shell scheme the weak mixing angle is a derived quantity. Following Sirlin [26] we define it as

$$\sin^2 \theta_W = s_W^2 = 1 - \frac{M_W^2}{M_Z^2}, \quad (3.33)$$

using the renormalized gauge boson masses. This definition is independent of a specific process and valid to all orders of perturbation theory.

Since the dependent parameters s_W and c_W frequently appear, it is useful to introduce the corresponding counterterms

$$c_{W,0} = c_W + \delta c_W, \quad s_{W,0} = s_W + \delta s_W. \quad (3.34)$$

Because of (3.33) these are directly related to the counterterms to the gauge boson masses. To one-loop order we obtain

$$\begin{aligned} \frac{\delta c_W}{c_W} &= \frac{1}{2} \left(\frac{\delta M_W^2}{M_W^2} - \frac{\delta M_Z^2}{M_Z^2} \right) = \frac{1}{2} \widetilde{\text{Re}} \left(\frac{\Sigma_T^W(M_W^2)}{M_W^2} - \frac{\Sigma_T^{ZZ}(M_Z^2)}{M_Z^2} \right), \\ \frac{\delta s_W}{s_W} &= -\frac{c_W^2}{s_W^2} \frac{\delta c_W}{c_W} = -\frac{1}{2} \frac{c_W^2}{s_W^2} \widetilde{\text{Re}} \left(\frac{\Sigma_T^W(M_W^2)}{M_W^2} - \frac{\Sigma_T^{ZZ}(M_Z^2)}{M_Z^2} \right). \end{aligned} \quad (3.35)$$

We have now determined all renormalization constants in terms of unrenormalized self energies. In the next sections we will describe the methods to calculate these self energies and more general diagrams at the one-loop level.

4 One-loop integrals

Perturbative calculations at one-loop order involve integrals over the loop momentum. In this chapter we discuss their classification and techniques for their calculation. The methods described here are to a large extent based on the work of Passarino and Veltman [18], 't Hooft and Veltman [28], and Melrose [29].

4.1 Definitions

The one-loop integrals in D dimensions are classified according to the number N of propagator factors in the denominator and the number P of integration momenta in the numerator. For $P + D - 2N \geq 0$ these integrals are UV-divergent. These divergencies are regularized by calculating the integrals in general dimensions $D \neq 4$ (dimensional regularization). The UV-divergencies drop out in renormalized quantities. For renormalizable theories we have $P \leq N$ and thus a finite number of divergent integrals.

We define the general one-loop tensor integral (see Fig. 4.1) as

$$T_{\mu_1 \dots \mu_P}^N(p_1, \dots, p_{N-1}, m_0, \dots, m_{N-1}) = \frac{(2\pi\mu)^{4-D}}{i\pi^2} \int d^D q \frac{q_{\mu_1} \dots q_{\mu_P}}{D_0 D_1 \dots D_{N-1}} \quad (4.1)$$

with the denominator factors

$$D_0 = q^2 - m_0^2 + i\varepsilon, \quad D_i = (q + p_i)^2 - m_i^2 + i\varepsilon, \quad i = 1, \dots, N-1, \quad (4.2)$$

originating from the propagators in the Feynman diagram. Furthermore we introduce

$$p_{i0} = p_i \quad \text{and} \quad p_{ij} = p_i - p_j. \quad (4.3)$$

Evidently the tensor integrals are invariant under arbitrary permutations of the propagators D_i , $i \neq 0$ and totally symmetric in the Lorentz indices μ_k . $i\varepsilon$ is an infinitesimal imaginary part which is needed to regulate singularities of the integrand. Its specific choice ensures causality. After integration it determines the correct imaginary parts of the logarithms and dilogarithms. The parameter μ has mass dimension and serves to keep

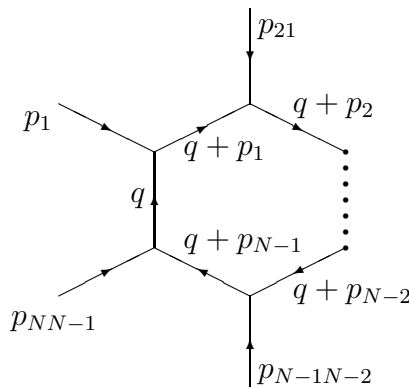


Figure 4.1: Conventions for the N-point integral.

the dimension of the integrals fixed for varying D . Conventionally T^N is denoted by the N th character of the alphabet, i.e. $T^1 \equiv A$, $T^2 \equiv B$, \dots , and the scalar integrals carry an index 0.

Lorentz covariance of the integrals allows to decompose the tensor integrals into tensors constructed from the external momenta p_i , and the metric tensor $g_{\mu\nu}$ with totally symmetric coefficient functions $T_{i_1\dots i_P}^N$. We formally introduce an artificial momentum p_0 in order to write the terms containing $g_{\mu\nu}$ in a compact way

$$T_{\mu_1\dots\mu_P}^N(p_1, \dots, p_{N-1}, m_0, \dots, m_{N-1}) = \sum_{i_1, \dots, i_P=0}^{N-1} T_{i_1\dots i_P}^N p_{i_1\mu_1} \cdots p_{i_P\mu_P}. \quad (4.4)$$

From this formula the correct $g_{\mu\nu}$ terms are recovered by omitting all terms containing an odd number of p_0 's and replacing products of even numbers of p_0 's by the corresponding totally symmetric tensor constructed from the $g_{\mu\nu}$, e.g.

$$\begin{aligned} p_{0\mu_1} p_{0\mu_2} &\rightarrow g_{\mu_1\mu_2}, \\ p_{0\mu_1} p_{0\mu_2} p_{0\mu_3} p_{0\mu_4} &\rightarrow g_{\mu_1\mu_2} g_{\mu_3\mu_4} + g_{\mu_1\mu_3} g_{\mu_2\mu_4} + g_{\mu_1\mu_4} g_{\mu_2\mu_3}. \end{aligned} \quad (4.5)$$

The explicit Lorentz decompositions for the lowest order integrals read

$$B_\mu = p_{1\mu} B_1, \quad (4.6)$$

$$B_{\mu\nu} = g_{\mu\nu} B_{00} + p_{1\mu} p_{1\nu} B_{11},$$

$$C_\mu = p_{1\mu} C_1 + p_{2\mu} C_2 = \sum_{i=1}^2 p_{i\mu} C_i,$$

$$C_{\mu\nu} = g_{\mu\nu} C_{00} + p_{1\mu} p_{1\nu} C_{11} + p_{2\mu} p_{2\nu} C_{22} + (p_{1\mu} p_{2\nu} + p_{2\mu} p_{1\nu}) C_{12}$$

$$= g_{\mu\nu} C_{00} + \sum_{i,j=1}^2 p_{i\mu} p_{j\nu} C_{ij},$$

$$C_{\mu\nu\rho} = (g_{\mu\nu} p_{1\rho} + g_{\nu\rho} p_{1\mu} + g_{\mu\rho} p_{1\nu}) C_{001} + (g_{\mu\nu} p_{2\rho} + g_{\nu\rho} p_{2\mu} + g_{\mu\rho} p_{2\nu}) C_{002} \quad (4.7)$$

$$+ p_{1\mu} p_{1\nu} p_{1\rho} C_{111} + p_{2\mu} p_{2\nu} p_{2\rho} C_{222}$$

$$+ (p_{1\mu} p_{1\nu} p_{2\rho} + p_{1\mu} p_{2\nu} p_{1\rho} + p_{2\mu} p_{1\nu} p_{1\rho}) C_{112}$$

$$+ (p_{2\mu} p_{2\nu} p_{1\rho} + p_{2\mu} p_{1\nu} p_{2\rho} + p_{1\mu} p_{2\nu} p_{2\rho}) C_{122}$$

$$= \sum_{i=1}^2 (g_{\mu\nu} p_{i\rho} + g_{\nu\rho} p_{i\mu} + g_{\mu\rho} p_{i\nu}) C_{00i} + \sum_{i,j,k=1}^2 p_{i\mu} p_{j\nu} p_{k\rho} C_{ijk},$$

$$\begin{aligned}
D_\mu &= \sum_{i=1}^3 p_{i\mu} D_i, \\
D_{\mu\nu} &= g_{\mu\nu} D_{00} + \sum_{i,j=1}^3 p_{i\mu} p_{j\nu} D_{ij}, \\
D_{\mu\nu\rho} &= \sum_{i=1}^3 (g_{\mu\nu} p_{i\rho} + g_{\nu\rho} p_{i\mu} + g_{\mu\rho} p_{i\nu}) D_{00i} + \sum_{i,j,k=1}^3 p_{i\mu} p_{j\nu} p_{k\rho} D_{ijk}, \\
D_{\mu\nu\rho\sigma} &= (g_{\mu\nu} g_{\rho\sigma} + g_{\mu\rho} g_{\nu\sigma} + g_{\mu\sigma} g_{\nu\rho}) D_{0000} \\
&\quad + \sum_{i,j=1}^3 (g_{\mu\nu} p_{i\rho} p_{j\sigma} + g_{\nu\rho} p_{i\mu} p_{j\sigma} + g_{\mu\rho} p_{i\nu} p_{j\sigma} \\
&\quad\quad + g_{\mu\sigma} p_{i\nu} p_{j\rho} + g_{\nu\sigma} p_{i\mu} p_{j\rho} + g_{\rho\sigma} p_{i\mu} p_{j\nu}) D_{00ij} \\
&\quad + \sum_{i,j,k,l=1}^3 p_{i\mu} p_{j\nu} p_{k\rho} p_{l\sigma} D_{ijkl}.
\end{aligned} \tag{4.8}$$

Since the four dimensional space is spanned by four Lorentz vectors the terms involving $g_{\mu\nu}$ should be omitted for $N \geq 5$ and at most four Lorentz vectors should be used in the decomposition (4.4). Consequently the Lorentz decomposition for a general tensor integral with $N \geq 5$ in four dimensions can be written as

$$T_{\mu_1 \dots \mu_P}^N(p_1, \dots, p_{N-1}, m_0, \dots, m_{N-1}) = \sum_{i_1, \dots, i_P=1}^4 T_{i_1 \dots i_P}^N p_{i_1 \mu_1} \dots p_{i_P \mu_P}, \tag{4.9}$$

where p_1, \dots, p_4 is any set of four linear independent Lorentz vectors out of p_1, \dots, p_{N-1} . The symmetry of the tensor integrals under exchange of the propagators yields relations between the scalar coefficient functions. Exchanging the arguments $(p_i, m_i) \leftrightarrow (p_j, m_j)$ together with the corresponding indices $i \leftrightarrow j$ leaves the scalar coefficient functions invariant

$$\begin{aligned}
&T_{\dots \underbrace{i \dots i}_n \dots \underbrace{j \dots j}_m \dots}^N(p_1, \dots, p_i, \dots, p_j, \dots, p_{N-1}, m_0, \dots, m_i, \dots, m_j, \dots, m_{N-1}) \\
&= T_{\dots \underbrace{i \dots i}_m \dots \underbrace{j \dots j}_n \dots}^N(p_1, \dots, p_j, \dots, p_i, \dots, p_{N-1}, m_0, \dots, m_j, \dots, m_i, \dots, m_{N-1}),
\end{aligned} \tag{4.10}$$

e.g.

$$\begin{aligned}
C_1(p_1, p_2, m_0, m_1, m_2) &= C_2(p_2, p_1, m_0, m_2, m_1), \\
C_{00}(p_1, p_2, m_0, m_1, m_2) &= C_{00}(p_2, p_1, m_0, m_2, m_1), \\
C_{12}(p_1, p_2, m_0, m_1, m_2) &= C_{12}(p_2, p_1, m_0, m_2, m_1).
\end{aligned} \tag{4.11}$$

All one-loop tensor integrals can be reduced to the scalar ones T_0^N . This is done in Sect. 4.2. General analytical results for the scalar integrals A_0, B_0, C_0 are D_0 are listed in Sect. 4.3. The scalar integrals for $N > 4$ can be expressed in terms of D_0 's in four dimensions. The relevant formulae are given in Sect. 4.4. They apply as well to the

tensor integrals with $N \leq 4$ in the kinematical regions, where the usual tensor integral reduction breaks down, because the Gram determinants appearing there are zero. The UV-divergent parts of the one-loop integrals are explicitly given in Sect. 4.5

4.2 Reduction of tensor integrals to scalar integrals

Using the Lorentz decomposition of the tensor integrals (4.4) the invariant functions $T_{i_1 \dots i_P}^N$ can be iteratively reduced to the scalar integrals T_0^N [18]. We derive the relevant formulae for the general tensor integral.

The product of the integration momentum q_μ with an external momentum can be expressed in terms of the denominators

$$qp_k = \frac{1}{2}[D_k - D_0 - f_k], \quad f_k = p_k^2 - m_k^2 + m_0^2. \quad (4.12)$$

Multiplying (4.1) with p_k and substituting (4.12) yields

$$\begin{aligned} R_{\mu_1 \dots \mu_{P-1}}^{N,k} &= T_{\mu_1 \dots \mu_P}^N p_k^{\mu_P} \\ &= \frac{1}{2} \frac{(2\pi\mu)^{4-D}}{i\pi^2} \int d^D q \left[\frac{q_{\mu_1} \dots q_{\mu_{P-1}}}{D_0 \dots D_{k-1} D_{k+1} \dots D_{N-1}} \right. \\ &\quad \left. - \frac{q_{\mu_1} \dots q_{\mu_{P-1}}}{D_1 \dots D_{N-1}} - f_k \frac{q_{\mu_1} \dots q_{\mu_{P-1}}}{D_0 \dots D_{N-1}} \right] \\ &= \frac{1}{2} \left[T_{\mu_1 \dots \mu_{P-1}}^{N-1}(k) - T_{\mu_1 \dots \mu_{P-1}}^{N-1}(0) - f_k T_{\mu_1 \dots \mu_{P-1}}^N \right], \end{aligned} \quad (4.13)$$

where the argument k of the tensor integrals in the last line indicates that the propagator D_k was cancelled. Note that $T_{\mu_1 \dots \mu_{P-1}}^{N-1}(0)$ has an external momentum in its first propagator. Therefore a shift of the integration momentum has to be performed in this integral in order to bring it to the form (4.1). All tensor integrals on the right-hand side of eq. (4.13) have one Lorentz index less than the original tensor integral. In two of them also one propagator is eliminated.

For $P \geq 2$ we obtain one more relation by contracting (4.1) with $g^{\mu\nu}$ and using

$$g^{\mu\nu} q_\mu q_\nu = q^2 = D_0 + m_0^2. \quad (4.14)$$

This gives

$$\begin{aligned} R_{\mu_1 \dots \mu_{P-2}}^{N,00} &= T_{\mu_1 \dots \mu_P}^N g^{\mu_{P-1}\mu_P} \\ &= \frac{(2\pi\mu)^{4-D}}{i\pi^2} \int d^D q \left[\frac{q_{\mu_1} \dots q_{\mu_{P-2}}}{D_1 \dots D_N} + m_0^2 \frac{q_{\mu_1} \dots q_{\mu_{P-2}}}{D_0 \dots D_N} \right] \\ &= \left[T_{\mu_1 \dots \mu_{P-2}}^{N-1}(0) + m_0^2 T_{\mu_1 \dots \mu_{P-2}}^N \right]. \end{aligned} \quad (4.15)$$

Inserting the Lorentz decomposition (4.4) for the tensor integrals T into (4.13) and (4.15) we obtain set of linear equations for the corresponding coefficient functions. This set

decomposes naturally into disjoint sets of $N - 1$ equations for each tensor integral. If the inverse of the matrix

$$X_{N-1} = \begin{pmatrix} p_1^2 & p_1 p_2 & \cdots & p_1 p_{N-1} \\ p_2 p_1 & p_2^2 & \cdots & p_2 p_{N-1} \\ \vdots & \vdots & \ddots & \vdots \\ p_{N-1} p_1 & p_{N-1} p_2 & \cdots & p_{N-1}^2 \end{pmatrix} \quad (4.16)$$

exists, these can be solved for the invariant functions $T_{i_1 \dots i_p}^N$ yielding them in terms of invariant functions of tensor integrals with fewer indices (see eqs. (4.18) and (4.19) below). In this way all tensor integrals are expressed iteratively in terms of scalar integrals T_0^L with $L \leq N$.

If the matrix X_{N-1} becomes singular, the reduction algorithm breaks down. If this is due to the linear dependence of the momenta we can leave out the linear dependent vectors of the set p_1, \dots, p_{N-1} in the Lorentz decomposition resulting in a smaller matrix X_M . If X_M is nonsingular the reduction algorithm works again. This happens usually at the edge of phase space where some of the momenta p_i become collinear.

If the determinant of X_{N-1} , the Gram determinant, is zero but the momenta are not linear dependent¹ one has to use a different reduction algorithm [29, 30]. This will be discussed in Sect. 4.4.

Here we give the results for the reduction of arbitrary N-point integrals depending on $M \leq N - 1$ linear independent Lorentz vectors in D dimensions for nonsingular X_M . Inserting the Lorentz decomposition of T_N and $R^{N,k}$ as well as $R^{N,00}$

$$\begin{aligned} R_{\mu_1 \dots \mu_{P-1}}^{N,k} &= T_{\mu_1 \dots \mu_P}^N p_k^{\mu_P} = \sum_{i_1, \dots, i_{P-1}=0}^M R_{i_1 \dots i_{P-1}}^{N,k} p_{i_1 \mu_1} \cdots p_{i_{P-1} \mu_{P-1}}, \\ R_{\mu_1 \dots \mu_{P-2}}^{N,00} &= T_{\mu_1 \dots \mu_P}^N g^{\mu_{P-1} \mu_P} = \sum_{i_1, \dots, i_{P-2}=0}^M R_{i_1 \dots i_{P-2}}^{N,00} p_{i_1 \mu_1} \cdots p_{i_{P-2} \mu_{P-2}}, \end{aligned} \quad (4.17)$$

into the first lines of (4.13) and (4.15) these equations can be solved for the $T_{i_1 \dots i_p}^N$:

$$\begin{aligned} T_{00 i_1 \dots i_{P-2}}^N &= \frac{1}{D + P - 2 - M} \left[R_{i_1 \dots i_{P-2}}^{N,00} - \sum_{k=1}^M R_{k i_1 \dots i_{P-2}}^{N,k} \right], \\ T_{k i_1 \dots i_{P-1}}^N &= (X_M^{-1})_{kk'} \left[R_{i_1 \dots i_{P-1}}^{N,k'} - \sum_{r=1}^{P-1} \delta_{i_r}^{k'} T_{00 i_1 \dots i_{r-1} i_{r+1} \dots i_{P-1}}^N \right]. \end{aligned} \quad (4.18)$$

Note that the numerator of the prefactor in the first equation is always positive in the relevant cases $P \geq 2$ and $D > M$. Using the third lines of (4.13) and (4.15) the R 's can be expressed in terms of $T_{i_1 \dots i_{P-1}}^N$, $T_{i_1 \dots i_{P-2}}^N$, and $T_{i_1 \dots i_q}^{N-1}$, with $q < P$ as follows

$$\begin{aligned} R_{i_1 \dots i_q}^{N,00} \underbrace{M \dots M}_{P-2-q} &= m_0^2 T_{i_1 \dots i_q}^N \underbrace{M \dots M}_{P-2-q} \\ &+ (-1)^{P-q} \left[\tilde{T}_{i_1 \dots i_q}^{N-1}(0) + \binom{P-2-q}{1} \sum_{k_1=1}^{M-1} \tilde{T}_{i_1 \dots i_q k_1}^{N-1}(0) \right] \end{aligned}$$

¹This can happen, because of the indefinite metric of space time.

$$\begin{aligned}
& + \binom{P-2-q}{2} \sum_{k_1, k_2=1}^{M-1} \tilde{T}_{i_1 \dots i_q k_1 k_2}^{N-1}(0) + \dots \\
& + \left[\binom{P-2-q}{P-2-q} \sum_{k_1, \dots, k_{P-2-q}=1}^{M-1} \tilde{T}_{i_1 \dots i_q k_1 \dots k_{P-2-q}}^{N-1}(0) \right], \\
R_{i_1 \dots i_q \underbrace{M \dots M}_{P-1-q}}^{N,k} & = \frac{1}{2} \left\{ T_{i_1 \dots \tilde{i}_q \underbrace{\tilde{M} \dots \tilde{M}}_{P-1-q}}^{N-1}(k) \theta(k | i_1, \dots, i_q, \underbrace{M, \dots, M}_{P-1-q}) - f_k T_{i_1 \dots i_q \underbrace{M \dots M}_{P-1-q}}^N \right. \\
& - (-1)^{P-1-q} \left[\tilde{T}_{i_1 \dots i_q}^{N-1}(0) + \binom{P-1-q}{1} \sum_{k_1=1}^{M-1} \tilde{T}_{i_1 \dots i_q k_1}^{N-1}(0) \right. \\
& + \binom{P-1-q}{2} \sum_{k_1, k_2=1}^{M-1} \tilde{T}_{i_1 \dots i_q k_1 k_2}^{N-1}(0) + \dots \\
& \left. \left. + \binom{P-1-q}{P-1-q} \sum_{k_1, \dots, k_{P-1-q}=1}^{M-1} \tilde{T}_{i_1 \dots i_q k_1 \dots k_{P-1-q}}^{N-1}(0) \right] \right\} \quad (4.19)
\end{aligned}$$

where $i_1, \dots, i_q \neq M$ and

$$\theta(k | i_1, \dots, i_{P-1}) = \begin{cases} 1 & i_r \neq k, \quad r = 1, \dots, P-1, \\ 0 & \text{else.} \end{cases} \quad (4.20)$$

The indices \tilde{i} refer to the i -th momentum of the corresponding N -point function T^N but to the $(i-1)$ -th momentum of the $N-1$ -point function $T^{N-1}(k)$ if $i > k$. Again the arguments of the T 's indicate the cancelled propagators. The tilde in $\tilde{T}(0)$ means that a shift of the integration variable $q \rightarrow q - p_M$ has been performed in order to obtain the standard form of these integrals. This shift generates the terms in the square brackets of (4.19). It is also the reason for the unsymmetric appearance of the index M in the above equations. A different shift would result in similar results. An explicit example illustrating the use of these reduction formulae is given in App. C.

The recursion formulae above determine the coefficients $T_{i_1 \dots i_P}$ regardless of their symmetries. Consequently coefficients whose indices are not all equal are obtained in different ways. This allows for checks on the analytical results as well as on numerical stability.

If the number M of linear independent momenta equals the dimension D of space-time then the terms containing $g_{\mu\nu}$ in the Lorentz decomposition have to be omitted, since $g_{\mu\nu}$ can be built up from the D momenta. In this case the coefficients $T_{i_1 \dots i_P}^N$ are obtained from the second equations in (4.18) and (4.19) with $T_{00i_1 \dots i_{P-2}}^N = 0$.

4.3 Scalar one-loop integrals for $N \leq 4$

With the methods described in the last section all one-loop integrals can be reduced to the scalar ones T_0^N provided the matrices X_M are nonsingular. General analytical results

for A_0, B_0, C_0 and D_0 were derived in [28]. Algorithms for the numerical calculation of the scalar one-loop integrals based on these results have been presented in [31]. Here we give a new formula [32] for D_0 involving only 16 dilogarithms compared to 24 of the solution of [28]. For completeness we first list the results for A_0, B_0 and C_0 .

4.3.1 Scalar one-point function

The scalar one-point function reads

$$A_0(m) = -m^2 \left(\frac{m^2}{4\pi\mu^2} \right)^{\frac{D-4}{2}} \Gamma\left(1 - \frac{D}{2}\right) = m^2 \left(\Delta - \log \frac{m^2}{\mu^2} + 1 \right) + O(D-4), \quad (4.21)$$

with the UV-divergence contained in

$$\Delta = \frac{2}{4-D} - \gamma_E + \log 4\pi \quad (4.22)$$

and γ_E is Euler's constant. The terms of order $O(D-4)$ are only relevant for two- or higher-loop calculations.

4.3.2 Scalar two-point function

The two-point function is given by

$$\begin{aligned} B_0(p_{10}, m_0, m_1) &= \Delta - \int_0^1 dx \log \frac{[p_{10}^2 x^2 - x(p_{10}^2 - m_0^2 + m_1^2) + m_1^2 - i\varepsilon]}{\mu^2} + O(D-4) \\ &= \Delta + 2 - \log \frac{m_0 m_1}{\mu^2} + \frac{m_0^2 - m_1^2}{p_{10}^2} \log \frac{m_1}{m_0} - \frac{m_0 m_1}{p_{10}^2} \left(\frac{1}{r} - r \right) \log r \\ &\quad + O(D-4), \end{aligned} \quad (4.23)$$

where r and $\frac{1}{r}$ are determined from

$$x^2 + \frac{m_0^2 + m_1^2 - p_{10}^2 - i\varepsilon}{m_0 m_1} x + 1 = (x+r)\left(x + \frac{1}{r}\right). \quad (4.24)$$

The variable r never crosses the negative real axis even for complex physical masses (m^2 has a negative imaginary part!). For $r < 0$ the $i\varepsilon$ prescription yields $\text{Im } r = \varepsilon \text{sgn}(r - \frac{1}{r})$. Consequently the result (4.23) is valid for arbitrary physical parameters.

For the field renormalization constants we need the derivative of B_0 with respect to p_{10}^2 . This is easily obtained by differentiating the above result

$$\begin{aligned} \frac{\partial}{\partial p_{10}^2} B_0(p_{10}, m_0, m_1) &= -\frac{m_0^2 - m_1^2}{p_{10}^4} \log \frac{m_1}{m_0} + \frac{m_0 m_1}{p_{10}^4} \left(\frac{1}{r} - r \right) \log r \\ &\quad - \frac{1}{p_{10}^2} \left(1 + \frac{r^2 + 1}{r^2 - 1} \log r \right) + O(D-4). \end{aligned} \quad (4.25)$$

4.3.3 Scalar three-point function

The general result for the scalar three-point function valid for all real momenta and physical masses was calculated by [28]. It can be brought into the symmetric form

$$\begin{aligned}
C_0(p_{10}, p_{20}, m_0, m_1, m_2) &= \\
& - \int_0^1 dx \int_0^x dy [p_{21}^2 x^2 + p_{10}^2 y^2 + (p_{20}^2 - p_{10}^2 - p_{21}^2)xy \\
& \quad + (m_1^2 - m_2^2 - p_{21}^2)x + (m_0^2 - m_1^2 + p_{21}^2 - p_{20}^2)y + m_2^2 - i\varepsilon]^{-1} \quad (4.26) \\
&= \frac{1}{\alpha} \sum_{i=0}^2 \left\{ \sum_{\sigma=\pm} \left[\text{Li}_2\left(\frac{y_{0i} - 1}{y_{i\sigma}}\right) - \text{Li}_2\left(\frac{y_{0i}}{y_{i\sigma}}\right) \right. \right. \\
& \quad \left. \left. + \eta\left(1 - x_{i\sigma}, \frac{1}{y_{i\sigma}}\right) \log \frac{y_{0i} - 1}{y_{i\sigma}} - \eta\left(-x_{i\sigma}, \frac{1}{y_{i\sigma}}\right) \log \frac{y_{0i}}{y_{i\sigma}} \right] \right. \\
& \quad \left. - \left[\eta(-x_{i+}, -x_{i-}) - \eta(y_{i+}, y_{i-}) - 2\pi i \theta(-p_{jk}^2) \theta(-\text{Im}(y_{i+} y_{i-})) \right] \log \frac{1 - y_{i0}}{-y_{i0}} \right\},
\end{aligned}$$

with $(i, j, k = 0, 1, 2$ and cyclic)

$$\begin{aligned}
y_{0i} &= \frac{1}{2\alpha p_{jk}^2} [p_{jk}^2 (p_{jk}^2 - p_{ki}^2 - p_{ij}^2 + 2m_i^2 - m_j^2 - m_k^2) \\
& \quad - (p_{ki}^2 - p_{ij}^2)(m_j^2 - m_k^2) + \alpha(p_{jk}^2 - m_j^2 + m_k^2)], \\
x_{i\pm} &= \frac{1}{2p_{jk}^2} [p_{jk}^2 - m_j^2 + m_k^2 \pm \alpha_i], \\
y_{i\pm} &= y_{0i} - x_{i\pm}, \quad (4.27) \\
\alpha &= \kappa(p_{10}^2, p_{21}^2, p_{20}^2), \\
\alpha_i &= \kappa(p_{jk}^2, m_j^2, m_k^2) (1 + i\varepsilon p_{jk}^2),
\end{aligned}$$

and κ is the Källén function

$$\kappa(x, y, z) = \sqrt{x^2 + y^2 + z^2 - 2(xy + yz + zx)}. \quad (4.28)$$

The dilogarithm or Spence function $\text{Li}_2(x)$ is defined as

$$\text{Li}_2(x) = - \int_0^1 \frac{dt}{t} \log(1 - xt), \quad |\arg(1 - x)| < \pi. \quad (4.29)$$

The η -function compensates for cut crossings on the Riemann-sheet of the logarithms and dilogarithms. For a, b on the first Riemann sheet it is defined by

$$\log(ab) = \log(a) + \log(b) + \eta(a, b). \quad (4.30)$$

All η -functions in (4.26) vanish if α and all the masses m_i are real. Note that α is real in particular for all on-shell decay and scattering processes.

4.3.4 Scalar four-point function

The scalar four-point function $D_0(p_{10}, p_{20}, p_{30}, m_0, m_1, m_2, m_3)$ can be expressed in terms of 16 dilogarithms [32].

Before we give the result we first introduce some useful variables and functions. We define

$$k_{ij} = \frac{m_i^2 + m_j^2 - p_{ij}^2}{m_i m_j}, \quad i, j = 0, 1, 2, 3, \quad (4.31)$$

and r_{ij} and \tilde{r}_{ij} by

$$x^2 + k_{ij}x + 1 = (x + r_{ij})(x + 1/r_{ij}), \quad (4.32)$$

and

$$x^2 + (k_{ij} - i\varepsilon)x + 1 = (x + \tilde{r}_{ij})(x + 1/\tilde{r}_{ij}). \quad (4.33)$$

Note that for real k_{ij} the r_{ij} 's lie either on the real axis or on the complex unit circle. Furthermore

$$P(y_0, y_1, y_2, y_3) = \sum_{0 \leq i < j \leq 3} k_{ij} y_i y_j + \sum_{j=0}^3 y_j^2, \quad (4.34)$$

$$Q(y_0, y_1, 0, y_3) = (1/r_{02} - r_{02})y_0 + (k_{12} - r_{02}k_{01})y_1 + (k_{23} - r_{02}k_{03})y_3, \quad (4.35)$$

$$\bar{Q}(y_0, 0, y_2, y_3) = (1/r_{13} - r_{13})y_3 + (k_{12} - r_{13}k_{23})y_2 + (k_{01} - r_{13}k_{03})y_0. \quad (4.36)$$

and $x_{1,2}$ is defined by

$$\begin{aligned} & \frac{r_{02}r_{13}}{x} \left\{ \left[P\left(1, \frac{x}{r_{13}}, 0, 0\right) - i\varepsilon \right] \left[P\left(0, 0, \frac{1}{r_{02}}, x\right) - i\varepsilon \right] \right. \\ & \quad \left. - \left[P\left(0, \frac{x}{r_{13}}, \frac{1}{r_{02}}, 0\right) - i\varepsilon \right] \left[P(1, 0, 0, x) - i\varepsilon \right] \right\} \\ & = ax^2 + bx + c + i\varepsilon d = a(x - x_1)(x - x_2), \end{aligned} \quad (4.37)$$

where

$$\begin{aligned} a &= k_{23}/r_{13} + r_{02}k_{01} - k_{03}r_{02}/r_{13} - k_{12}, \\ b &= (r_{13} - 1/r_{13})(r_{02} - 1/r_{02}) + k_{01}k_{23} - k_{03}k_{12}, \\ c &= k_{01}/r_{02} + r_{13}k_{23} - k_{03}r_{13}/r_{02} - k_{12}, \\ d &= k_{12} - r_{02}k_{01} - r_{13}k_{23} + r_{02}r_{13}k_{03}. \end{aligned} \quad (4.38)$$

In addition we introduce

$$\gamma_{kl} = \text{sgn Re}[a(x_k - x_l)], \quad k, l = 1, 2, \quad (4.39)$$

and

$$\begin{aligned} x_{k0} &= x_k, & s_0 &= \tilde{r}_{03}, \\ x_{k1} &= x_k/r_{13}, & s_1 &= \tilde{r}_{01}, \\ x_{k2} &= x_k r_{02}/r_{13}, & s_2 &= \tilde{r}_{12}, \\ x_{k3} &= x_k r_{02}, & s_3 &= \tilde{r}_{23}. \end{aligned} \quad (4.40)$$

as well as

$$x_{kj}^{(0)} = \lim_{\varepsilon \rightarrow 0} x_{kj} \quad \text{as} \quad r_{ij} = \lim_{\varepsilon \rightarrow 0} \tilde{r}_{ij}. \quad (4.41)$$

Finally we need

$$\tilde{\eta}(a, \tilde{b}) = \begin{cases} \eta(a, b) & \text{for } b \text{ not real,} \\ 2\pi i \left[\theta(-\text{Im } a)\theta(-\text{Im } \tilde{b}) - \theta(\text{Im } a)\theta(\text{Im } \tilde{b}) \right] & \text{for } b < 0, \\ 0 & \text{for } b > 0 \end{cases} \quad (4.42)$$

with $b = \lim_{\varepsilon \rightarrow 0} \tilde{b}$.

Then the result for real r_{02} can be written as

$$\begin{aligned} D_0(p_{10}, p_{20}, p_{30}, m_0, m_1, m_2, m_3) &= \frac{1}{m_1 m_2 m_3 m_4 a (x_1 - x_2)} \\ &\left\{ \sum_{j=0}^3 \sum_{k=1}^2 (-1)^{j+k} \left[\text{Li}_2(1 + s_j x_{kj}) + \eta(-x_{kj}, s_j) \log(1 + s_j x_{kj}) \right. \right. \\ &\quad \left. \left. + \text{Li}_2\left(1 + \frac{x_{kj}}{s_j}\right) + \eta\left(-x_{kj}, \frac{1}{s_j}\right) \log\left(1 + \frac{x_{kj}}{s_j}\right) \right] \right. \\ &+ \sum_{k=1}^2 (-1)^{k+1} \left[\tilde{\eta}(-x_k, \tilde{r}_{02}) \left[\log(r_{02} x_k) + \log\left(Q\left(\frac{1}{x_k^{(0)}}, 0, 0, 1\right) - i\varepsilon\right) \right. \right. \\ &\quad \left. \left. + \log\left(\frac{\overline{Q}(0, 0, 1, r_{02} x_k^{(0)})}{d} + i\varepsilon \gamma_{k,3-k} \text{sgn}(r_{02} \text{Im } \tilde{r}_{13})\right) \right] \right. \\ &\quad \left. + \tilde{\eta}\left(-x_k, \frac{1}{\tilde{r}_{13}}\right) \left[\log\left(\frac{x_k}{r_{13}}\right) + \log\left(Q\left(\frac{r_{13}}{x_k^{(0)}}, 1, 0, 0\right) - i\varepsilon\right) \right. \right. \\ &\quad \left. \left. + \log\left(\frac{\overline{Q}(1, 0, 0, x_k^{(0)})}{d} + i\varepsilon \gamma_{k,3-k} \text{sgn}(\text{Im } \tilde{r}_{13})\right) \right] \right. \\ &\quad \left. - \left[\tilde{\eta}\left(-x_k, \frac{\tilde{r}_{02}}{\tilde{r}_{13}}\right) + \eta\left(\tilde{r}_{02}, \frac{1}{\tilde{r}_{13}}\right) \right] \left[\log\left(\frac{r_{02} x_k}{r_{13}}\right) + \log\left(Q\left(\frac{r_{13}}{x_k^{(0)}}, 1, 0, 0\right) - i\varepsilon\right) \right. \right. \\ &\quad \left. \left. + \log\left(\frac{\overline{Q}(0, 0, 1, r_{02} x_k^{(0)})}{d} + i\varepsilon \gamma_{k,3-k} \text{sgn}(r_{02} \text{Im } \tilde{r}_{13})\right) \right] \right. \\ &\quad \left. \left. + \eta\left(\tilde{r}_{02}, \frac{1}{\tilde{r}_{13}}\right) \tilde{\eta}\left(-x_k, -\frac{\tilde{r}_{02}}{\tilde{r}_{13}}\right) \right] \right\}. \quad (4.43) \end{aligned}$$

In the case that $|r_{ij}| = 1$ for all r_{ij} , the result reads:

$$\begin{aligned} D_0(p_{10}, p_{20}, p_{30}, m_0, m_1, m_2, m_3) &= \frac{1}{m_1 m_2 m_3 m_4 a (x_1 - x_2)} \\ &\left\{ \sum_{j=0}^3 \sum_{k=1}^2 (-1)^{j+k} \left[\text{Li}_2(1 + s_j x_{kj}) + \eta(-x_{kj}, s_j) \log(1 + s_j x_{kj}) \right. \right. \\ &\quad \left. \left. + \text{Li}_2\left(1 + \frac{x_{kj}}{s_j}\right) + \eta\left(-x_{kj}, \frac{1}{s_j}\right) \log\left(1 + \frac{x_{kj}}{s_j}\right) \right] \right. \\ &+ \sum_{k=1}^2 (-1)^{k+1} \left[\eta\left(-x_k, \frac{1}{r_{13}}\right) \left[\log\left(\frac{r_{13}}{x_k^{(0)}} P\left(1, \frac{x_k^{(0)}}{r_{13}}, 0, 0\right) - \frac{x_k^{(0)}}{r_{13}} \varepsilon b \gamma_{k,3-k}\right) + \log\left(\frac{x_k^{(0)}}{r_{13}}\right) \right] \right. \end{aligned}$$

$$\begin{aligned}
& + \eta(-x_k, r_{02}) \left[\log\left(\frac{1}{r_{02}x_k^{(0)}} P(0, 0, 1, r_{02}x_k^{(0)}) - r_{02}x_k^{(0)} \varepsilon b \gamma_{k,3-k}\right) + \log(r_{02}x_k^{(0)}) \right] \\
& - \left[\eta\left(-x_k, \frac{r_{02}}{r_{13}}\right) + \eta\left(r_{02}, \frac{1}{r_{13}}\right) \right] \left[\log\left(\frac{r_{13}}{r_{02}x_k^{(0)}} P(0, 1, \frac{r_{02}x_k^{(0)}}{r_{13}}, 0) - \frac{r_{02}x_k^{(0)}}{r_{13}} \varepsilon b \gamma_{k,3-k}\right) \right. \\
& \left. + \log\left(\frac{r_{02}x_k^{(0)}}{r_{13}}\right) \right] + \left(1 - \gamma_{k,3-k} \text{sgn}(b)\right) \eta\left(-x_k, -\frac{r_{02}}{r_{13}}\right) \eta\left(r_{02}, \frac{1}{r_{13}}\right) \left. \right\}.
\end{aligned}$$

ε is understood as infinitesimally small.

4.4 Reduction of scalar and tensor integrals for vanishing Gram determinant

Using the four-dimensionality of space-time the scalar five-point function can be reduced to five scalar four-point functions [29, 31]. Furthermore if the Gram determinant of the external momenta of a tensor integral T^N vanishes,

$$|X_{N-1}| = \begin{vmatrix} p_1^2 & p_1 p_2 & \cdots & p_1 p_{N-1} \\ p_2 p_1 & p_2^2 & \cdots & p_2 p_{N-1} \\ \vdots & \vdots & \ddots & \vdots \\ p_{N-1} p_1 & p_{N-1} p_2 & \cdots & p_{N-1}^2 \end{vmatrix} = 0, \quad (4.44)$$

this tensor integral can be expressed in terms of N integrals T^{N-1} . This is always the case for $N \geq 6$, because any five momenta are linear dependent in four dimensions.

4.4.1 Reduction of scalar five-point functions

Here we assume that the four external momenta appearing in the five-point function span the whole four-dimensional space². Then the integration momentum q depends linearly on these four external momenta and the following equations holds

$$0 = \begin{vmatrix} 2q^2 & 2qp_1 & \cdots & 2qp_4 \\ 2p_1q & 2p_1^2 & \cdots & 2p_1p_4 \\ \vdots & \vdots & \ddots & \vdots \\ 2p_4q & 2p_4p_1 & \cdots & 2p_4^2 \end{vmatrix} = \begin{vmatrix} 2D_0 + Y_{00} & 2qp_1 & \cdots & 2qp_4 \\ D_1 - D_0 + Y_{10} - Y_{00} & 2p_1^2 & \cdots & 2p_1p_4 \\ \vdots & \vdots & \ddots & \vdots \\ D_4 - D_0 + Y_{40} - Y_{00} & 2p_4p_1 & \cdots & 2p_4^2 \end{vmatrix} \quad (4.45)$$

with

$$Y_{ij} = m_i^2 + m_j^2 - (p_i - p_j)^2. \quad (4.46)$$

and D_i as defined in (4.2). Thus we have

$$\frac{1}{i\pi^2} \int d^Dq \frac{1}{D_0 D_1 \cdots D_4} \begin{vmatrix} 2D_0 + Y_{00} & 2qp_1 & \cdots & 2qp_4 \\ D_1 - D_0 + Y_{10} - Y_{00} & 2p_1^2 & \cdots & 2p_1p_4 \\ \vdots & \vdots & \ddots & \vdots \\ D_4 - D_0 + Y_{40} - Y_{00} & 2p_4p_1 & \cdots & 2p_4^2 \end{vmatrix} = 0. \quad (4.47)$$

²The exceptional case, when they are linear dependent will be covered in the next section.

Expanding the determinant along the first column we obtain

$$\begin{aligned}
0 = & \left[2T_0^4(0) + Y_{00}T_0^5 \right] \begin{vmatrix} 2p_1p_1 & \dots & 2p_1p_4 \\ \vdots & \ddots & \vdots \\ 2p_4p_1 & \dots & 2p_4p_4 \end{vmatrix} \\
& + \sum_{k=1}^4 (-1)^k \left[T_\mu^4(k) - T_\mu^4(0) - p_{4\mu}T_0^4(0) \right. \\
& \quad \left. + p_{4\mu}T_0^4(0) + (Y_{k0} - Y_{00})T_\mu^5 \right] \\
& \quad \times \begin{vmatrix} 2p_{1\mu} & \dots & 2p_{4\mu} \\ 2p_1p_1 & \dots & 2p_1p_4 \\ \vdots & \ddots & \vdots \\ 2p_{k-1}p_1 & \dots & 2p_{k-1}p_4 \\ 2p_{k+1}p_1 & \dots & 2p_{k+1}p_4 \\ \vdots & \ddots & \vdots \\ 2p_4p_1 & \dots & 2p_4^2 \end{vmatrix}
\end{aligned} \tag{4.48}$$

where the arguments of the functions T^4 denote again the cancelled propagators.

The Lorentz decomposition of the vector integrals in (4.48) involves only the momenta p_1, \dots, p_4 . $T_{\mu\mu_1\dots\mu_P}^4(k)$ does not depend on p_k , consequently each term in its Lorentz decomposition contains a factor $p_{i\mu}$, $i \neq k$ and its contraction with the corresponding determinant in (4.48) vanishes. Similarly all terms in the tensor integral decomposition of $T_\mu^4(0) + p_{4\mu}T_0^4(0)$ involve a factor $p_{i\mu} - p_{4\mu}$, $i = 1, 2, 3$, if one performs the shift $q \rightarrow q - p_4$ to bring the tensor integral to the standard form. Multiplying with the determinants and performing the sum in (4.48) these terms drop out. Finally in the term $p_{4\mu}T_0^4(0)$ the determinant is nonzero only for $k = 4$ where it can be combined with the first term in (4.48). Rewriting the resulting equation as a determinant and reinserting the explicit form of the tensor integrals we find

$$\frac{1}{i\pi^2} \int d^Dq \frac{1}{D_0 D_1 \dots D_4} \begin{vmatrix} D_0 + Y_{00} & 2qp_1 & \dots & 2qp_4 \\ Y_{10} - Y_{00} & 2p_1^2 & \dots & 2p_1p_4 \\ \vdots & \vdots & \ddots & \vdots \\ Y_{40} - Y_{00} & 2p_4p_1 & \dots & 2p_4^2 \end{vmatrix} = 0. \tag{4.49}$$

Using

$$\begin{aligned}
2p_i p_j &= Y_{ij} - Y_{i0} - Y_{0j} + Y_{00}, \\
2qp_j &= D_j - D_0 + Y_{0j} - Y_{00},
\end{aligned} \tag{4.50}$$

adding the first column to each of the other columns and then enlarging the determinant by one column and one row this can be written as

$$\begin{vmatrix} 1 & Y_{00} & \dots & Y_{04} \\ 0 & T_0^4(0) + Y_{00}T_0^5 & \dots & T_0^4(4) + Y_{40}T_0^5 \\ 0 & Y_{10} - Y_{00} & \dots & Y_{14} - Y_{04} \\ \vdots & \vdots & \ddots & \vdots \\ 0 & Y_{40} - Y_{00} & \dots & Y_{44} - Y_{04} \end{vmatrix} = 0 \quad (4.51)$$

This is equivalent to

$$\begin{vmatrix} T_0^5 & -T_0^4(0) & -T_0^4(1) & -T_0^4(2) & -T_0^4(3) & -T_0^4(4) \\ 1 & Y_{00} & Y_{01} & Y_{02} & Y_{03} & Y_{04} \\ 1 & Y_{10} & Y_{11} & Y_{12} & Y_{13} & Y_{14} \\ 1 & Y_{20} & Y_{21} & Y_{22} & Y_{23} & Y_{24} \\ 1 & Y_{30} & Y_{31} & Y_{32} & Y_{33} & Y_{34} \\ 1 & Y_{40} & Y_{41} & Y_{42} & Y_{43} & Y_{44} \end{vmatrix} = 0, \quad (4.52)$$

which can be solved for T_0^5 if the determinant of the matrix Y_{ij} , $i, j = 0, \dots, 4$ is nonzero. Note that in the integral $T_0^4(0)$ the momenta have not been shifted. In particular (4.52) yields the scalar five-point function T_0^5 in terms of five scalar four-point functions.

4.4.2 Reduction of N-point functions for zero Gram determinant

For vanishing Gram determinant $|X_{N-1}|$ the following relation holds, if the Lorentz decomposition of the appearing tensor integrals contains only momenta and no metric tensors, which is the case for $N \geq 6$ or $P = 0$ (scalar integrals)

$$\frac{(2\pi\mu)^{4-D}}{i\pi^2} \int d^Dq \frac{q_{\mu_1} \dots q_{\mu_P}}{D_0 D_1 \dots D_{N-1}} \begin{vmatrix} D_0 + Y_{00} & 2qp_1 & \dots & 2qp_{N-1} \\ Y_{10} - Y_{00} & 2p_1^2 & \dots & 2p_1 p_{N-1} \\ \vdots & \vdots & \ddots & \vdots \\ Y_{N-10} - Y_{00} & 2p_{N-1} p_1 & \dots & 2p_{N-1}^2 \end{vmatrix} = 0. \quad (4.53)$$

Performing the same manipulations of the determinant as in (4.49) to (4.52) above this results in

$$\begin{vmatrix} T_{\mu_1 \dots \mu_P}^N & -T_{\mu_1 \dots \mu_P}^{N-1}(0) & -T_{\mu_1 \dots \mu_P}^{N-1}(1) & \dots & -T_{\mu_1 \dots \mu_P}^{N-1}(N-1) \\ 1 & Y_{00} & Y_{01} & \dots & Y_{0N-1} \\ 1 & Y_{10} & Y_{11} & \dots & Y_{1N-1} \\ \vdots & \vdots & \vdots & \ddots & \vdots \\ 1 & Y_{N-10} & Y_{N-11} & \dots & Y_{N-1N-1} \end{vmatrix} = 0, \quad (4.54)$$

valid for $|X_{N-1}| = 0$ and $N \geq 6$ or $P = 0$. We stress again that in the tensor integral $T_{\mu_1 \dots \mu_P}^N(0)$ appearing in (4.54) the momenta have not been shifted. Eq. (4.54) determines $T_{\mu_1 \dots \mu_P}^N$ in terms of $T_{\mu_1 \dots \mu_P}^{N-1}(i)$, $i = 0, \dots, N-1$, if the determinant of the matrix Y_{ij} is

nonzero. The vanishing of this determinant corresponds to the leading Landau singularity of T^N which is clearly not contained in T^{N-1} . In this case one has to calculate T^N directly [30].

Eq. (4.54) in particular expresses T_0^N by T_0^{N-1} . For $N = 5$ and $P = 0$ (4.54) coincides with (4.52), which is thus valid for arbitrary momenta. For $N > 6$ one can choose any six out of the N denominator factors resulting in different reductions. For $N \leq 4$, where (4.54) is only valid for scalar integrals, the Gram determinant is singular at the edge of phase space where some of the momenta p_i become collinear, i.e. for forward or backward scattering or at the threshold of a certain process. Because in this special situations all integrals can be reduced to lower ones one can obtain considerably simpler formulae than in the general case (see e.g. [33]).

With the methods described in this section all tensor integrals with $N \geq 6$ can be reduced directly to tensor integrals with smaller N . Note that this may yield tensor integrals with $P > N$ because P is not reduced simultaneously as in the reduction method described in Sect. 4.2. These tensor integrals are not directly present in renormalizable theories. Nevertheless their reduction to scalar integrals can be done with the formulae given in Sect. 4.2.

4.5 UV-divergent parts of tensor integrals

For practical calculations it is useful to know the UV-divergent parts of the tensor integrals explicitly. We give directly the products of $D - 4$ with all divergent one-loop tensor coefficient integrals appearing in renormalizable theories up to terms of the order $O(D - 4)$

$$\begin{aligned}
(D - 4) A_0(m) &= -2m^2, \\
(D - 4) B_0(p_{10}, m_0, m_1) &= -2, \\
(D - 4) B_1(p_{10}, m_0, m_1) &= 1, \\
(D - 4) B_{00}(p_{10}, m_0, m_1) &= \frac{1}{6}(p_{10}^2 - 3m_0^2 - 3m_1^2), \\
(D - 4) B_{11}(p_{10}, m_0, m_1) &= -\frac{2}{3}, \\
(D - 4) C_{00}(p_{10}, p_{20}, m_0, m_1, m_2) &= -\frac{1}{2}, \\
(D - 4) C_{00i}(p_{10}, p_{20}, m_0, m_1, m_2) &= \frac{1}{6}, \\
(D - 4) D_{0000}(p_{10}, p_{20}, p_{30}, m_0, m_1, m_2, m_3) &= -\frac{1}{12}.
\end{aligned} \tag{4.55}$$

All other scalar coefficients defined in (4.7) and (4.8) are UV-finite.

5 Standard matrix elements

5.1 Definition

The invariant matrix elements for scattering and decay processes involving external fermions and/or vector bosons depend on the polarizations σ_i , σ'_i and λ_i of these particles. This dependence is completely contained in the polarization vectors $\varepsilon_{\mu_i}(k_i, \lambda_i)$ and spinors $\bar{v}_{\alpha_i}(p'_i, \sigma'_i)$ and $u_{\alpha_i}(p_i, \sigma_i)$. k_i , p'_i and p_i denote the incoming momenta of the vector bosons, antifermions and fermions, respectively. For outgoing fermions one has to replace p , p' by $-p$, $-p'$ and one must use $u(-p) = v(p)$. If we split off the polarization vectors and spinors from the invariant matrix element \mathcal{M} we are left with a tensor involving Lorentz and Dirac indices in the general case

$$\mathcal{M} = \bar{v}_{\alpha_1}(p'_1, \sigma'_1) \dots \bar{v}_{\alpha_n}(p'_n, \sigma'_n) \mathcal{M}_{\alpha_1 \dots \alpha_n \beta_1 \dots \beta_n}^{\mu_1 \dots \mu_m} u_{\beta_1}(p_1, \sigma_1) \dots u_{\beta_n}(p_n, \sigma_n) \times \varepsilon_{\mu_1}(k_1, \lambda_1) \dots \varepsilon_{\mu_m}(k_m, \lambda_m). \quad (5.1)$$

To be definite we choose m external vector bosons and n external fermion-antifermion pairs. The tensor $\mathcal{M}_{\alpha_1 \dots \alpha_n \beta_1 \dots \beta_n}^{\mu_1 \dots \mu_m}$ can be decomposed into a set of covariant operators together with the corresponding scalar formfactors F_i

$$\mathcal{M}_{\alpha_1 \dots \alpha_n \beta_1 \dots \beta_n}^{\mu_1 \dots \mu_m} = \sum_i \mathcal{M}_{i, \alpha_1 \dots \alpha_n \beta_1 \dots \beta_n}^{\mu_1 \dots \mu_m} F_i. \quad (5.2)$$

We call the covariant operators $\mathcal{M}_{i, \alpha_1 \dots \alpha_n \beta_1 \dots \beta_n}^{\mu_1 \dots \mu_m}$ multiplied by the corresponding polarization vectors and spinors standard matrix elements \mathcal{M}_i

$$\mathcal{M}_i = \bar{v}_{\alpha_1}(p'_1, \sigma'_1) \dots \bar{v}_{\alpha_n}(p'_n, \sigma'_n) \mathcal{M}_{i, \alpha_1 \dots \alpha_n \beta_1 \dots \beta_n}^{\mu_1 \dots \mu_m} u_{\beta_1}(p_1, \sigma_1) \dots u_{\beta_n}(p_n, \sigma_n) \times \varepsilon_{\mu_1}(k_1, \lambda_1) \dots \varepsilon_{\mu_m}(k_m, \lambda_m). \quad (5.3)$$

In this way the invariant amplitude \mathcal{M} is decomposed into polarization independent formfactors F_i and the standard matrix elements \mathcal{M}_i

$$\mathcal{M} = \sum_i \mathcal{M}_i F_i. \quad (5.4)$$

The formfactors F_i are complicated model dependent functions involving in general the invariant integrals T^N and the counterterms. The standard matrix elements in contrast are simple model independent expressions which depend on the external particles only but contain the whole information on their polarization. They are purely kinematical objects. All of the dynamical information is contained in the formfactors.

The covariant tensor operators forming the standard matrix elements can be constructed from the external four-momenta p_i , p'_i and k_i , the Lorentz tensors $g^{\mu\nu}$ and $\varepsilon^{\mu\nu\rho\sigma}$ and the Dirac matrices γ^μ , γ_5 . In general one thus obtains an overcomplete set. Dirac algebra and momentum conservation are used to eliminate superfluous operators. Since the external particles are on-shell, the Dirac equation for the fermion spinors

$$\begin{aligned} \not{p}_i u(p_i, \sigma_i) &= m_i u(p_i, \sigma_i), \\ \bar{v}(p'_i, \sigma'_i) \not{p}'_i &= -m'_i \bar{v}(p'_i, \sigma'_i) \end{aligned} \quad (5.5)$$

and the transversality condition for the polarization vectors

$$k_i^{\mu_i} \varepsilon_{\mu_i}(k_i, \lambda_i) = 0 \quad (5.6)$$

reduce the number of independent standard matrix elements further.

The number of independent standard matrix elements cannot be larger than the number of independent polarization combinations of the external particles. In four dimensions there are only four linear independent four-vectors. Expressing all four-vectors in a definite basis allows to derive the missing relations between the remaining standard matrix elements. Thus a minimal set of standard matrix elements can be constructed.

If there are only few external particles there may be less independent standard matrix elements than different polarization combinations, since there are only few momenta available for their construction. In this case some of the polarized amplitudes are related.

The number of standard matrix elements can be reduced further if the model under consideration exhibits certain symmetries. These evidently also apply to the relevant standard matrix elements.

For many applications it is not essential to minimize the number of standard matrix elements. All one needs is a complete set.

Furthermore the choice of the standard matrix elements is not unique. This allows to arrange for the most convenient set according to simplicity, the structure of the lowest order amplitudes and, if present, symmetries. At least some of the formfactors can be chosen as generalizations of the lowest order couplings. This is useful in establishing improved Born approximations.

The concept of standard matrix elements is not indispensable for the calculation of amplitudes in higher orders. It is, however, extremely helpful in organizing lengthy calculations, which often are inevitable. All complicated expressions are cast into the formfactors which are polarization independent and thus have to be evaluated only once.

An alternative method would be to calculate directly the polarized amplitudes. This requires a definite representation for the spinors and/or polarization vectors from the start. The whole calculation has to be done for each polarization separately. A closer look shows that this method can be represented as a particular case of the standard matrix element approach. The corresponding covariant operators are constructed from the polarization vectors and spinors instead of the momenta, Lorentz tensors and Dirac matrices. Their explicit form is

$$\begin{aligned} \mathcal{M}_{i, \alpha_1 \dots \alpha_n \beta_1 \dots \beta_n}^{\mu_1 \dots \mu_m} &= (-1)^n \frac{v_{\alpha_1}(p'_1, \sigma'_1)}{2m'_1} \dots \frac{v_{\alpha_n}(p'_n, \sigma'_n)}{2m'_n} \frac{\bar{u}_{\beta_1}(p_1, \sigma_1)}{2m_1} \dots \frac{\bar{u}_{\beta_n}(p_n, \sigma_n)}{2m_n} \\ &\times \varepsilon_{\mu_1}^*(k_1, \lambda_1) \dots \varepsilon_{\mu_m}^*(k_m, \lambda_m), \end{aligned} \quad (5.7)$$

where m, m' are the masses of the external spinors. The indices i correspond to different polarization combinations. Consequently the number of different standard matrix elements equals the number of polarizations of the external particles. For each polarization only one standard matrix element is nonzero. In this sense the set of standard matrix elements (5.7) is orthogonal. The formfactors equal the polarization amplitudes and are directly obtained by inserting explicitly the polarization vectors and spinors in the invariant matrix element. Unlike in the approach outlined above these formfactors are no direct generalizations of the lowest order couplings.

In the following we list complete sets of standard matrix elements relevant for the production of bosons in fermion-antifermion annihilation.

5.2 Standard matrix elements for processes with two external fermions

In this section we will give the standard matrix elements for processes involving two external fermions ($F\bar{F}$) and one [or two] scalar (S) or vector (V) bosons. The momenta and spinors of the fermions are denoted by p_1, p_2 and $\bar{v}(p_1) = \bar{v}(p_1, \sigma_1), u(p_2) = u(p_2, \sigma_2)$, the momenta and polarization vectors of the bosons by $k_1, \varepsilon_1 = \varepsilon(k_1, \lambda_1)$ [and $k_2, \varepsilon_2 = \varepsilon(k_2, \lambda_2)$]. The numbers of different polarizations for each scalar, fermion and vector boson are 1, 2 and 3, respectively. If we use momentum conservation to eliminate k_1 [or $k_1 + k_2$] the standard matrix elements are constructed from the momenta p_2 and p_1 [and $k_1 - k_2$], the polarization vectors of the vector bosons, the totally antisymmetric tensor $\varepsilon^{\mu\nu\rho\sigma}$ and Dirac matrices between the spinors. If there are products of ε -tensors, pairs of them can be eliminated using

$$\varepsilon^{\mu\nu\rho\sigma}\varepsilon^{\alpha\beta\gamma\delta} = - \begin{vmatrix} g^{\mu\alpha} & g^{\mu\beta} & g^{\mu\gamma} & g^{\mu\delta} \\ g^{\nu\alpha} & g^{\nu\beta} & g^{\nu\gamma} & g^{\nu\delta} \\ g^{\rho\alpha} & g^{\rho\beta} & g^{\rho\gamma} & g^{\rho\delta} \\ g^{\sigma\alpha} & g^{\sigma\beta} & g^{\sigma\gamma} & g^{\sigma\delta} \end{vmatrix}. \quad (5.8)$$

If any of the left over ε -tensors are contracted with four four-momenta, we write for one of these momenta $p^\alpha = \frac{1}{2}\{\not{p}, \gamma^\alpha\}$ between the spinors. Now all remaining ε -tensors are contracted with one γ -matrix at least and can be eliminated using the Chisholm identity¹

$$\varepsilon_{\mu\nu\rho\sigma}\gamma^\sigma = -i[\gamma_\mu\gamma_\nu\gamma_\rho - g_{\mu\nu}\gamma_\rho + g_{\mu\rho}\gamma_\nu - g_{\nu\rho}\gamma_\mu]\gamma_5. \quad (5.9)$$

All Dirac matrices contracted with p_1 or p_2 can be eliminated using Dirac algebra and the Dirac equation. Consequently the only remaining Dirac matrices are contracted with polarization vectors [and $k_1 - k_2$] and there is at most one of each type. Finally in the scalar products involving the polarization vectors only one [or two] independent momenta may appear because of transversality and momentum conservation.

Thus we arrive at the following sets of standard matrix elements (we suppress polarization indices in the following):

5.2.1 $S \rightarrow F\bar{F}$

There are $2 \times 2 = 4$ different polarization combinations but only two standard matrix elements

$$\mathcal{M}^\sigma = \bar{u}(p_1) \omega_\sigma v(p_2), \quad (5.10)$$

where $\sigma = \pm$ and $\omega_\pm = \frac{1 \pm \gamma_5}{2}$ and the fermions are outgoing.

5.2.2 $V \rightarrow F\bar{F}$

Replacing the scalar by a vector results in $3 \times 2 \times 2 = 12$ different polarizations and yet only four standard matrix elements

$$\begin{aligned} \mathcal{M}_1^\sigma &= \bar{u}(p_1) \not{\varepsilon}_1 \omega_\sigma v(p_2), \\ \mathcal{M}_2^\sigma &= \bar{u}(p_1) \omega_\sigma v(p_2) \varepsilon_1 p_1. \end{aligned} \quad (5.11)$$

¹Eq. (5.8) and (5.9) can be applied because the standard matrix elements involve only external vectors and spinors which remain four-dimensional also in dimensional regularization.

5.2.3 $F\bar{F} \rightarrow SS$

Here the number of independent polarizations four equals the number of standard matrix elements

$$\begin{aligned}\mathcal{M}_1^\sigma &= \bar{v}(p_1) \frac{1}{2}(\not{k}_1 - \not{k}_2) \omega_\sigma u(p_2), \\ \mathcal{M}_2^\sigma &= \bar{v}(p_1) \omega_\sigma u(p_2).\end{aligned}\tag{5.12}$$

5.2.4 $F\bar{F} \rightarrow SV$

In this case we find twelve standard matrix elements for $2 \times 2 \times 3 = 12$ different polarizations

$$\begin{aligned}\mathcal{M}_1^\sigma &= \bar{v}(p_1) \not{\epsilon}_2 \omega_\sigma u(p_2), \\ \mathcal{M}_2^\sigma &= \bar{v}(p_1) \frac{1}{2}(\not{k}_1 - \not{k}_2) \omega_\sigma u(p_2) \varepsilon_2 p_1, \\ \mathcal{M}_3^\sigma &= \bar{v}(p_1) \frac{1}{2}(\not{k}_1 - \not{k}_2) \omega_\sigma u(p_2) \varepsilon_2 p_2, \\ \mathcal{M}_4^\sigma &= \bar{v}(p_1) \not{\epsilon}_2 \not{k}_2 \omega_\sigma u(p_2), \\ \mathcal{M}_5^\sigma &= \bar{v}(p_1) \omega_\sigma u(p_2) \varepsilon_2 p_1, \\ \mathcal{M}_6^\sigma &= \bar{v}(p_1) \omega_\sigma u(p_2) \varepsilon_2 p_2.\end{aligned}\tag{5.13}$$

5.2.5 $F\bar{F} \rightarrow VV$

There are $2 \times 2 \times 3 \times 3 = 36$ different polarization combinations, however, we can construct 40 standard matrix elements

$$\begin{aligned}\mathcal{M}_1^\sigma &= \bar{v}(p_1) \not{\epsilon}_1 (\not{k}_1 - \not{p}_1) \not{\epsilon}_2 \omega_\sigma u(p_2), \\ \mathcal{M}_2^\sigma &= \bar{v}(p_1) \frac{1}{2}(\not{k}_1 - \not{k}_2) (\varepsilon_1 \varepsilon_2) \omega_\sigma u(p_2), \\ \mathcal{M}_{3,1}^\sigma &= \bar{v}(p_1) \not{\epsilon}_1 \omega_\sigma u(p_2) (\varepsilon_2 k_1), \\ \mathcal{M}_{3,2}^\sigma &= -\bar{v}(p_1) \not{\epsilon}_2 \omega_\sigma u(p_2) (\varepsilon_1 k_2), \\ \mathcal{M}_{4,1}^\sigma &= \bar{v}(p_1) \not{\epsilon}_1 \omega_\sigma u(p_2) (\varepsilon_2 p_2), \\ \mathcal{M}_{4,2}^\sigma &= -\bar{v}(p_1) \not{\epsilon}_2 \omega_\sigma u(p_2) (\varepsilon_1 p_1), \\ \mathcal{M}_5^\sigma &= \bar{v}(p_1) \frac{1}{2}(\not{k}_1 - \not{k}_2) \omega_\sigma u(p_2) (\varepsilon_1 k_2) (\varepsilon_2 k_1), \\ \mathcal{M}_6^\sigma &= \bar{v}(p_1) \frac{1}{2}(\not{k}_1 - \not{k}_2) \omega_\sigma u(p_2) (\varepsilon_1 p_1) (\varepsilon_2 p_2), \\ \mathcal{M}_{7,1}^\sigma &= \bar{v}(p_1) \frac{1}{2}(\not{k}_1 - \not{k}_2) \omega_\sigma u(p_2) (\varepsilon_1 k_2) (\varepsilon_2 p_2), \\ \mathcal{M}_{7,2}^\sigma &= \bar{v}(p_1) \frac{1}{2}(\not{k}_1 - \not{k}_2) \omega_\sigma u(p_2) (\varepsilon_1 p_1) (\varepsilon_2 k_1), \\ \mathcal{M}_{11}^\sigma &= \bar{v}(p_1) \not{\epsilon}_1 \not{\epsilon}_2 \omega_\sigma u(p_2), \\ \mathcal{M}_{12}^\sigma &= \bar{v}(p_1) \omega_\sigma u(p_2) (\varepsilon_1 \varepsilon_2), \\ \mathcal{M}_{13,1}^\sigma &= \bar{v}(p_1) \not{\epsilon}_1 \not{k}_1 \omega_\sigma u(p_2) (\varepsilon_2 k_1), \\ \mathcal{M}_{13,2}^\sigma &= \bar{v}(p_1) \not{k}_2 \not{\epsilon}_2 \omega_\sigma u(p_2) (\varepsilon_1 k_2), \\ \mathcal{M}_{14,1}^\sigma &= \bar{v}(p_1) \not{\epsilon}_1 \not{k}_1 \omega_\sigma u(p_2) (\varepsilon_2 p_2),\end{aligned}\tag{5.14}$$

$$\begin{aligned}
\mathcal{M}_{14,2}^\sigma &= \bar{v}(p_1) \not{k}_2 \not{\epsilon}_2 \omega_\sigma u(p_2) (\varepsilon_1 p_1), \\
\mathcal{M}_{15}^\sigma &= \bar{v}(p_1) \omega_\sigma u(p_2) (\varepsilon_1 k_2) (\varepsilon_2 k_1), \\
\mathcal{M}_{16}^\sigma &= \bar{v}(p_1) \omega_\sigma u(p_2) (\varepsilon_1 p_1) (\varepsilon_2 p_2), \\
\mathcal{M}_{17,1}^\sigma &= \bar{v}(p_1) \omega_\sigma u(p_2) (\varepsilon_1 k_2) (\varepsilon_2 p_2), \\
\mathcal{M}_{17,2}^\sigma &= \bar{v}(p_1) \omega_\sigma u(p_2) (\varepsilon_1 p_1) (\varepsilon_2 k_1).
\end{aligned}$$

We have obtained more than 36 standard matrix elements because we have not yet used the four dimensionality of space time, i.e. the fact that the five vectors p_1 , p_2 , $k_1 - k_2$, ε_1 and ε_2 are linear dependent. The relations between the 40 standard matrix elements can be found by representing these vectors in a certain basis using for example $v_1 = p_1 + p_2$, $v_2 = p_1 - p_2$, $v_3 = k_1 - k_2$, $v_{4,\mu} = \varepsilon_{\mu\nu\rho\sigma} v_1^\nu v_2^\rho v_3^\sigma$. In this way one can derive the relation

$$\begin{aligned}
0 &= 2(p_1 p_2 - m_1 m_2) (\mathcal{M}_1^\sigma + \mathcal{M}_2^\sigma) \\
&\quad - 2(p_2 k_2 - m_2^2 - m_1 m_2) \mathcal{M}_{3,1}^\sigma - 2(p_1 k_1 - m_1^2 - m_1 m_2) \mathcal{M}_{3,2}^\sigma \\
&\quad - 2(k_1^2 + (k_1 k_2)) \mathcal{M}_{4,1}^\sigma - 2(k_2^2 + (k_1 k_2)) \mathcal{M}_{4,2}^\sigma - 2\mathcal{M}_5^\sigma + 2(\mathcal{M}_{7,1}^\sigma + \mathcal{M}_{7,2}^\sigma) \\
&\quad - 2(m_1(m_2^2 - p_2 k_2) + m_2(m_1^2 - p_1 k_1)) (\mathcal{M}_{11}^\sigma - \mathcal{M}_{12}^\sigma) \\
&\quad + (m_1 + m_2)(p_1 p_2 - m_1 m_2) \mathcal{M}_{12}^\sigma - 2m_2 \mathcal{M}_{13,1}^\sigma - 2m_1 \mathcal{M}_{13,2}^\sigma \\
&\quad + (m_1 + m_2) (2\mathcal{M}_{14,1}^\sigma + 2\mathcal{M}_{14,2}^\sigma - \mathcal{M}_{15}^\sigma - 4\mathcal{M}_{16}^\sigma) \\
&\quad + (3m_1 + m_2) \mathcal{M}_{17,1}^\sigma + (3m_2 + m_1) \mathcal{M}_{17,2}^\sigma
\end{aligned} \tag{5.15}$$

and a similar independent one allowing to eliminate four of the 40 standard matrix elements (5.14).

The construction of complete sets of standard matrix elements described above is straightforward. The reduction of general structures to these standard matrix elements is therefore easy to implement into computer algebra programs. In practical applications some of the standard matrix elements may not contribute due to the presence of symmetries and/or the neglect of fermion masses. These aspects will be discussed together with the applications in the following chapters.

5.3 Calculation of standard matrix elements

For the calculation of the standard matrix elements one has to choose a certain representation for the polarization vectors and spinors. This has to be done only once for each process and not in the calculation of individual Feynman diagrams. If there are at least four external particles the polarization vectors can be constructed from their four-momenta respecting

$$\begin{aligned}
k_i \cdot \varepsilon_i(k_i, \lambda_i) &= 0, \\
\varepsilon_i(k_i, \lambda_i) \varepsilon_i(k_i, \lambda'_i) &= -\delta_{\lambda_i, \lambda'_i}.
\end{aligned} \tag{5.16}$$

We thus obtain for ε_2

$$\varepsilon_2^\mu(k_2, \parallel) = \frac{1}{\sqrt{[p_1 p_2 (2p_1 k_2 p_2 k_2 - k_2^2 p_1 p_2) + p_1^2 p_2^2 k_2^2 - p_2^2 (p_1 k_2)^2 - p_1^2 (p_2 k_2)^2]}}$$

$$\begin{aligned}
& \times \frac{1}{\sqrt{[(p_2 k_2 + p_1 k_2)^2 - k_2^2 (p_1 + p_2)^2]}} \\
& \times \left[p_2^\mu (p_1 (p_1 + p_2) k_2^2 - p_1 k_2 (p_2 k_2 + p_1 k_2)) \right. \\
& \quad - p_1^\mu (p_2 (p_1 + p_2) k_2^2 - p_2 k_2 (p_2 k_2 + p_1 k_2)) \\
& \quad \left. + k_2^\mu (p_1 p_2 (p_1 k_2 - p_2 k_2) + p_2^2 p_1 k_2 - p_1^2 p_2 k_2) \right] \\
& = (0, \cos \vartheta, 0, -\sin \vartheta) \tag{5.17}
\end{aligned}$$

$$\begin{aligned}
\varepsilon_2^\mu(k_2, \perp) &= \frac{1}{\sqrt{p_1 p_2 (2p_1 k_2 p_2 k_2 - k_2^2 p_1 p_2) + p_1^2 p_2^2 k_2^2 - p_2^2 (p_1 k_2)^2 - p_1^2 (p_2 k_2)^2}} \varepsilon_{\nu\rho\sigma}^\mu p_2^\nu p_1^\rho k_2^\sigma \\
&= (0, 0, 1, 0) \tag{5.18}
\end{aligned}$$

$$\begin{aligned}
\varepsilon_2^\mu(k_2, L) &= \frac{1}{\sqrt{k_2^2 [(p_2 k_2 + p_1 k_2)^2 - k_2^2 (p_2 + p_1)^2]}} \left[k_2^\mu (p_2 k_2 + p_1 k_2) - (p_1 + p_2)^\mu k_2^2 \right] \\
&= (k, E_2 \sin \vartheta, 0, E_2 \cos \vartheta) / \sqrt{k_2^2}. \tag{5.19}
\end{aligned}$$

where we have also given the simple expressions in the CMS-system of the fermions and bosons. In this system the four-momenta of the external particles read

$$\begin{aligned}
p_{1,2} &= (\tilde{E}_{1,2}, 0, 0, \mp |\mathbf{p}|), \\
k_{1,2} &= (E_{1,2}, \mp |\mathbf{k}| \sin \vartheta, 0, \mp |\mathbf{k}| \cos \vartheta). \tag{5.20}
\end{aligned}$$

$\tilde{E}_{1,2}$ are the energies and \mathbf{p} the three-momentum of the fermions and $E_{1,2}$ the energies and \mathbf{k} the three-momentum of the bosons. ϑ is the angle between the spatial vectors \mathbf{p} and \mathbf{k} ,

From the polarization vectors given above the ones for helicity states are obtained as

$$\varepsilon_2^\mu(k_2, \pm) = \frac{1}{\sqrt{2}} \left[\varepsilon_2^\mu(k_2, \parallel) \pm i \varepsilon_2^\mu(k_2, \perp) \right], \quad \varepsilon_2^\mu(k_2, 0) = \varepsilon_2^\mu(k_2, L). \tag{5.21}$$

The polarization vector ε_1 can be obtained by interchanging $1 \leftrightarrow 2$.

For the case of only three external particles one needs a further independent vector. It can be chosen freely but linear independent of the momenta. Using this additional vector as one of the polarization vectors the others can be constructed using (5.16).

Inserting the polarization vectors (5.19) into the standard matrix elements these can be reduced to the ones for external scalars, i.e. to (5.10) for the decay $V \rightarrow F\bar{F}$, and to (5.12) for the annihilation processes $F\bar{F} \rightarrow VV, VS$. To calculate these remaining Dirac matrix elements one either inserts a definite representation for the spinors or evaluates the

quantities $\mathcal{M}_i^{\sigma*} \mathcal{M}_j^{\sigma'}$ via traces and reconstructs \mathcal{M}_i^{σ} from those if needed. Note that for the calculation of $|\mathcal{M}|^2$ to one-loop order one only has to evaluate the products $\mathcal{M}_i^{\sigma*} \mathcal{M}_j^{\sigma'}$ for those values of i , where F_i^{σ} is nonzero in lowest order

$$\begin{aligned} |\mathcal{M}|^2 &= |\mathcal{M}_0 + \delta\mathcal{M}_1|^2 \approx |\mathcal{M}_0|^2 + 2\text{Re}\{\mathcal{M}_0^* \delta\mathcal{M}_1\} \\ &= \sum_{i,j} F_{i,0}^{\sigma*} (F_{j,0}^{\sigma} + 2\delta F_{j,1}^{\sigma}) \text{Re}\{\mathcal{M}_i^{\sigma*} \mathcal{M}_j^{\sigma}\}. \end{aligned} \quad (5.22)$$

Here \mathcal{M}_0 , $F_{i,0}^{\sigma}$ denote the lowest order quantities and $\delta\mathcal{M}_1$, $\delta F_{i,1}^{\sigma}$ the one-loop quantities.

For massless external fermions the Dirac matrix elements (5.10) and (5.12) are equivalent to the helicity matrix elements. They do not interfere and can thus easily be obtained from $|\mathcal{M}_i^{\sigma}|^2$ as

$$\begin{aligned} \bar{v}(p_1) \omega_{\sigma} u(p_2) &= \sqrt{2p_1 p_2}, \\ \bar{v}(p_1) (\not{k}_1 - \not{k}_2) \omega_{\sigma} u(p_2) &= \sqrt{4p_1(k_1 - k_2) p_2(k_1 - k_2) - 2p_1 p_2 (k_1 - k_2)^2}. \end{aligned} \quad (5.23)$$

If one is only interested in unpolarized quantities it suffices to calculate $\sum_{pol} \mathcal{M}_i^{\sigma*} \mathcal{M}_j^{\sigma}$ using the polarization sums for vector bosons and spinors.

6 Calculation of one-loop amplitudes

We have described all the ingredients necessary for the calculation of one-loop radiative corrections. This chapter shows how one-loop amplitudes are evaluated in practice.

First one has to specify a Lagrangian and to derive the corresponding Feynman rules. Then renormalization has to be carried out and the counterterms have to be determined. Both were done in Chap. 2 and 3 for the SM. Once the Feynman rules and the counterterms are fixed, the following steps apply to any renormalizable model.

To calculate the amplitude of a certain process at the one-loop level one has to construct all tree and one-loop Feynman diagrams with the given external particles allowed by the specified model. Next each Feynman diagram has to be reduced algebraically to a form suitable for numerical evaluation. This procedure is explained in more detail in Sect. 6.1. Finally the expressions for all diagrams have to be put together into a numerical program which calculates the amplitude and the corresponding cross section or decay rate.

6.1 Algebraic reduction of Feynman diagrams

The algorithm for the reduction of one-loop diagrams is the following. The loop integral obtained from the Feynman rules contains a product of propagators as denominator and a numerator composed of Lorentz vectors and tensors, Dirac matrices and spinors and polarization vectors of the external particles. The numerator is simplified using tensor and Dirac algebra, the mass shell conditions for the external particles and momentum conservation. One can also try to separate terms proportional to one or more of the denominators. Cancelling these yields N-point functions of lower degree. Next the loop integral is organized into the tensor integrals defined in Sect. 4.1. The Lorentz decomposition of these integrals is inserted and the whole Dirac and Lorentz structure is separated off from the integrals. Using again Dirac algebra and mass shell conditions it can be reduced to the appropriate standard matrix elements as discussed in Chap. 5.

We thus arrive at an expression of the form

$$\delta\mathcal{M} = \sum_i \mathcal{M}_i \delta F_i \quad (6.1)$$

for each one-loop Feynman diagram. The formfactors are linear combinations of the invariant coefficient functions of the tensor integrals with coefficients being functions of the kinematical invariants.

The formfactors can be further evaluated by applying the reduction scheme for the invariant integrals described in Sects. 4.2 and 4.4. Finally they are obtained as linear combinations of the scalar one-loop integrals A_0 , B_0 , C_0 and D_0 which are given explicitly in Sect. 4.3. This last step may lead to very lengthy expressions. Their algebraic evaluation needs a lot of time and space. This can be avoided by performing the reduction to scalar integrals numerically.

The evaluation of the counterterm diagrams and the Born diagrams is done in a similar way. Since no integrations have to be performed their calculation is much easier. In most cases the counterterm diagrams can be obtained from the Born diagrams by replacing the lowest order couplings by the corresponding counterterm.

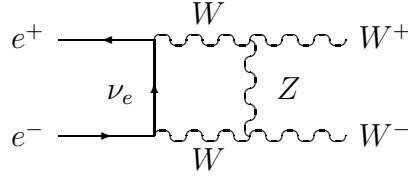


Figure 6.1: Box diagram contributing to $e^+e^- \rightarrow W^+W^-$.

As an illustration of the reduction method we present the explicit calculation of a box diagram contributing to $e^+e^- \rightarrow W^+W^-$ (Fig. 6.1). According to the Feynman rules the corresponding contribution to the invariant matrix element $\delta\mathcal{M}$ is given by (we include a global factor i in the Feynman rules in order to obtain real amplitudes)

$$\delta\mathcal{M} = -i \frac{e^4 c_W^2}{2s_W^4} \mu^{4-D} \int \frac{d^D q}{(2\pi)^D} \frac{\bar{v}(p_1) \gamma^\mu (\not{q} + \not{k}_1 - \not{p}_1) \gamma^\nu \omega_- u(p_2) \Gamma_{\lambda\mu\rho} \Gamma_{\sigma\nu}^\lambda \varepsilon_1^\rho \varepsilon_2^\sigma}{[q^2 - M_Z^2] [(q + k_1)^2 - M_W^2] (q + k_1 - p_1)^2 [(q - k_2)^2 - M_W^2]}, \quad (6.2)$$

with

$$\begin{aligned} \Gamma_{\lambda\mu\rho} &= g_{\lambda\mu}(2q + k_1)_\rho + g_{\mu\rho}(-q - 2k_1)_\lambda + g_{\rho\lambda}(k_1 - q)_\mu, \\ \Gamma_{\lambda\sigma\nu} &= g_{\lambda\sigma}(-k_2 - q)_\nu + g_{\sigma\nu}(2k_2 - q)_\lambda + g_{\nu\lambda}(2q - k_2)_\sigma. \end{aligned} \quad (6.3)$$

Evaluating the numerator and introducing the tensor integrals D and C we arrive at

$$\begin{aligned} \delta\mathcal{M} &= \frac{\alpha^2 c_W^2}{2s_W^4} \bar{v}(p_1) \left\{ -8\gamma^\mu \varepsilon_1^\nu \varepsilon_2^\rho D_{\mu\nu\rho} \right. \\ &+ D_{\mu\nu} \left[\not{\varepsilon}_1 \gamma^\mu \not{\varepsilon}_2 2(k_1 - k_2)^\nu \right. \\ &+ \not{\varepsilon}_1 \left(-2\varepsilon_2^\mu k_2^\nu - 8p_1^\mu \varepsilon_2^\nu + 2p_2^\mu \varepsilon_2^\nu \right) + \not{\varepsilon}_1 \gamma^\mu \not{k}_2 8\varepsilon_2^\nu \\ &- \not{\varepsilon}_2 \left(-2\varepsilon_1^\mu k_1^\nu - 8p_2^\mu \varepsilon_1^\nu + 2p_1^\mu \varepsilon_1^\nu \right) - \not{k}_1 \gamma^\mu \not{\varepsilon}_2 8\varepsilon_1^\nu \\ &\left. \left. + \not{k}_1 8\varepsilon_1^\mu \varepsilon_2^\nu + \gamma^\mu \left(-16\varepsilon_1^\nu p_2 \varepsilon_2 + 16\varepsilon_2^\nu p_1 \varepsilon_1 + 2(k_1 - p_1)^\nu \varepsilon_1 \varepsilon_2 \right) \right] \right\} \\ &+ D_\mu \left[\not{\varepsilon}_1 (\not{k}_1 - \not{p}_1) \not{\varepsilon}_2 2(k_1 - k_2)^\mu + \not{\varepsilon}_1 \gamma^\mu \not{\varepsilon}_2 (M_Z^2 - 4k_1 k_2) \right. \\ &+ \not{\varepsilon}_1 \left(-\varepsilon_2^\mu (3M_Z^2 + 3M_W^2 + 2p_1 k_1) - 4k_2^\mu \varepsilon_2 k_1 + 4p_2^\mu \varepsilon_2 k_1 \right) \\ &- \not{\varepsilon}_2 \left(\varepsilon_1^\mu (3M_Z^2 + 3M_W^2 + 2p_2 k_2) + 4k_1^\mu \varepsilon_1 k_2 - 4p_1^\mu \varepsilon_1 k_2 \right) \\ &\left. + \not{k}_1 \left(2(k_1 - p_1)^\mu \varepsilon_1 \varepsilon_2 - 8\varepsilon_1^\mu \varepsilon_2 p_2 + 8\varepsilon_2^\mu \varepsilon_1 p_1 \right) \right] \quad (6.4) \end{aligned}$$

$$\begin{aligned}
& +\gamma^\mu \varepsilon_1 \varepsilon_2 (M_Z^2 - 3M_W^2 + 6p_1 k_1) + \not{k}_1 \gamma^\mu \not{\varepsilon}_2 4\varepsilon_1 k_2 + 4\not{\varepsilon}_1 \gamma^\mu \not{k}_2 4\varepsilon_2 k_1 \Big] \\
& +D_0 \Big[\not{\varepsilon}_1 (\not{k}_1 - \not{p}_1) \not{\varepsilon}_2 (M_Z^2 - 4k_1 k_2) + \not{k}_1 \varepsilon_1 \varepsilon_2 (M_W^2 - 2p_1 k_1 - 3M_Z^2) \\
& \quad + \not{\varepsilon}_1 \varepsilon_2 k_1 (4p_2 k_2 - 2M_W^2 + 2M_Z^2) - \not{\varepsilon}_2 \varepsilon_1 k_2 (4p_1 k_1 - 2M_W^2 + 2M_Z^2) \Big] \\
& +C_\mu \Big[\not{\varepsilon}_1 \gamma^\mu \not{\varepsilon}_2 - \not{\varepsilon}_2 3\varepsilon_1^\mu - \not{\varepsilon}_1 3\varepsilon_2^\mu + \gamma^\mu \varepsilon_1 \varepsilon_2 \Big] \\
& +C_0 \Big[\not{\varepsilon}_1 2\varepsilon_2 k_1 - \not{\varepsilon}_2 2\varepsilon_1 k_2 + \not{\varepsilon}_1 3\varepsilon_2 p_2 - \not{\varepsilon}_2 3\varepsilon_1 p_1 - \not{k}_1 4\varepsilon_1 \varepsilon_2 \Big] \omega_{-u}(p_2).
\end{aligned}$$

The three-point integrals arise from q^2 terms in the numerator by writing $q^2=(q^2 - M_Z^2)+M_Z^2$ and cancelling the first denominator factor. After that the shift $q \rightarrow q - k_1 + p_1$ was performed in the three-point integrals (this shift conserves the manifest CP symmetry of the diagram). The arguments of the C and D functions are as follows

$$\begin{aligned}
D &= D(k_1, k_1 - p_1, -k_2, M_Z, M_W, 0, M_W), \\
C &= C(p_1, -p_2, 0, M_W, M_W).
\end{aligned} \tag{6.5}$$

Inserting the tensor integral decomposition eqs. (4.7, 4.8) yields the final expression

$$\begin{aligned}
\delta\mathcal{M} &= \frac{\alpha^2 c_W^2}{2s_W^4} \left\{ \mathcal{M}_1^- \left[20 D_{00} + 2(4M_W^2 - s)D_{33} + 2(M_W^2 + t)D_{22} \right. \right. \\
& \quad + (12M_W^2 + 4t - 2s)D_{23} + 2(4M_W^2 - s)D_{13} + (16M_W^2 - 6s + 2M_Z^2)D_3 \\
& \quad \left. \left. + (2t - 2s + 6M_W^2 + M_Z^2)D_2 + (4M_W^2 - 2s + M_Z^2)D_0 \right] \right. \\
& \quad + \mathcal{M}_2^- \left[-4C_0 - 16 D_{003} - 8 D_{002} + 10 D_{00} + 2tD_{22} + 2(M_W^2 + t)(D_{33} + D_{13}) \right. \\
& \quad \left. + 2(M_W^2 + 3t)D_{23} + 2(M_W^2 - 2t + M_Z^2)D_3 + (M_Z^2 - t)D_2 + (t - 3M_Z^2)D_0 \right] \\
& \quad + \left[\mathcal{M}_{3,1}^- + \mathcal{M}_{3,2}^- \right] \left[-3C_2 + 2C_0 - 8D_{003} - 8D_{00} + (4s - 11M_W^2 + 5t)D_{13} \right. \\
& \quad \left. - 3(M_W^2 + t)D_{33} - 2(2M_W^2 + t)D_{23} + (t - 4M_W^2 - 3M_Z^2)D_3 + 2(M_Z^2 - t)D_0 \right]^{(6.6)} \\
& \quad + \left[\mathcal{M}_{4,1}^- + \mathcal{M}_{4,2}^- \right] \left[4C_2 + 3C_0 - 8D_{002} - 26D_{00} + 2(s - 4M_W^2)(D_{33} + D_{13}) \right. \\
& \quad \left. - 2(t + 2M_W^2)D_{22} + (4s - 2t - 18M_W^2)D_{23} \right. \\
& \quad \left. + (4s - 8M_W^2 - 2M_Z^2)D_3 + (t - 4M_W^2 - 3M_Z^2)D_2 \right] \\
& \quad + \mathcal{M}_5^- \left[16D_{113} + 8D_{123} - 8D_{13} \right] \\
& \quad \left. + \mathcal{M}_6^- \left[8D_{222} + 16D_{223} + 24D_{22} + 32D_{23} + 16D_2 \right] \right\}
\end{aligned}$$

$$+ [\mathcal{M}_{7,1}^- + \mathcal{M}_{7,2}^-] [8D_{332} + 8D_{223} + 8D_{123} + 8D_{23} + 16D_{13}] \},$$

where we introduced the standard matrix elements (5.14), the Mandelstam variables

$$s = (p_1 + p_2)^2, \quad t = (p_1 - k_1)^2, \quad (6.7)$$

and put

$$k_1^2 = k_2^2 = M_W^2, \quad p_1^2 = p_2^2 = 0. \quad (6.8)$$

Furthermore we made use of the relations which follow from the symmetry of the diagram under the exchange $e^+ \leftrightarrow e^-, W^+ \leftrightarrow W^-$ (CP invariance)

$$\begin{aligned} D_1 &= D_3, & D_{11} &= D_{33}, & D_{12} &= D_{23}, \\ D_{001} &= D_{003}, & D_{112} &= D_{332}, & D_{122} &= D_{223}, \\ D_{111} &= D_{333}, & D_{113} &= D_{133}, & C_1 &= C_2. \end{aligned} \quad (6.9)$$

These reduce the number of independent invariant integrals considerably. Note that not all of the 40 standard matrix elements of (5.14) appear in (6.6). This is due to the neglect of fermion masses and CP invariance of the box diagram.

This example shows that the reduction method is straightforward and universally applicable to one-loop Feynman diagrams, since they all have a similar structure.

6.2 Generic Feynman diagrams

The huge number of algebraic calculations makes the evaluation of each Feynman diagram very lengthy and tedious. Furthermore there are a large number of diagrams contributing to each process. Fortunately many of the diagrams resemble each other in their algebraic structure and can be considered as special cases of generic diagrams. These are the Feynman diagrams of a theory with only one generic scalar, fermion, vector boson and Faddeev-Popov ghost each and arbitrary renormalizable couplings between those fields (for more details see [34]). It suffices to do the algebraic calculations for these generic diagrams only. All actual diagrams are obtained from those by substituting the actual fields together with their coupling constants and masses. This saves a lot of work especially if there are many fields in the theory.

Clearly the generic diagrams can be calculated with the methods described above. The efficiency of generic diagrams is illustrated in the next section using the decay of the W -boson into massless fermions as example.

6.3 The decay $W \rightarrow f_i \bar{f}'_j$ for massless fermions

We will now apply the methods described above by calculating the one-loop amplitude for the decay of the W -boson into massless fermions

$$W^+(k) \rightarrow f_i(p_1) \bar{f}'_j(p_2). \quad (6.10)$$

In lowest order there is only one Feynman diagram (Fig.6.2) leading to the amplitude

$$\mathcal{M}_0 = -\frac{eV_{ij}}{\sqrt{2}s_W} \bar{u}(p_1) \not{\epsilon}(k) \omega_- v(p_2) = -\frac{eV_{ij}}{\sqrt{2}s_W} \mathcal{M}_1^-. \quad (6.11)$$

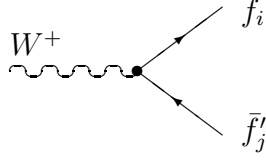


Figure 6.2: Born diagram to $W \rightarrow f_i \bar{f}'_j$.

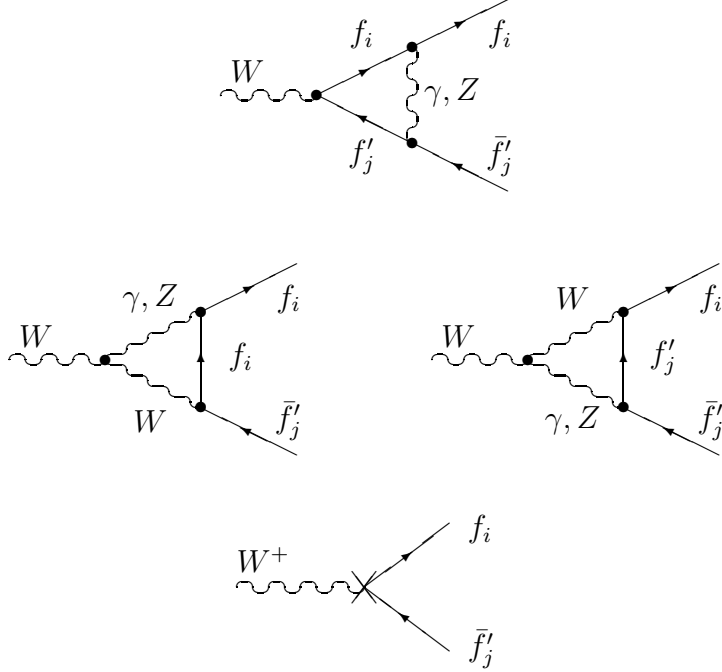


Figure 6.3: One-loop diagrams and corresponding counterterm diagram to $W \rightarrow f_i \bar{f}'_j$.

Neglecting the fermion masses the amplitude (6.11) leads to the following lowest order decay width

$$\Gamma_0 = \frac{\alpha M_W}{6 2s_W^2} |V_{ij}|^2. \quad (6.12)$$

At one-loop order there are six loop diagrams and one counterterm diagram (Fig. 6.3; the counterterm is indicated by a cross).

The first two loop diagrams correspond to one generic diagram and the other four to another generic one. We first calculate the two generic diagrams. The expression for the first reads

$$\delta\mathcal{M}_1 = i\mu^{4-D} \int \frac{d^D q}{(2\pi)^D} \frac{1}{(q^2 - M^2)(q + p_1)^2(q - p_2)^2} \bar{u}(p_1)\gamma^\nu(g_1^- \omega_- + g_1^+ \omega_+)(\not{q} + \not{p}_1)\not{\epsilon}(g_3^- \omega_- + g_3^+ \omega_+)(\not{q} - \not{p}_2)\gamma_\nu(g_2^- \omega_- + g_2^+ \omega_+)v(p_2), \quad (6.13)$$

where g^\pm denote the generic left- and right-handed fermion-fermion-vector couplings. Simplification and decomposition into tensor integrals yields

$$\begin{aligned}
\delta\mathcal{M}_1 &= i\mu^{4-D} \int \frac{d^D q}{(2\pi)^D} \frac{1}{(q^2 - M^2)(q + p_1)^2(q - p_2)^2} \\
&\quad \bar{u}(p_1)[-2(\not{q} - \not{p}_2)\not{\epsilon}(\not{q} + \not{p}_1) + (4 - D)(\not{q}\not{\epsilon})](g_1^- g_3^- g_2^- \omega_- + g_1^+ g_2^+ g_3^+ \omega_+)v(p_2) \\
&= -\frac{1}{16\pi^2} \bar{u}(p_1)[(2 - D)C_{\mu\nu}\gamma^\mu\not{\epsilon}\gamma^\nu + 2C_\mu(\not{p}_2\not{\epsilon}\gamma^\mu - \gamma^\mu\not{\epsilon}\not{p}_1) + 2C_0\not{p}_2\not{\epsilon}\not{p}_1] \\
&\quad (g_1^- g_2^- g_3^- \omega_- + g_1^+ g_2^+ g_3^+ \omega_+)v(p_2).
\end{aligned} \tag{6.14}$$

Insertion of the Lorentz decomposition and further simplification gives

$$\begin{aligned}
\delta\mathcal{M}_1 &= -\frac{1}{16\pi^2}(g_1^- g_3^- g_2^- \mathcal{M}_1^- + g_1^+ g_3^+ g_2^+ \mathcal{M}_1^+) \\
&\quad [(2 - D)^2 C_{00} - 2k^2(C_{12} + C_1 + C_2 + C_0)].
\end{aligned} \tag{6.15}$$

Finally the reduction of the invariant integrals and the use of (4.55) leads to

$$\begin{aligned}
\delta\mathcal{M}_1 &= -\frac{1}{16\pi^2}(g_1^- g_3^- g_2^- \mathcal{M}_1^- + g_1^+ g_3^+ g_2^+ \mathcal{M}_1^+) \\
&\quad [-2k^2 C_0(0, k^2, 0, M, 0, 0)(1 + \frac{M^2}{k^2})^2 \\
&\quad - B_0(k^2, 0, 0)(3 + 2\frac{M^2}{k^2}) + 2B_0(0, M, 0)(2 + \frac{M^2}{k^2}) - 2] \\
&= -\frac{1}{16\pi^2}(g_1^- g_3^- g_2^- \mathcal{M}_1^- + g_1^+ g_3^+ g_2^+ \mathcal{M}_1^+)\mathcal{V}_a(0, k^2, 0, M, 0, 0),
\end{aligned} \tag{6.16}$$

where we introduced the generic vertex function \mathcal{V}_a which is defined in the general case in App. C.

Similarly we obtain for the second generic diagram

$$\begin{aligned}
\delta\mathcal{M}_2 &= -i\mu^{4-D} \int \frac{d^D q}{(2\pi)^D} \frac{\bar{u}(p_1)\gamma^\nu(g_1^- \omega_- + g_1^+ \omega_+)(-\not{q})\gamma_\rho(g_2^- \omega_- + g_2^+ \omega_+)v(p_2)}{q^2[(q + p_1)^2 - M_1^2][(q - p_2)^2 - M_2^2]} \\
&\quad g_3 [g_{\rho\mu}(p_1 + 2p_2 - q)_\nu - g_{\mu\nu}(2p_1 + p_2 + q)_\rho + g_{\nu\rho}(2q + p_1 - p_2)_\mu]\varepsilon^\mu \\
&= \frac{1}{16\pi^2} g_3 (g_1^- g_2^- \mathcal{M}_1^- + g_1^+ g_2^+ \mathcal{M}_1^+) [4(D - 1)C_{00} - 2k^2(C_{12} + C_1 + C_2)] \\
&= \frac{1}{16\pi^2} g_3 (g_1^- g_2^- \mathcal{M}_1^- + g_1^+ g_2^+ \mathcal{M}_1^+) \\
&\quad [2(M_1^2 + M_2^2 + \frac{M_1^2 M_2^2}{k^2})C_0(0, k^2, 0, 0, M_1, M_2) - (1 + \frac{M_1^2 + M_2^2}{k^2})B_0(k^2, M_1, M_2) \\
&\quad + (2 + \frac{M_1^2}{k^2})B_0(0, 0, M_1) + (2 + \frac{M_2^2}{k^2})B_0(0, 0, M_2)] \\
&= \frac{1}{16\pi^2} g_3 (g_1^- g_2^- \mathcal{M}_1^- + g_1^+ g_2^+ \mathcal{M}_1^+)\mathcal{V}_b^-(0, k^2, 0, 0, M_1, M_2).
\end{aligned} \tag{6.17}$$

The general definition of \mathcal{V}_b^- can again be found in App. C.

Inserting the actual couplings and masses of the six actual diagrams into the generic diagrams and adding the counterterm diagram, which can be easily obtained from the

Feynman rules or the Born diagram, we find for the virtual one-loop corrections to the invariant amplitude for $W \rightarrow f_i \bar{f}'_j$

$$\begin{aligned}
\delta\mathcal{M} = & -\frac{e}{\sqrt{2}s_W} \frac{\alpha}{4\pi} V_{ij} \mathcal{M}_1^- \\
& \{ Q_f Q_{f'} \mathcal{V}_a(0, M_W^2, 0, \lambda, 0, 0) \\
& + g_f^- g_{f'}^- \mathcal{V}_a(0, M_W^2, 0, M_Z, 0, 0) \\
& + Q_f \mathcal{V}_b^-(0, M_W^2, 0, 0, \lambda, M_W) \\
& - Q_{f'} \mathcal{V}_b^-(0, M_W^2, 0, 0, M_W, \lambda) \\
& + \frac{c_W}{s_W} g_f^- \mathcal{V}_b^-(0, M_W^2, 0, 0, M_Z, M_W) \\
& - \frac{c_W}{s_W} g_{f'}^- \mathcal{V}_b^-(0, M_W^2, 0, 0, M_W, M_Z) \\
& + \frac{1}{2} \delta Z_{ii}^{f, L\dagger} + \frac{1}{2} \delta Z_{jj}^{f', L} + \frac{1}{2} \delta Z_W + \delta Z_e - \frac{\delta s_W}{s_W} \}.
\end{aligned} \tag{6.18}$$

The left- and right-handed couplings g_f^σ of the fermions to the Z -boson are defined in (A.14). Note that only one out of the four standard matrix elements (5.11) is contributing there and that we need no counterterm to the quark mixing matrix for massless fermions. The counterterms are expressed in terms of the self energies in Sect. 3.3. These have to be calculated to one-loop order to determine $\delta\mathcal{M}$ completely.

$\delta\mathcal{M}$ contains infrared divergencies. These are regularized with a photon mass λ . They drop out in the decay width if the contribution from the decay $W \rightarrow f_i \bar{f}'_j \gamma$ is added. This will be discussed in more detail in Chap. 7.

The example above was rather simple. If we keep the fermion masses finite or consider processes with more external particles the number and complexity of Feynman diagrams raises considerably.

6.4 Computer algebraic calculation of one-loop diagrams

The procedure of generation and algebraic reduction of Feynman diagrams as described above is algorithmic and can be implemented in symbolic computation systems. There are several attempts to create such systems for high energy physics calculations [35]. In addition there exist special packages written in general purpose languages [9, 10, 11, 12]. In particular the *MATHEMATICA* packages *FEYN ARTS* [11] and *FEYN CALC* [12] have been developed for the automatic calculation of one-loop diagrams following the approach outlined in this paper.

FEYN ARTS generates all graphs to a given process in a specified model together with their combinatorial factors (weights). It yields both analytical expressions and drawings of the graphs. There is a version under development which uses the concept of generic diagrams. It creates all relevant generic graphs together with a list of all possible substitutions yielding the actual graphs.

FEYN CALC performs the algebraic evaluation of Feynman diagrams. It starts from the output of *FEYN ARTS* and uses exactly the reduction algorithm described above. It can deal with generic diagrams. The *FEYN CALC* output can easily be translated into *FORTTRAN* code.

7 Soft photon bremsstrahlung

As mentioned in the last chapter the virtual one-loop corrections to the decay matrix element $W \rightarrow f_i \bar{f}'_j$ are infrared divergent. These divergencies originate from photonic corrections and show up in any process with charged external particles.

However, these processes are not of direct physical relevance since they cannot be distinguished experimentally from those involving additional soft external photons. Since the photons are massless their energies can be arbitrarily small and thus less than the resolution of any detector. Therefore in observable processes in addition to the basic process those with arbitrary numbers of soft photons are included.

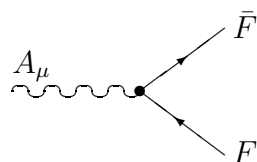
For these observable processes one obtains theoretically satisfactory results. Adding incoherently the cross sections of all the different processes with arbitrary numbers of photons, all infrared divergencies cancel [36]. This cancellation takes place between the virtual photonic corrections and the real bremsstrahlung corrections order by order in perturbation theory. To one-loop order one only needs to consider single photon radiation. For the cancellations only the soft photons, i.e. photons with energy $k_0 \leq \Delta E$, are relevant, where ΔE is a cutoff parameter, which should be small compared to all relevant energy scales. Photons with energies $k_0 > \Delta E$ are called hard. They can also yield sizable contributions especially arising from photon emission collinear to the external charged particles.

In Sect. 7.1 we introduce the soft photon approximation and show that in this approximation the bremsstrahlung diagrams are proportional to the Born diagrams. The corresponding soft photon cross section for arbitrary Born diagrams is given in Sect. 7.2.

7.1 Soft photon approximation

Attaching soft photons to a charged external particle line of an arbitrary Feynman diagram yields diagrams which become singular for vanishing momentum of the soft photon. This divergence arises from the propagator of the charged particle generated by the inclusion of the radiated photon line. In the soft photon approximation the momenta of the radiated photons are neglected everywhere but in this singular propagator. This approximation is valid if the matrix element of the basic process does not change much if a photon with energy ΔE is emitted, i.e. the basic matrix element is a slowly varying function of the photon energy for $k_0 < \Delta E$. This is not the case if the basic process contains a narrow resonance as e.g. in $e^+e^- \rightarrow \mu^+\mu^-$. Then one must either choose ΔE small compared to the width of the resonance or take into account the strong variation exactly [37, 38].

We now extract the soft photon matrix elements for external fermions, scalars and vector bosons. The general renormalizable couplings of these particles to the photon allowed by electromagnetic gauge invariance are (momenta are considered as incoming):



$$= -ieQ_F\gamma_\mu, \tag{7.1}$$

where

$$\omega_k = \sqrt{\mathbf{k}^2 + \lambda^2} \quad (7.15)$$

and \pm refers to the relative sign of the i -th and j -th term in (7.13). As in the virtual corrections the IR-singularities are regularized by the photon mass λ . Note that these integrals are not Lorentz-invariant due to the integration region. The basic integrals

$$I_{ij} = \int_{|\mathbf{k}| \leq \Delta E} \frac{d^3k}{2\omega_k} \frac{2p_i p_j}{p_i k p_j k} \quad (7.16)$$

have been worked out e.g. by 't Hooft and Veltman [28].

The result is

$$I_{ij} = 4\pi \frac{\alpha p_i p_j}{(\alpha p_i)^2 - p_j^2} \left\{ \frac{1}{2} \log \frac{(\alpha p_i)^2}{p_j^2} \log \frac{4\Delta E^2}{\lambda^2} \right. \quad (7.17)$$

$$\left. + \left[\frac{1}{4} \log^2 \frac{u_0 - |\mathbf{u}|}{u_0 + |\mathbf{u}|} + \text{Li}_2 \left(1 - \frac{u_0 + |\mathbf{u}|}{v} \right) + \text{Li}_2 \left(1 - \frac{u_0 - |\mathbf{u}|}{v} \right) \right]_{u=p_j}^{u=\alpha p_i} \right\},$$

with

$$v = \frac{(\alpha p_i)^2 - p_j^2}{2(\alpha p_{i0} - p_{j0})}, \quad (7.18)$$

and α defined through

$$\alpha^2 p_i^2 - 2\alpha p_i p_j + p_j^2 = 0, \quad \frac{\alpha p_{i0} - p_{j0}}{p_{j0}} > 0. \quad (7.19)$$

For $p_i = p_j$ this simplifies to

$$I_{ii} = 2\pi \left\{ \log \frac{4\Delta E^2}{\lambda^2} + \frac{p_0}{|\mathbf{p}|} \log \frac{p_0 - |\mathbf{p}|}{p_0 + |\mathbf{p}|} \right\}, \quad (7.20)$$

and for $\mathbf{p}_i = -\mathbf{p}_j = \mathbf{p}$

$$I_{ij} = 2\pi \frac{pq}{(p_0 + q_0)|\mathbf{p}|} \left\{ \frac{1}{2} \log \frac{p_0 + |\mathbf{p}|}{p_0 - |\mathbf{p}|} \log \frac{4\Delta E^2}{\lambda^2} - \text{Li}_2 \left(\frac{2|\mathbf{p}|}{p_0 + |\mathbf{p}|} \right) - \frac{1}{4} \log^2 \frac{p_0 + |\mathbf{p}|}{p_0 - |\mathbf{p}|} \right. \quad (7.21)$$

$$\left. + \frac{1}{2} \log \frac{q_0 + |\mathbf{p}|}{q_0 - |\mathbf{p}|} \log \frac{4\Delta E^2}{\lambda^2} - \text{Li}_2 \left(\frac{2|\mathbf{p}|}{q_0 + |\mathbf{p}|} \right) - \frac{1}{4} \log^2 \frac{q_0 + |\mathbf{p}|}{q_0 - |\mathbf{p}|} \right\}.$$

Inserting the results for I_{ij} into (7.14) yields the soft photon cross section. Adding it to the one-loop corrected cross section for the corresponding basic process the IR-divergencies cancel and the limit $\lambda \rightarrow 0$ can be taken.

Although the inclusion of the real soft photon emission is sufficient to obtain IR-finite results, it is often not adequate for real experiments, because realistic detectors do not provide a sufficiently small resolution $\Delta E/E$ necessary for the validity of the soft photon approximation. Therefore also hard photons (with $k_0 > \Delta E$) are important. Their contribution is UV- and IR-finite and can be treated separately. One merely has to make sure that the soft and hard part are properly adapted to each other.

Hard photon corrections are treated with methods different from the ones presented in this work. Their contribution depends sensitively on the experimental setup. They are usually incorporated by Monte Carlo simulations [15].

8 Input parameters and leading higher order contributions

In order to complete all ingredients necessary for the calculation of radiative corrections we have to specify the input parameters. This is done in Sect. 8.1. The leading higher order corrections which become important for precision experiments are discussed in Sect. 8.2.

8.1 Input parameters

In its original symmetric version the SM depends on the parameters (2.21), which are essentially the couplings allowed by the $SU(2)_W \times U(1)_Y$ symmetry. These were replaced by the physical parameters (2.22), i.e. the particle masses, the electromagnetic coupling constant, and the quark mixing matrix. In the on-shell renormalization scheme the renormalized parameters are equal to these physical parameters in all orders of perturbation theory.

The numerical values of the physical parameters must be fixed through experimental input. However, this input may not necessarily consist of direct measurements of the renormalized parameters; it may be obtained from any suitable set of experimental results. In practice one uses those experiments which have the highest experimental accuracy and theoretical reliability. This criterion is certainly fulfilled for the following set of parameters whose numerical values are taken from [39]:

- the fine structure constant

$$\alpha = 1/137.0359895(61)$$

corresponding to the classical electron charge $e = \sqrt{4\pi\alpha}$,

- the masses of the charged leptons

$$m_e = 0.51099906(15) \text{ MeV}, \quad m_\mu = 105.658387(34) \text{ MeV},$$
$$m_\tau = 1784.1_{-3.6}^{+2.7} \text{ MeV},$$

- the mass of the Z -boson [5]

$$M_Z = 91.177(21) \text{ GeV},$$

- and the Fermi constant

$$G_F = 1.16637(2)10^{-5} \text{ GeV}^{-2},$$

which is directly related to the muon lifetime.

We do not use the W -mass as input parameter because it is experimentally not known with comparable accuracy.

Besides the above listed well known parameters the still unknown masses of the top quark and the Higgs scalar are kept as free parameters. If the minimal SM is correct, the present experimental data restrict the top quark mass to the region $80 \text{ GeV} < m_t <$

200 GeV [5, 8]. For the Higgs mass we use $40 \text{ GeV} < M_H < 1 \text{ TeV}$, where the lower bound is experimental [5] and the upper bound is favored by theoretical consistency arguments. If not stated otherwise we will use the values $m_t = 140 \text{ GeV}$ and $M_H = 100 \text{ GeV}$.

The quark mixing matrix elements V_{ij} are directly taken from experiment. We use the parametrization of Harari and Leurer [40] as advocated by the Particle Data Group and choose the following numerical values for the parameters in agreement with [39]

$$s_{12} = 0.220, \quad s_{23} = 0.046, \quad s_{13} = 0.007 \quad (8.1)$$

and $\delta = 0$ for simplicity. This yields approximately the following numbers for the quark mixing matrix elements:

$$\begin{aligned} V_{ud} &= 0.975, & V_{us} &= 0.220, & V_{ub} &= 0.007, \\ V_{cd} &= -0.220, & V_{cs} &= 0.974, & V_{cb} &= 0.046, \\ V_{td} &= 0.003, & V_{ts} &= -0.046, & V_{tb} &= 0.999. \end{aligned} \quad (8.2)$$

It remains to discuss the masses m_q of the light quarks ($q = d, u, s, c, b$). In the electroweak Lagrangian the quarks are treated as free particles with appropriate masses. This is not correct due to the presence of the strong interaction. Therefore the quark masses can at best be considered as somewhat effective parameters. Fortunately in typical high energy experiments ($s \gg m_q^2$) theoretical predictions depend on the quark masses only through universal quantities such as the hadronic vacuum polarization or the quark structure functions. These can be directly determined from experiment. Nonuniversal contributions are suppressed as m_q^2/s and thus negligible for sufficiently high energies.

For processes without external quarks only the hadronic contribution to the vacuum polarization

$$\Pi^{AA}(s) = \frac{\Sigma_T^{AA}(s)}{s} \quad (8.3)$$

is relevant. In perturbation theory the contribution of light quarks is given by

$$\hat{\Pi}_{had}^{AA}(s) = 3 \frac{\alpha}{3\pi} \sum_{d,u,s,c,b} Q_q^2 \left(\frac{5}{3} - \log \frac{-s - i\varepsilon}{m_q^2} \right). \quad (8.4)$$

The large logarithmic terms contained in (8.4) constitute a dominant contribution to the radiative corrections. They originate from the charge renormalization in the on-shell scheme at zero momentum transfer (see eq. 3.32) involving

$$\Pi^{AA}(0) = \left. \frac{\partial \Sigma_T^{AA}(k^2)}{\partial k^2} \right|_{k^2=0}. \quad (8.5)$$

In this quantity nonperturbative strong interaction effects cannot be neglected. Since no reliable theoretical predictions are available one has to extract $\Pi_{had}^{AA}(0)$ from experimental data. Writing

$$\begin{aligned} \Pi_{had}^{AA}(0) &= \Pi_{had}^{AA}(0) - \text{Re} \Pi_{had}^{AA}(s) + \text{Re} \Pi_{had}^{AA}(s) \\ &= -\text{Re} \hat{\Pi}_{had}^{AA}(s) + \text{Re} \Pi_{had}^{AA}(s), \end{aligned} \quad (8.6)$$

the unrenormalized hadronic vacuum polarization $\Pi_{had}^{AA}(s)$ can be evaluated perturbatively for $s \gg m_q^2$ and the renormalized one $\text{Re } \hat{\Pi}_{had}^{AA}(s)$ is given by the dispersion relation

$$\text{Re } \hat{\Pi}_{had}^{AA}(s) = \frac{\alpha}{3\pi} s \text{Re} \int_{4m_\pi^2}^{\infty} ds' \frac{R^{AA}(s')}{s'(s' - s - i\varepsilon)} \quad (8.7)$$

with

$$R^{AA}(s') = \frac{\sigma(e^+e^- \rightarrow \gamma^* \rightarrow \text{hadrons})}{\sigma(e^+e^- \rightarrow \gamma^* \rightarrow \mu^+\mu^-)}. \quad (8.8)$$

$R^{AA}(s)$ can be taken from experiment up to some scale s , for larger s perturbative QCD is used. A recent analysis [41] involving data for the energy range below 40 GeV yields for the contribution of the 5 light quarks in the energy region $50 \text{ GeV} < s < 200 \text{ GeV}$

$$\text{Re } \hat{\Pi}_{had}^{AA(5)}(s) = -0.0288 \pm 0.0009 \quad (8.9)$$

$$-0.002980 \left[\log \left(\frac{s}{(92 \text{ GeV})^2} \right) + 0.006307 \left(\frac{s}{(92 \text{ GeV})^2} - 1 \right) \right].$$

For energies around the Z -boson mass this can be approximated by (8.4) using the effective quark masses

$$\begin{aligned} m_u &= 0.041 \text{ GeV}, & m_c &= 1.5 \text{ GeV}, \\ m_d &= 0.041 \text{ GeV}, & m_s &= 0.15 \text{ GeV}, & m_b &= 4.5 \text{ GeV}. \end{aligned} \quad (8.10)$$

These quark masses, in particular the ones for the three lightest quarks, are effective parameters adjusted to fit the dispersion integral and have no further significance.

In addition to the above parameters we need the strong coupling constant α_s for the QCD corrections. Its value at the scale of the Z -boson mass is given by [5]

$$\alpha_s = 0.115 \pm 0.010. \quad (8.11)$$

For the numerical evaluation we use in the following

$$\alpha_s = 0.12. \quad (8.12)$$

The W -mass is determined from the parameters given above through the relation

$$M_W^2 \left(1 - \frac{M_W^2}{M_Z^2} \right) = \frac{\pi\alpha}{\sqrt{2}G_F} [1 + \Delta r]. \quad (8.13)$$

Δr summarizes the radiative corrections to muon decay [26] apart from the QED corrections which coincide with those of the Fermi model. It depends on all parameters of the SM and is given by

$$\begin{aligned} \Delta r &= \Pi^{AA}(0) - \frac{c_W^2}{s_W^2} \left(\frac{\Sigma_T^{ZZ}(M_Z^2)}{M_Z^2} - \frac{\Sigma_T^W(M_W^2)}{M_W^2} \right) + \frac{\Sigma_T^W(0) - \Sigma_T^W(M_W^2)}{M_W^2} \\ &\quad + 2 \frac{c_W}{s_W} \frac{\Sigma_T^{AZ}(0)}{M_Z^2} + \frac{\alpha}{4\pi s_W^2} \left(6 + \frac{7 - 4s_W^2}{2s_W^2} \log c_W^2 \right). \end{aligned} \quad (8.14)$$

The relation (8.13) can be improved by summing the leading higher order reducible corrections. This is done in the next section (eq. 8.23). For the set of parameters specified above we obtain for the W -boson mass

$$M_W = 80.23 \text{ GeV}. \quad (8.15)$$

8.2 Leading higher order contributions

The natural order of magnitude of one-loop radiative corrections is set by the loop expansion parameter $\frac{\alpha}{\pi} \sim 0.0023$. Consequently typical one-loop corrections are of the order of one percent. There are, however, two important types of radiative corrections which are enhanced by large mass ratios. The first type is associated with light fermions the second with a heavy top quark. These corrections can reach several percent. Consequently the corresponding higher loop corrections may become as big as several permill and thus have to be taken into account in predictions for precision experiments.

8.2.1 Leading logarithms from light fermion masses

The first type of enhanced corrections originates from the renormalization of α at zero momentum transfer where the relevant scale is set by the fermion masses. These are much smaller than the relevant scales in high energy experiments. The large ratio of these different scales leads to large logarithms which can be summarized in the universal quantity

$$\Delta\alpha(s) = -\text{Re}\hat{\Pi}^{AA}(s) = \frac{\alpha}{3\pi} \sum_f N_C^f Q_f^2 \log \frac{|s|}{m_f^2} + \dots = (\Delta\alpha)_{LL} + \dots, \quad (8.16)$$

where N_C^f is the colour factor of the fermions and the dots indicate nonleading contributions. Renormalization group arguments can be used to show [42] that the leading logarithms $(\Delta\alpha)_{LL}$ are correctly summed to all orders in perturbation theory by the replacement

$$1 + (\Delta\alpha)_{LL} \rightarrow \frac{1}{1 - (\Delta\alpha)_{LL}}. \quad (8.17)$$

Since not only the leading logarithms but the whole fermionic contribution to $\Delta\alpha$ are gauge invariant we will sum the latter. The gauge dependent bosonic contribution can not be summed, however, because this would violate gauge invariance in higher orders. Thus we arrive at

$$1 + \Delta\alpha = 1 + (\Delta\alpha)_{ferm} + (\Delta\alpha)_{bos} \rightarrow \frac{1}{1 - (\Delta\alpha)_{ferm}} + (\Delta\alpha)_{bos}. \quad (8.18)$$

This corresponds to a resummation of the iterated one-loop fermionic vacuum polarization to all orders.

Since the leading logarithms contained in $\Delta\alpha$ originate from the charge renormalization constant δZ_e they are universal, i.e. they appear everywhere where α appears in lowest order. They can be taken into account by replacing the lowest order α by a running $\alpha(s)$ defined as

$$\alpha = \alpha(0) \rightarrow \alpha(s) = \frac{\alpha}{1 - (\Delta\alpha(s))_{ferm}}. \quad (8.19)$$

$\Delta\alpha(0) = 0$ due to the on-shell renormalization condition for α . Using $\alpha(s)$ instead of α effectively corresponds to renormalize α not at zero momentum transfer but at momentum transfer s . Then the light fermion masses can be neglected everywhere and no large logarithms appear.

There are similar large logarithms associated with external fermion lines. These are related to collinear singularities, arising from the radiation of photons collinear to external particles. They can be consistently treated with the structure function method [43].

8.2.2 Leading m_t^2 contributions

The second type of important corrections is also connected to the fermionic sector. The top quark gives rise to corrections $\propto m_t^2/M_W^2$, which become large if the top quark mass is large compared to the W -boson mass. For $m_t = 200$ GeV they reach several percent. These terms arise from fermion loop contributions to the boson self energies and from the Yukawa couplings of the physical and unphysical Higgs fields, which show up in vertex and fermionic self energy corrections. The latter are process dependent and are therefore not discussed here. The former, however, are universal, they can be traced back to the renormalization of s_W in the on-shell scheme

$$\begin{aligned} \frac{\delta s_W}{s_W} &= -\frac{1}{2} \frac{c_W^2}{s_W^2} \widetilde{\text{Re}} \left(\frac{\Sigma_T^W(M_W^2)}{M_W^2} - \frac{\Sigma_T^{ZZ}(M_Z^2)}{M_Z^2} \right) \\ &= \frac{1}{2} \frac{c_W^2}{s_W^2} \frac{\alpha}{4\pi} \frac{3}{4s_W^2} \frac{m_t^2}{M_W^2} + \dots = \frac{1}{2} \frac{c_W^2}{s_W^2} \Delta\rho + \dots \end{aligned} \quad (8.20)$$

where the dots indicate again nonleading contributions.

There is no general principle that determines the resummation of these corrections. The following recipe has been shown to yield the correct leading terms to $O(\alpha^2)$ [44]

$$\begin{aligned} s_W^2 &\rightarrow s_W^2 + c_W^2 \Delta\bar{\rho} = \bar{s}_W^2, \\ c_W^2 &\rightarrow c_W^2(1 - \Delta\bar{\rho}) = \bar{c}_W^2, \end{aligned} \quad (8.21)$$

where

$$\Delta\bar{\rho} = \frac{3G_F m_t^2}{8\sqrt{2}\pi^2} \left[1 + \frac{G_F m_t^2}{8\sqrt{2}\pi^2} (19 - 2\pi^2) \right] \quad (8.22)$$

incorporates the result [45] from two-loop irreducible diagrams. Note that α has been replaced by G_F in order to obtain the correct leading $O(\alpha^2)$ terms.

In particular for the relation between M_W and G_F the correct resummation of the leading corrections is given by

$$G_F = \frac{\pi}{M_W^2 \sqrt{2}} \frac{\alpha}{s_W^2} \frac{1}{1 - (\Delta\alpha)_{\text{ferm}}} \frac{1}{1 + \frac{c_W^2}{s_W^2} \Delta\bar{\rho}} \left[1 + \Delta r - (\Delta\alpha)_{\text{ferm}} + \frac{c_W^2}{s_W^2} \Delta\rho \right]. \quad (8.23)$$

Note that the two types of leading corrections are summed separately. Inserting $s_W^2 = 1 - M_W^2/M_Z^2$ this relation can be used to determine the W -boson mass M_W including leading higher order contributions.

Neglecting the nonleading contributions and using (8.19) and (8.21) eq. (8.23) can be written as

$$\frac{\pi\alpha(M_W^2)}{\bar{s}_W^2} \approx \sqrt{2} G_F M_W^2. \quad (8.24)$$

With this relation the appearance of G_F in $\Delta\bar{\rho}$ can be easily understood. All leading universal corrections arise from the renormalization constants of α and s_W . Consequently they can be absorbed by incorporating the leading finite parts of these renormalization constants into the effective parameters $\alpha(s)$ and \bar{s}_W^2 (including the leading higher order corrections). Thus one obtains from the lowest order result directly the corresponding result including the leading universal corrections. In particular (8.24) can be obtained in this way. Applying this recipe to $\Delta\rho$ and using (8.24) introduces naturally G_F .

8.2.3 Recipes for leading universal corrections

From the discussion above we infer that the universal leading higher order contributions can be taken into account by the following replacements

$$\begin{aligned}
 \alpha &\rightarrow \alpha(s), \\
 s_W^2 &\rightarrow \bar{s}_W^2, & c_W^2 &\rightarrow \bar{c}_W^2, \\
 \frac{e^2}{2s_W^2} &= \frac{2\pi\alpha}{s_W^2} \rightarrow \frac{2\pi\alpha(s)}{\bar{s}_W^2} \approx 2\sqrt{2}G_F M_W^2, \\
 \frac{e^2}{4s_W^2 c_W^2} &= \frac{\pi\alpha}{s_W^2 c_W^2} \rightarrow \frac{\pi\alpha(s)}{\bar{s}_W^2 \bar{c}_W^2} \approx \sqrt{2}G_F M_Z^2 \frac{1}{1 - \Delta\bar{\rho}}.
 \end{aligned} \tag{8.25}$$

Note that this does not include the nonuniversal corrections $\propto \alpha m_t^2/M_W^2$ arising from enhanced Yukawa couplings. These have to be evaluated for each process directly.

9 The width of the W -boson

In the coming years the upgrade of the LEP electron positron storage ring to 180 – 190 GeV CM-energy will allow to study the properties of the W -boson in detail in a model independent way. Besides its mass M_W also its total and partial decay widths are of interest. While the leptonic partial widths allow to test lepton universality the hadronic partial widths can serve to determine the quark mixing matrix elements [46]. The expected accuracy is $\delta M_W \approx 100$ MeV and $\delta \Gamma_W \approx 200$ MeV [47].

An accurate comparison between these experiments and theoretical predictions of the SM requires at least the inclusion of one-loop radiative corrections both for the production and the decay of W -bosons. The W -bosons decay dominantly into fermion-antifermion pairs. The total and partial widths of the W -boson and the corresponding one-loop radiative corrections are discussed in this chapter.

The electroweak and QCD corrections for decays into massless fermions ($m_f \ll M_W$) have been calculated in [48, 49, 50]. The hard bremsstrahlung contribution has been investigated in [52, 53]. The QCD corrections for the decay into a massive top quark and a massless bottom quark were given in [54]. The full one-loop electroweak and QCD corrections together with the complete photonic and gluonic bremsstrahlung were evaluated for arbitrary finite fermion masses in [55].

Since the top quark is probably heavier than the W -boson and since all other quark masses are small compared to the W -boson mass, the fermion mass effects are not of great importance for the W -decay. However, the matrix element for the W -decay into two fermions is directly related via crossing to the one for the decay of the top quark into a W -boson and a bottom quark. In this case the fermion masses are crucial. Since we will discuss top decay in Chap. 10 we give the results for W -decay for finite fermion masses.

9.1 Lowest order

The Born amplitude for the decay $W^+ \rightarrow f_i \bar{f}'_j$ was already given in (6.11). For finite fermion masses the following result is obtained for the corresponding partial decay width

$$\Gamma_0^{W f_i \bar{f}'_j}(M_W, m_{f,i}, m_{f',j}) = N_C^f \frac{\alpha}{12} \frac{1}{2s_W^2} |V_{ij}|^2 \frac{\kappa(M_W^2, m_{f,i}^2, m_{f',j}^2)}{M_W^3} G_1^-, \quad (9.1)$$

where κ/M_W^3 originates from phase space and

$$G_1^- = \sum_{pol} \mathcal{M}_1^{\dagger} \mathcal{M}_1^- = 2M_W^2 - m_{f,i}^2 - m_{f',j}^2 - \frac{(m_{f,i}^2 - m_{f',j}^2)^2}{M_W^2} \quad (9.2)$$

from the polarization sum of the matrix element squared. The Källén function κ was defined in (4.28). The colour factor N_C^f is given by

$$N_C^f = \begin{cases} 3 & \text{for quarks,} \\ 1 & \text{for leptons.} \end{cases} \quad (9.3)$$

For leptonic decays we have $V_{ij} = \delta_{ij}$. The total width is obtained as a sum over the partial fermionic decay widths with $m_{f,i} + m_{f',j} < M_W$

$$\Gamma_0^W = \sum_{ij} \Gamma_0^{W u_i d_j} + \sum_i \Gamma_0^{W \nu_i l_i}. \quad (9.4)$$

We can write down another possible tree level representation for the partial decay width by eliminating α/s_W^2 in favour of G_F

$$\bar{\Gamma}_0^{Wf_i f'_j}(M_W, m_{f,i}, m_{f',j}) = N_C^f \frac{G_F}{12\pi\sqrt{2}} |V_{ij}|^2 \frac{\kappa(M_W^2, m_{f,i}^2, m_{f',j}^2)}{M_W} G_1^-. \quad (9.5)$$

9.2 Electroweak virtual corrections

In our formulation of the on-shell renormalization scheme the invariant matrix element to one-loop order has the following form

$$\begin{aligned} \mathcal{M}^{Wf_i f'_j} = & -\frac{e}{\sqrt{2}s_W} \left\{ V_{ij} \mathcal{M}_1^- \left[1 + \delta Z_e - \frac{\delta s_W}{s_W} \right] + \mathcal{M}_1^- \delta V_{ij} \right. \\ & + V_{ij} \mathcal{M}_1^- \frac{1}{2} \delta Z_W + \mathcal{M}_1^- \frac{1}{2} \sum_k [\delta Z_{ik}^{f,L\dagger} V_{kj} + V_{ik} \delta Z_{kj}^{f',L}] \\ & \left. + \sum_{a=1}^2 \sum_{\sigma=\pm} \mathcal{M}_a^\sigma \delta F_a^\sigma(M_W, m_{f,i}, m_{f',j}) \right\}. \end{aligned} \quad (9.6)$$

The standard matrix elements M_a^σ were defined in (5.11). The functions δF_a^σ summarize the loop corrections to the $Wf_i f'_j$ -vertex. There are no explicit self energy corrections from the external lines. These are all absorbed into the field renormalization constants δZ_W , $\delta Z^{f,L}$ and $\delta Z^{f',L}$. These and the parameter renormalization constants were given in terms of self energies in Sect. 3.3. The explicit forms of the self energies can be found in App. B.

Fig. 9.1 shows the Feynman diagrams contributing to the vertex corrections for massive fermions. They yield the following vertex form factors

$$\begin{aligned} \delta F_1^-(M_W, m_1, m_2) = & \frac{\alpha}{4\pi} \times \\ & \left\{ Q_f Q_{f'} \mathcal{V}_a(m_1^2, M_W^2, m_2^2, \lambda, m_1, m_2) + g_f^- g_{f'}^- \mathcal{V}_a(m_1^2, M_W^2, m_2^2, M_Z, m_1, m_2) \right. \\ & + \sum_{\sigma=\pm} \left[Q_f \mathcal{V}_b^\sigma(m_1^2, M_W^2, m_2^2, m_1, \lambda, M_W) - Q_{f'} \mathcal{V}_b^\sigma(m_2^2, M_W^2, m_1^2, m_2, \lambda, M_W) \right. \\ & \left. \left. + \frac{c_W}{s_W} g_f^\sigma \mathcal{V}_b^\sigma(m_1^2, M_W^2, m_2^2, m_1, M_Z, M_W) - \frac{c_W}{s_W} g_{f'}^\sigma \mathcal{V}_b^\sigma(m_2^2, M_W^2, m_1^2, m_2, M_Z, M_W) \right] \right. \\ & + \frac{1}{4s_W^2} \mathcal{V}_c(m_1^2, M_W^2, m_2^2, M_H, m_1, m_2) \\ & \left. + \frac{1}{2s_W^2} \left[\mathcal{V}_d(m_1^2, M_W^2, m_2^2, m_1, M_H, M_W) + \mathcal{V}_d(m_2^2, M_W^2, m_1^2, m_2, M_H, M_W) \right] \right. \\ & \left. + \frac{1}{2s_W^2} \left[\mathcal{V}_e(m_1^2, M_W^2, m_2^2, m_1, M_H, M_W) + \mathcal{V}_e(m_2^2, M_W^2, m_1^2, m_2, M_H, M_W) \right] \right\} \end{aligned} \quad (9.7)$$

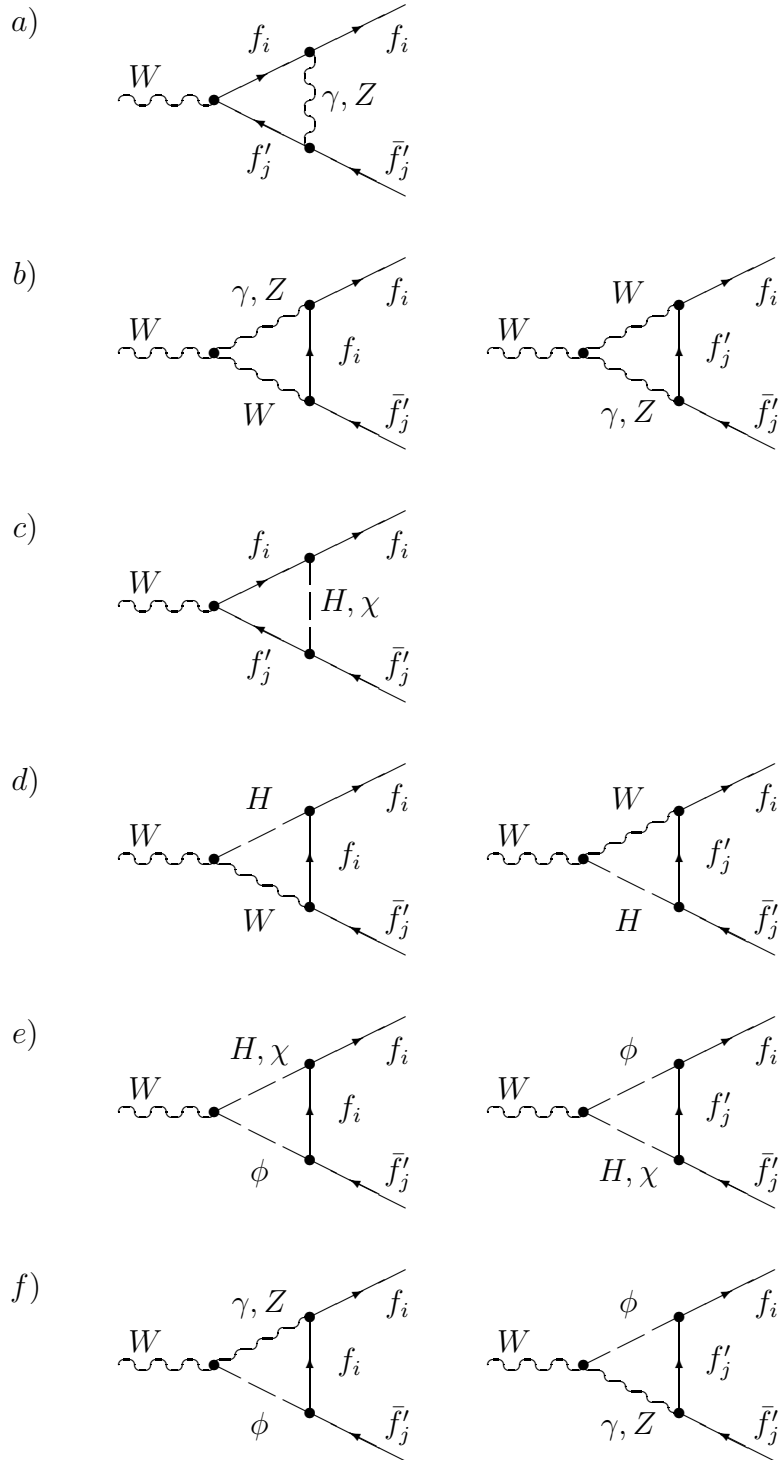


Figure 9.1: One-loop diagrams for $W \rightarrow f_i \bar{f}_j$.

$$\begin{aligned}
& + \mathcal{V}_e(m_1^2, M_W^2, m_2^2, m_1, M_Z, M_W) + \mathcal{V}_e(m_2^2, M_W^2, m_1^2, m_2, M_Z, M_W) \Big] \\
& + \sum_{\sigma=\pm} \left[Q_f \mathcal{V}_f^\sigma(m_1^2, M_W^2, m_2^2, m_1, \lambda, M_W) - Q_{f'} \mathcal{V}_f^\sigma(m_2^2, M_W^2, m_1^2, m_2, \lambda, M_W) \right. \\
& \quad \left. - \frac{s_W}{c_W} g_f^\sigma \mathcal{V}_f^\sigma(m_1^2, M_W^2, m_2^2, m_1, M_Z, M_W) + \frac{s_W}{c_W} g_{f'}^\sigma \mathcal{V}_f^\sigma(m_2^2, M_W^2, m_1^2, m_2, M_Z, M_W) \right] \Big\}, \\
\delta F_1^+(M_W, m_1, m_2) &= \frac{\alpha}{4\pi} m_1 m_2 \times \\
& \left\{ \sum_{\sigma=\pm} \left[Q_f Q_{f'} \mathcal{W}_a^\sigma(m_1^2, M_W^2, m_2^2, \lambda, m_1, m_2) + g_f^\sigma g_{f'}^\sigma \mathcal{W}_a^\sigma(m_1^2, M_W^2, m_2^2, M_Z, m_1, m_2) \right. \right. \\
& \quad + Q_f \mathcal{W}_b^\sigma(m_1^2, M_W^2, m_2^2, m_1, \lambda, M_W) - Q_{f'} \mathcal{W}_b^\sigma(m_2^2, M_W^2, m_1^2, m_2, \lambda, M_W) \\
& \quad \left. + \frac{c_W}{s_W} g_f^\sigma \mathcal{W}_b^\sigma(m_1^2, M_W^2, m_2^2, m_1, M_Z, M_W) - \frac{c_W}{s_W} g_{f'}^\sigma \mathcal{W}_b^\sigma(m_2^2, M_W^2, m_1^2, m_2, M_Z, M_W) \right] \\
& + \frac{1}{4s_W^2} \left[\sum_{\sigma=\pm} \mathcal{W}_c^\sigma(m_1^2, M_W^2, m_2^2, M_H, m_1, m_2) - \mathcal{W}_c^-(m_1^2, M_W^2, m_2^2, M_Z, m_1, m_2) \right] \\
& + \frac{1}{2s_W^2} \left[\mathcal{W}_d(m_1^2, M_W^2, m_2^2, m_1, M_H, M_W) + \mathcal{W}_d(m_2^2, M_W^2, m_1^2, m_2, M_H, M_W) \right] \quad (9.8) \\
& + \frac{1}{2s_W^2} \left[\mathcal{W}_e(m_1^2, M_W^2, m_2^2, m_1, M_H, M_W) + \mathcal{W}_e(m_2^2, M_W^2, m_1^2, m_2, M_H, M_W) \right. \\
& \quad \left. - \mathcal{W}_e(m_1^2, M_W^2, m_2^2, m_1, M_Z, M_W) - \mathcal{W}_e(m_2^2, M_W^2, m_1^2, m_2, M_Z, M_W) \right] \\
& + \sum_{\sigma=\pm} \left[Q_f \mathcal{W}_f^\sigma(m_1^2, M_W^2, m_2^2, m_1, \lambda, M_W) - Q_{f'} \mathcal{W}_f^\sigma(m_2^2, M_W^2, m_1^2, m_2, \lambda, M_W) \right. \\
& \quad \left. - \frac{s_W}{c_W} g_f^\sigma \mathcal{W}_f^\sigma(m_1^2, M_W^2, m_2^2, m_1, M_Z, M_W) + \frac{s_W}{c_W} g_{f'}^\sigma \mathcal{W}_f^\sigma(m_2^2, M_W^2, m_1^2, m_2, M_Z, M_W) \right] \Big\},
\end{aligned}$$

$$\begin{aligned}
\delta F_2^-(M_W, m_1, m_2) &= \frac{\alpha}{4\pi} m_1 \times \\
& \left\{ \sum_{\sigma=\pm} \left[Q_f Q_{f'} \mathcal{X}_a^\sigma(m_1^2, M_W^2, m_2^2, \lambda, m_1, m_2) + g_f^\sigma g_{f'}^\sigma \mathcal{X}_a^\sigma(m_1^2, M_W^2, m_2^2, M_Z, m_1, m_2) \right. \right. \\
& \quad \left. + Q_f \mathcal{X}_b^\sigma(m_1^2, M_W^2, m_2^2, m_1, \lambda, M_W) + \frac{c_W}{s_W} g_f^\sigma \mathcal{X}_b^\sigma(m_1^2, M_W^2, m_2^2, m_1, M_Z, M_W) \right] \\
& \quad \left. - Q_{f'} \mathcal{X}_b^-(m_1^2, M_W^2, m_2^2, m_2, M_W, \lambda) - \frac{c_W}{s_W} g_{f'}^\sigma \mathcal{X}_b^-(m_1^2, M_W^2, m_2^2, m_2, M_W, M_Z) \right\}
\end{aligned}$$

$$\begin{aligned}
& + \frac{1}{4s_W^2} \left[\sum_{\sigma=\pm} \mathcal{X}_c^-(m_1^2, M_W^2, m_2^2, M_H, m_1, m_2) - \mathcal{X}_c^-(m_1^2, M_W^2, m_2^2, M_Z, m_1, m_2) \right] \\
& + \frac{1}{2s_W^2} \mathcal{X}_d(m_1^2, M_W^2, m_2^2, m_1, M_H, M_W) \tag{9.9} \\
& - \frac{1}{2s_W^2} \sum_{\sigma=\pm} \left[\sigma \left(\mathcal{X}_e^\sigma(m_1^2, M_W^2, m_2^2, m_1, M_H, M_W) - \mathcal{X}_e^\sigma(m_2^2, M_W^2, m_1^2, m_2, M_H, M_W) \right) \right. \\
& \quad \left. - \mathcal{X}_e^\sigma(m_1^2, M_W^2, m_2^2, m_1, M_Z, M_W) - \mathcal{X}_e^\sigma(m_2^2, M_W^2, m_1^2, m_2, M_Z, M_W) \right] \\
& - \frac{1}{2s_W^2} \frac{m_2^2}{M_W^2} \left[\mathcal{X}_e^0(m_1^2, M_W^2, m_2^2, m_1, M_H, M_W) - \mathcal{X}_e^0(m_2^2, M_W^2, m_1^2, m_2, M_H, M_W) \right. \\
& \quad \left. - \mathcal{X}_e^0(m_1^2, M_W^2, m_2^2, m_1, M_Z, M_W) - \mathcal{X}_e^0(m_2^2, M_W^2, m_1^2, m_2, M_Z, M_W) \right] \\
& + Q_f \mathcal{X}_f(m_1^2, M_W^2, m_2^2, m_1, \lambda, M_W) + Q_{f'} \mathcal{X}_f(m_2^2, M_W^2, m_1^2, m_2, \lambda, M_W) \\
& - \frac{s_W}{c_W} \left[g_f^+ \mathcal{X}_f(m_1^2, M_W^2, m_2^2, m_1, M_Z, M_W) + g_{f'}^- \mathcal{X}_f(m_2^2, M_W^2, m_1^2, m_2, M_Z, M_W) \right] \Big\}.
\end{aligned}$$

To obtain these results we had to evaluate six generic diagrams labeled by a, b, c, d, e and f in Fig. 9.1. The corresponding invariant functions \mathcal{V} , \mathcal{W} and \mathcal{X} are listed in App. C. The formfactor δF_2^+ can be obtained from δF_2^- by the substitutions $m_1 \leftrightarrow m_2$, $Q_f \leftrightarrow -Q_{f'}$, $g_f \leftrightarrow -g_{f'}$.

Squaring the matrix element (9.6), summing over the polarizations of the external particles and multiplying the phase space factor yields the one-loop corrected width

$$\begin{aligned}
\Gamma_1^{Wfif'_j} &= N_C^f \frac{\alpha}{12} \frac{1}{2s_W^2} \frac{\kappa(M_W^2, m_{f,i}^2, m_{f',j}^2)}{M_W^3} \\
& \left\{ |V_{ij}|^2 G_1^- \left[1 + 2\delta Z_e - 2\frac{\delta s_W}{s_W} + \delta Z_W \right] \right. \\
& + \frac{1}{2} G_1^- \sum_k [(\delta Z_{ik}^{f,L\dagger} + \delta Z_{ik}^{f,L}) V_{kj} + V_{ik} (\delta Z_{kj}^{f',L\dagger} + \delta Z_{kj}^{f',L})] V_{ij}^\dagger \\
& \left. + 2|V_{ij}|^2 \sum_{a=1}^2 \sum_{\sigma=\pm} G_a^\sigma \delta F_a^\sigma(M_W, m_{f,i}, m_{f',j}) \right\} \tag{9.10} \\
& = \Gamma_0^{Wfif'_j} (1 + \delta_{virt}^{ew}),
\end{aligned}$$

where

$$G_1^+ = \sum_{pol} \mathcal{M}_1^{-\dagger} \mathcal{M}_1^+ = 6 m_{f,i} m_{f',j}, \tag{9.11}$$

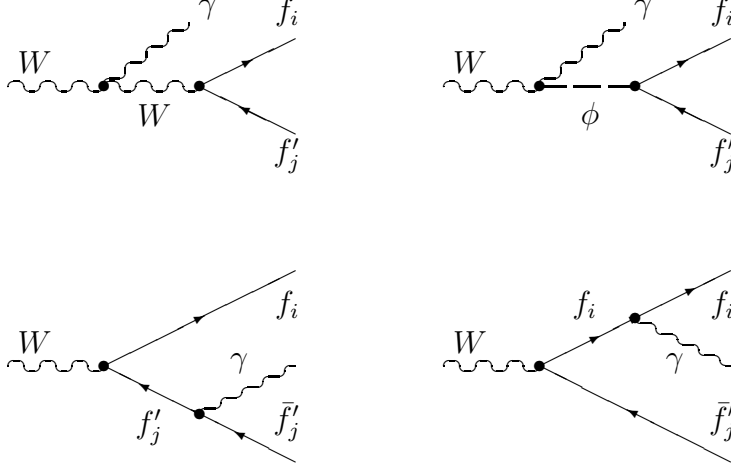


Figure 9.2: Bremsstrahlung Feynman diagrams for $W \rightarrow f_i \bar{f}'_j \gamma$.

$$G_2^- = \sum_{pol} \mathcal{M}_1^{-\dagger} \mathcal{M}_2^- = -\frac{m_{f,i} \kappa^2 (M_W^2, m_{f,i}^2, m_{f',j}^2)}{2 M_W^2},$$

$$G_2^+ = \sum_{pol} \mathcal{M}_1^{-\dagger} \mathcal{M}_2^+ = -\frac{m_{f',j} \kappa^2 (M_W^2, m_{f,i}^2, m_{f',j}^2)}{2 M_W^2},$$

and we have inserted δV_{ij} from (3.23).

9.3 Photon bremsstrahlung

Like any one-loop amplitude with external charged particles (9.6) and consequently (9.10) are IR-divergent due to virtual photonic corrections. These singularities are compensated by the the real bremsstrahlung corrections, i.e. the three-body decay

$$W^+(k) \rightarrow f_i(p_1) \bar{f}'_j(p_2) \gamma(q). \quad (9.12)$$

The corresponding matrix element as given by the Feynman diagrams (Fig. 9.2) is

$$\begin{aligned} \mathcal{M}_b = V_{ij} \frac{e^2}{\sqrt{2} s_W} \bar{u}(p_1) \left\{ \frac{-Q_f}{2p_1 q} [2p_1 \eta \not{\epsilon} + \not{\eta} \not{q} \not{\epsilon}] + \frac{Q_{f'}}{2p_2 q} [2p_2 \eta \not{\epsilon} + \not{\epsilon} \not{q} \not{\eta}] \right. \\ \left. + \frac{(Q_f - Q_{f'})}{-2kq} [(q\eta - 2k\eta) \not{\epsilon} + 2\epsilon\eta \not{q} - 2q\epsilon \not{\eta}] \right\} \omega_{-v}(p_2), \end{aligned} \quad (9.13)$$

where η denotes the polarization vector of the photon. Performing the polarization sum over the square of the amplitude gives

$$\sum_{pol} |\mathcal{M}_b|^2 = \frac{\alpha^2}{2s_W^2} (64\pi^2) |V_{ij}|^2 \left\{ \frac{Q_f Q_{f'}}{(2p_1 q)(2p_2 q)} [(M_W^2 - m_{f,i}^2 - m_{f',j}^2) G_1^-] \right\}$$

$$\begin{aligned}
& -\frac{Q_f^2}{(2p_1q)^2} \left[(m_{f,i}^2 + 2p_1q)G_1^- + \left(1 + \frac{m_{f,i}^2 + m_{f',j}^2}{2M_W^2}\right)(2p_1q)(-2kq) + (2p_1q)^2 \right] \\
& -\frac{Q_{f'}^2}{(2p_2q)^2} \left[(m_{f',j}^2 + 2p_2q)G_1^- + \left(1 + \frac{m_{f,i}^2 + m_{f',j}^2}{2M_W^2}\right)(2p_2q)(-2kq) + (2p_2q)^2 \right] \\
& -\frac{(Q_f - Q_{f'})^2}{(-2kq)^2} \left[(M_W^2 - 2kq)G_1^- + \frac{m_{f,i}^2 + m_{f',j}^2}{2M_W^2}(-2kq)^2 - 2(2p_1q)(2p_2q) \right] \\
& -\frac{Q_f(Q_f - Q_{f'})}{-2kq \, 2p_1q} \left[(M_W^2 + m_{f,i}^2 - m_{f',j}^2)G_1^- - 2(2p_1q)(2p_2q) \right] \\
& +\frac{Q_{f'}(Q_f - Q_{f'})}{-2kq \, 2p_2q} \left[(M_W^2 - m_{f,i}^2 + m_{f',j}^2)G_1^- - 2(2p_1q)(2p_2q) \right] \Big\}. \tag{9.14}
\end{aligned}$$

From this the complete bremsstrahlung cross section (including soft and hard photons) is obtained by integrating over the phase space of the photon and the two fermions as

$$\begin{aligned}
\Gamma_b^{Wf_i f'_j}(M_W, m_{f,i}, m_{f',j}) &= \frac{1}{(2\pi)^5} \frac{N_C^f}{2M_W} \int \frac{d^3q}{2q_0} \frac{d^3p_1}{2p_{10}} \frac{d^3p_2}{2p_{20}} \delta^{(4)}(p_1 + p_2 + q - k) \frac{1}{3} \sum_{pol} |\mathcal{M}_b|^2 \\
&= \Gamma_0^{Wf_i f'_j} \delta_b^{ew}(M_W, m_{f,i}, m_{f',j}) \tag{9.15}
\end{aligned}$$

with

$$\begin{aligned}
\delta_b^{ew}(M_W, m_{f,i}, m_{f',j}) &= \\
& \left(-\frac{\alpha}{\pi} \right) \frac{4M_W^2}{\kappa(M_W^2, m_{f,i}^2, m_{f',j}^2)} \left\{ -Q_f Q_{f'} \left[(M_W^2 - m_{f,i}^2 - m_{f',j}^2) I_{12} \right] \right. \\
& + Q_f^2 \left[(m_{f,i}^2 I_{11} + I_1) + \left(1 + \frac{m_{f,i}^2 + m_{f',j}^2}{2M_W^2}\right) \frac{I_1^0}{G_1^-} + \frac{I}{G_1^-} \right] \\
& + Q_{f'}^2 \left[(m_{f',j}^2 I_{22} + I_2) + \left(1 + \frac{m_{f,i}^2 + m_{f',j}^2}{2M_W^2}\right) \frac{I_2^0}{G_1^-} + \frac{I}{G_1^-} \right] \\
& + (Q_f - Q_{f'})^2 \left[(M_W^2 I_{00} + I_0) + \frac{m_{f,i}^2 + m_{f',j}^2}{2M_W^2} \frac{I}{G_1^-} - 2 \frac{I_{00}^{12}}{G_1^-} \right] \\
& + Q_f(Q_f - Q_{f'}) \left[(M_W^2 + m_{f,i}^2 - m_{f',j}^2) I_{01} - 2 \frac{I_0^1}{G_1^-} \right] \\
& \left. - Q_{f'}(Q_f - Q_{f'}) \left[(M_W^2 - m_{f,i}^2 + m_{f',j}^2) I_{02} - 2 \frac{I_0^1}{G_1^-} \right] \right\}. \tag{9.16}
\end{aligned}$$

The bremsstrahlung phase space integrals $I_{kl} = I_{kl}(M_W, m_{f,i}, m_{f',j})$ are given in App. D. The IR-singularities contained in the I_{kl} are again regularized by a photon mass λ .

9.4 QCD corrections

Like the electroweak corrections also the QCD corrections consist of virtual and real contributions

$$\delta^{QCD}(M_W, m_{f,i}, m_{f',j}) = \delta_{virt}^{QCD} + \delta_b^{QCD}, \quad (9.17)$$

which are individually IR-divergent. They are obtained from the electroweak results of the previous sections by keeping only the terms containing Q_f^2 , $Q_{f'}^2$ or $Q_f Q_{f'}$, setting $Q_f = Q_{f'} = 1$, replacing α by the strong coupling constant α_s and multiplying an overall colour factor $C_F = \frac{4}{3}$. In particular the virtual QCD-corrections arise only from the diagram of Fig. 9.1a with the photon replaced by a gluon and the corresponding corrections to the fermion wave function renormalization constants. Since this allows many simplifications we give the explicit results

$$\begin{aligned} \delta_{virt}^{QCD} = & \left(-\frac{\alpha_s}{4\pi} \right) 2 C_F \left\{ 6 - B_0(M_W^2, m_{f,i}, m_{f',j}) \right. \\ & + \frac{1}{2} B_0(0, m_{f,i}, m_{f,i}) + \frac{1}{2} B_0(0, m_{f',j}, m_{f',j}) \\ & + 2(M_W^2 - m_{f,i}^2 - m_{f',j}^2)(C_0 + C_1 + C_2) - 2m_{f,i}^2 C_1 - 2m_{f',j}^2 C_2 \quad (9.18) \\ & - 2 \log\left(\frac{m_{f,i} m_{f',j}}{\lambda^2}\right) - 2 \frac{G_1^+}{G_1^-} m_{f,i} m_{f',j} [C_1 + C_2] \\ & \left. + 4 \frac{G_2^-}{G_1^-} m_{f,i} [C_{11} + C_{12} + C_1] + 4 \frac{G_2^+}{G_1^+} m_{f',j} [C_{22} + C_{12} + C_2] \right\}. \end{aligned}$$

The arguments of the three-point functions are $C = C(m_{f,i}^2, M_W^2, m_{f',j}^2, \lambda, m_{f,i}, m_{f',j})$. To the gluonic bremsstrahlung δ_b^{QCD} only the first three terms of (9.16) contribute. For zero fermion masses the total QCD-correction reduces to

$$\delta^{QCD}(M_W, 0, 0) = \frac{\alpha_s}{\pi}. \quad (9.19)$$

9.5 Results and Discussion

For numerical evaluation of the previous results we use the parameters listed in Sect. 8.1 including the values for the quark mixing matrix as given by (8.1). The W -mass is determined from the relation (8.23).

In the on-shell scheme the lowest order width is parametrized by α and the particle masses (9.1). In this scheme large electroweak corrections arise due to fermion loop contributions to the renormalization of α and s_W . We can improve the results in this scheme by resumming the corresponding one-loop contributions to all orders as discussed in Sect. 8.2. Thus we obtain for the corrected width

$$\begin{aligned} \Gamma &= \Gamma_0 \left[1 + \delta_1 - (\Delta\alpha)_{ferm} + \frac{c_W^2}{s_W^2} \Delta\rho \right] \frac{1}{1 - (\Delta\alpha)_{ferm}} \frac{1}{1 + \frac{c_W^2}{s_W^2} \Delta\bar{\rho}} \\ &= \Gamma_0 [1 + \delta], \end{aligned} \quad (9.20)$$

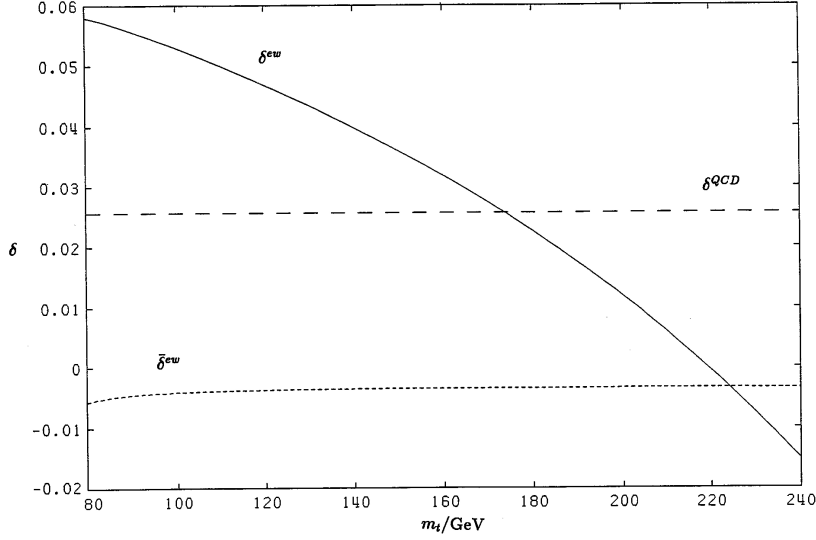


Figure 9.3: Electroweak radiative corrections δ^{ew} and $\bar{\delta}^{ew}$ and QCD-corrections δ^{QCD} to the total W -width Γ^W versus the top mass.

where

$$\delta_1 = \delta_{virt}^{ew} + \delta_b^{ew} + \delta_{virt}^{QCD} + \delta_b^{QCD} \quad (9.21)$$

is the proper one-loop correction without resummation. As in any charged current process we can avoid the large corrections by parametrizing the lowest order decay width with G_F and M_W instead of α and s_W^2 (9.5). Using (8.23) we find the relation between the decay width in both parametrizations

$$\bar{\Gamma}_0 = \Gamma_0 \frac{1}{1 - (\Delta\alpha)_{ferm}} \frac{1}{1 + \frac{c_W^2}{s_W^2} \Delta\bar{\rho}} \left[1 + \Delta r - (\Delta\alpha)_{ferm} + \frac{c_W^2}{s_W^2} \Delta\rho \right], \quad (9.22)$$

$$\bar{\Gamma} = \bar{\Gamma}_0 [1 + \delta_1 - \Delta r] = \bar{\Gamma}_0 (1 + \bar{\delta}).$$

The large fermionic contributions contained in δ_1 are exactly cancelled by equal contributions in Δr and consequently the remaining corrections $\bar{\delta}$ are small.

The relative corrections to the total W -boson decay width are shown in Fig. 9.3. They are large and strongly m_t -dependent in the on-shell scheme. This behaviour arises from the fermionic contributions to the renormalization of the weak mixing angle in (9.6) ($\delta s_W^2/s_W^2$) which contain terms $\propto \alpha m_t^2/M_W^2$. In contrast to this in the parametrization with G_F the corrections depend only weakly on m_t and remain below 0.6%. The QCD corrections are practically constant and equal to $2\alpha_s/(3\pi)$, their value for zero fermion masses.

m_t	M_W	Γ_0^W	$\bar{\Gamma}_0^W$	Γ_{ew}^W	$\bar{\Gamma}_{ew}^W$
80.0	79.87	1.8778	2.0056	1.9866	1.9940
100.0	79.99	1.8996	2.0147	2.0002	2.0063
120.0	80.10	1.9211	2.0235	2.0110	2.0158
140.0	80.23	1.9447	2.0330	2.0221	2.0256
160.0	80.37	1.9713	2.0435	2.0340	2.0363
180.0	80.52	2.0018	2.0553	2.0469	2.0481
200.0	80.69	2.0368	2.0684	2.0608	2.0612

Table 9.1: W -decay width Γ^W parametrized by α and $\bar{\Gamma}^W$ parametrized by G_F in lowest order and including electroweak corrections. All values are given in GeV.

Tab. 9.1 shows the lowest order width Γ_0 and the width including electroweak corrections Γ_{ew} in both parametrizations for various values of the top mass. The W -mass obtained from (8.23) is also listed there. While the results for the lowest order width in the two parametrizations differ by several percent, the deviation of the first order expressions is always less than 0.4%.

The analytical results were presented above for finite external fermion masses and with correct renormalization of the quark mixing matrix. However, since the top quark is presumably heavier than the W -boson [57] all relevant actual fermion masses are small compared to the W -boson mass. Therefore in addition to the completely corrected numerical results $\Gamma(M_W, m_{f,i}, m_{f',j})$ for finite fermion masses we also give those for vanishing fermion masses $\Gamma(M_W, 0, 0)$ in Tab. 9.2. The analytical results for vanishing fermion masses were listed in Sect. 6.3. Finally we include an improved Born approximation consisting of the Born widths with zero fermion masses parametrized by G_F and multiplied by the QCD correction factor for zero quark masses

$$\begin{aligned}\Gamma_{imp}^{W\nu l} &= \frac{G_F M_W^3}{6\sqrt{2}\pi}, \\ \Gamma_{imp}^{Wud} &= \frac{G_F M_W^3}{2\sqrt{2}\pi} |V_{ij}|^2 \left(1 + \frac{\alpha_s}{\pi}\right), \\ \Gamma_{imp}^W &= \frac{3G_F M_W^3}{2\sqrt{2}\pi} \left(1 + \frac{2}{3} \frac{\alpha_s}{\pi}\right),\end{aligned}\tag{9.23}$$

for the leptonic partial widths, the hadronic partial widths and for the total width, respectively.

The numerical values for the partial and total W -widths in these different approximations are given in Tab. 9.2 assuming a top quark mass of 140 GeV and a Higgs boson mass of 100 GeV. The improved Born approximation (9.23) reproduces the exact results up to 0.4% (0.6% for the decays into a b -quark). The effects of the fermion masses are below 0.3%. They are suppressed by m_q^2/s . There are no mass singularities since the

	Born width	complete one-loop	$m_f = 0$ in Γ	improved Born	Branching ratio
$\Gamma(W \rightarrow e\nu_e)$	0.2260	0.2252	0.2252	0.2260	0.1084
$\Gamma(W \rightarrow \mu\nu_\mu)$	0.2259	0.2252	0.2252	0.2260	0.1084
$\Gamma(W \rightarrow \tau\nu_\tau)$	0.2258	0.2250	0.2252	0.2260	0.1083
$\Gamma(W \rightarrow lep.)$	0.6777	0.6754	0.6756	0.6778	0.3251
$\Gamma(W \rightarrow ud)$	0.6450	0.6672	0.6672	0.6696	0.3211
$\Gamma(W \rightarrow us) \times 10$	0.3281	0.3393	0.3393	0.3406	0.0163
$\Gamma(W \rightarrow ub) \times 10^4$	0.3306	0.3428	0.3436	0.3448	0.00002
$\Gamma(W \rightarrow cd) \times 10$	0.3281	0.3396	0.3396	0.3409	0.0163
$\Gamma(W \rightarrow cs)$	0.6432	0.6656	0.6657	0.6682	0.3204
$\Gamma(W \rightarrow cb) \times 10^2$	0.1427	0.1480	0.1484	0.1489	0.0007
$\Gamma(W \rightarrow had.)$	1.3553	1.4022	1.4023	1.4075	0.6749
$\Gamma(W \rightarrow all)$	2.0330	2.0776	2.0779	2.0853	

Table 9.2: Partial and total W-decay widths $\bar{\Gamma}$ in different approximations for $m_t = 140$ GeV, $M_H = 100$ GeV and the corresponding W-mass $M_W = 80.23$ GeV.

width is obtained by integrating over the full phase space of the final state particles [56]. Consequently the exact numerical values of the masses of the external fermions masses are irrelevant¹. The branching ratios derived from (9.23)

$$\begin{aligned}
BR(W \rightarrow l\nu) &= \frac{1}{9(1 + 2\alpha_s/3\pi)}, \\
BR(W \rightarrow \text{leptons}) &= \frac{1}{3(1 + 2\alpha_s/3\pi)}, \\
BR(W \rightarrow u_i d_j) &= \frac{|V_{ij}|^2(1 + \alpha_s/\pi)}{3(1 + 2\alpha_s/3\pi)}, \\
BR(W \rightarrow \text{hadrons}) &= \frac{2(1 + \alpha_s/\pi)}{3(1 + 2\alpha_s/3\pi)} \tag{9.24}
\end{aligned}$$

agree numerically within 0.1% with those obtained from the full one loop results. They depend only on α_s and V_{ij} .

The dependence of the W-width on the unknown top and Higgs masses is shown in Tab. 9.3 for Γ^{Wud} and in Tab. 9.4 for $\Gamma^{W\ell\nu}$. A variation of m_t between 80 and 200 GeV affects the partial widths by $\sim 4\%$, a variation of M_H between 50 and 1000 GeV by

¹The values given in Sect. 8.1 are not appropriate for the external quarks. We only use them here to demonstrate the numerical irrelevance of the fermion mass effects.

m_t	$M_H = 50$	$M_H = 100$	$M_H = 300$	$M_H = 1000$
80.0	0.2212	0.2209	0.2202	0.2193
100.0	0.2227	0.2224	0.2217	0.2208
120.0	0.2239	0.2236	0.2229	0.2220
140.0	0.2251	0.2248	0.2241	0.2232
160.0	0.2264	0.2261	0.2254	0.2245
180.0	0.2278	0.2276	0.2269	0.2260
200.0	0.2294	0.2291	0.2284	0.2275

Table 9.3: Partial W-decay width $\Gamma^{W e\nu}$ including first order QCD and electroweak corrections for different values of the top and Higgs masses. All values are given in GeV.

m_t	$M_H = 50$	$M_H = 100$	$M_H = 300$	$M_H = 1000$
80.0	0.6539	0.6530	0.6509	0.6481
100.0	0.6585	0.6575	0.6554	0.6526
120.0	0.6622	0.6612	0.6591	0.6563
140.0	0.6659	0.6650	0.6629	0.6601
160.0	0.6700	0.6691	0.6670	0.6642
180.0	0.6745	0.6736	0.6715	0.6686
200.0	0.6793	0.6784	0.6763	0.6735

Table 9.4: Partial W-decay width $\Gamma^{W ud}$ including first order QCD and electroweak corrections for different values of the top and Higgs masses. All values are given in GeV.

$\sim 1\%$. This holds as well for the total width as shown in Tab. 9.5. All this is valid for constant α , G_F and M_Z . In this case the top mass dependence is mainly due to the variation of M_W with m_t . Keeping instead M_W , G_F and M_Z fixed the dependence on m_t is considerably smaller. Remember, however, that the prediction for the decay width has the same uncertainty in this parametrization due to the uncertainty of the experimental value for the W -boson mass.

We have compared our results for the partial leptonic width for zero fermion masses to those of Jegerlehner [50] and Bardin et al. [49], who both use the parametrization with G_F . Furthermore Jegerlehner includes two-loop QCD corrections into the boson self energies. If these are switched off the difference between his and our results is less than 0.1 MeV. Performing the same comparison with Bardin et al., our values for the partial widths are 0.7 MeV to 0.8 MeV larger than theirs. Our results for the QCD corrections agree with those obtained by Alvarez et al. [54].

m_t	$M_H = 50$	$M_H = 100$	$M_H = 300$	$M_H = 1000$
80.0	2.0375	2.0347	2.0283	2.0196
100.0	2.0517	2.0488	2.0423	2.0336
120.0	2.0630	2.0602	2.0537	2.0449
140.0	2.0747	2.0719	2.0654	2.0566
160.0	2.0872	2.0844	2.0780	2.0692
180.0	2.1009	2.0981	2.0917	2.0830
200.0	2.1157	2.1129	2.1066	2.0980

Table 9.5: Total W-decay width Γ^W including first order QCD and electroweak corrections for different values of the top and Higgs masses. All values are given in GeV.

10 The top width

The present lower limit from CDF data indicates that the top mass is at least 89 GeV [57]. Moreover, LEP data in combination with radiative correction calculations require $m_t = 137 \pm 40$ GeV within the minimal standard model [5, 8] at the 1σ level. Therefore the top mass lies presumably above the Wb threshold and the dominant decay of the top quark is the one into a W -boson and a bottom quark ($t \rightarrow Wb$) and the total width of the top quark can be well described by the partial width $\Gamma^{tWb} = \Gamma(t \rightarrow Wb)$.

While the measurement of the top mass will provide a long missing input parameter, the measurement of its width will serve as a consistency check on the standard model. With the operation of LHC, SSC and/or a high energy e^+e^- collider one expects to obtain a sufficiently large number of tops so that both the mass and the width can be measured with good accuracy.

The QCD corrections to the top decay $t \rightarrow Wb$ were already evaluated in [58, 59]. The first order electroweak corrections have been calculated by [60, 61].

The electroweak corrections to this decay involve particularly interesting contributions of $O(\alpha m_t^2/M_W^2)$ which are potentially large for large top masses. Those terms arise not only from fermion loop contributions to the boson self energies but also from the Yukawa couplings of the Higgs fields, which show up in vertex and fermionic self energy corrections. As discussed in Sect. 8.2 contributions of the first type can be eliminated if the Born approximation is expressed by G_F and M_W . Surprisingly the effects from strong Yukawa couplings turn out to be small, as will be demonstrated in the following.

We will only consider the decay of free top quarks and sum over the polarizations of the W -bosons. The results are obtained via crossing from the ones for $W \rightarrow t\bar{b}$.

10.1 Notation and lowest order decay width

Because we want to use our results for the decay $W^+ \rightarrow t\bar{b}$ we consider the decay of an anti-top quark. The corresponding decay width is identical to the one of the top quark because of the CPT theorem.

The lowest order decay of an anti-top quark

$$\bar{t}(p_1) \rightarrow W^-(k)\bar{b}(p_2) \quad (10.1)$$

is described by the Feynman diagram of Fig. 10.1 yielding the amplitude

$$\mathcal{M}_0 = \frac{-e}{\sqrt{2}s_W} V_{tb} \bar{v}(p_1)\not{\omega}_-v(p_2). \quad (10.2)$$

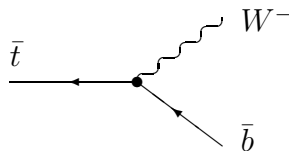


Figure 10.1: Born diagram for the decay $\bar{t} \rightarrow W^-\bar{b}$

It can be obtained from the Born amplitude (6.11) for the decay $W^+ \rightarrow t\bar{b}$ by crossing. This amounts to change the signs of p_1 and k and use $u(-p_1) = v(p_1)$ and $\varepsilon(-k) = \varepsilon(k)$. From (10.2) we get the lowest order width

$$\Gamma_0^{tWb}(m_t, M_W, m_b) = \frac{\alpha}{8} \frac{1}{2s_W^2} |V_{tb}|^2 \frac{\kappa(m_t^2, M_W^2, m_b^2)}{m_t^3} G_1^-, \quad (10.3)$$

with

$$G_1^- = \left[m_t^2 + m_b^2 - 2M_W^2 + \frac{(m_t^2 - m_b^2)^2}{M_W^2} \right]. \quad (10.4)$$

Eq. (10.3) can directly be derived from (9.1) by substituting $m_i \rightarrow m_t$ and $m_j \rightarrow m_b$ in G_1^- coming from the matrix element squared, exchanging M_W and m_t in the phase space factors, changing the spin average from $1/3$ to $1/2$ and supplying a minus sign originating from the different signs of the momenta entering the matrix element squared. This minus sign has been incorporated into the definition of G_1^- which differs from the one in Chap. 9.

Introducing G_F instead of α the lowest order width reads

$$\bar{\Gamma}_0^{tWb}(m_t, M_W, m_b) = \frac{G_F M_W^2}{8\pi\sqrt{2}} |V_{tb}|^2 \frac{\kappa(m_t^2, M_W^2, m_b^2)}{m_t^3} G_1^-. \quad (10.5)$$

10.2 Virtual corrections

With the four Dirac matrix elements

$$\begin{aligned} \mathcal{M}_1^- &= \bar{v}(p_1) \not{\epsilon} \omega_- v(p_2), \\ \mathcal{M}_1^+ &= \bar{v}(p_1) \not{\epsilon} \omega_+ v(p_2), \\ \mathcal{M}_2^- &= \bar{v}(p_1) \omega_- v(p_2) \epsilon \cdot p_1, \\ \mathcal{M}_2^+ &= \bar{v}(p_1) \omega_+ v(p_2) \epsilon \cdot p_1 \end{aligned} \quad (10.6)$$

obtained from (5.11) by setting $p_1 \rightarrow -p_1$ the virtual electroweak one-loop corrections take the form of (9.6) with t and b instead of i and j . The corresponding decay width Γ_1^{tWb} follows from (9.10) using the substitutions specified after (10.4).

The QCD corrections can be extracted from the electroweak ones in the same way as in Sect. 9.4.

10.3 Bremsstrahlung

The real photonic contributions of $O(\alpha)$ to the top width arise from the radiative decay

$$\bar{t}(p_1) \rightarrow W^-(k) \bar{b}(p_2) \gamma(q). \quad (10.7)$$

The corresponding amplitude squared, summed over all polarizations, can be derived from (9.14) by replacing the momenta $k \rightarrow -k$, $p_1 \rightarrow -p_1$ and multiplying an overall factor (-1) . From this we get the bremsstrahlung contribution to the top width by integrating over the appropriate phase space

$$\Gamma_b^{tWb}(m_t, M_W, m_b) = \frac{1}{(2\pi)^5} \frac{1}{2m_t} \int \frac{d^3q}{2q_0} \frac{d^3k}{2k_0} \frac{d^3p_2}{2p_{20}} \delta^{(4)}(p_1 - p_2 - q - k) \frac{1}{2} \sum_{pol} |\mathcal{M}_b|^2$$

$$= \Gamma_0^{tWb} \delta_b^{ew}(m_t, M_W, m_b). \quad (10.8)$$

The correction factor reads

$$\begin{aligned} \delta_b^{ew}(m_t, M_W, m_b) = & \left(-\frac{\alpha}{\pi}\right) \frac{4m_t^2}{\kappa(m_t^2, M_W^2, m_b^2)} \left\{ -Q_t Q_b \left[(M_W^2 - m_t^2 - m_b^2) I_{02} \right] \right. \\ & + Q_t^2 \left[(m_t^2 I_{00} + I_0) - \left(1 + \frac{m_t^2 + m_b^2}{2M_W^2}\right) \frac{I_0^1}{G_1^-} - \frac{I}{G_1^-} \right] \\ & + Q_b^2 \left[(m_b^2 I_{22} + I_2) - \left(1 + \frac{m_t^2 + m_b^2}{2M_W^2}\right) \frac{I_2^1}{G_1^-} - \frac{I}{G_1^-} \right] \\ & + (Q_t - Q_b)^2 \left[(M_W^2 I_{11} + I_1) - \frac{m_t^2 + m_b^2}{2M_W^2} \frac{I}{G_1^-} + 2 \frac{I_{11}^{02}}{G_1^-} \right] \\ & + Q_t(Q_t - Q_b) \left[(M_W^2 + m_t^2 - m_b^2) I_{01} + 2 \frac{I_1^2}{G_1^-} \right] \\ & \left. - Q_b(Q_t - Q_b) \left[(M_W^2 - m_t^2 + m_b^2) I_{12} + 2 \frac{I_1^0}{G_1^-} \right] \right\}. \quad (10.9) \end{aligned}$$

The bremsstrahlung phase space integrals carry the arguments $I_{\dots} = I_{\dots}(m_t, M_W, m_b)$. They are given in App. D.

From eq. (10.9) the gluonic bremsstrahlung corrections can be obtained by setting $Q_t = Q_b = 1$, replacing α by the strong coupling constant α_s and multiplying with the colour factor $C_F = \frac{4}{3}$.

10.4 Results and discussion

We again use the parameters listed in Sect. 8.1 as numerical input and calculate the W -mass from the relation (8.23). Unless stated otherwise, we choose for the Higgs mass $M_H = 100$ GeV.

We perform the same summation of the leading higher order corrections as discussed in Sect. 9.5, eq. (9.20), and introduce the parametrization with G_F and M_W as in (9.22). In this parametrization the large corrections arising from the renormalization of α and s_W^2 are absorbed into the lowest order expression. This is not the case for large contributions proportional to $\alpha m_t^2/M_W^2$ arising from vertex and fermion self energy diagrams with enhanced Yukawa couplings.

In Tab. 10.1 we give the lowest order width as well as the width including electroweak corrections in both parametrizations for various values of the top mass together with the W -mass obtained from (8.23). The results for the first order expressions of both parametrizations agree within 0.05%.

According to (10.3) the width increases with the top mass approximately like m_t^3/M_W^2 . The corresponding relative corrections are shown in Fig. 10.2. The QCD corrections yield about -10% with only a weak dependence on the top mass. In the on-shell scheme we find sizable electroweak corrections which range from $+7\%$ at $m_t = 100$ GeV to -13%

m_t	M_W	Γ_0^{tWb}	$\bar{\Gamma}_0^{tWb}$	Γ_{ew}^{tWb}	$\bar{\Gamma}_{ew}^{tWb}$
100.0	79.99	0.0887	0.0940	0.0951	0.0951
120.0	80.10	0.3095	0.3260	0.3306	0.3305
140.0	80.23	0.6393	0.6684	0.6788	0.6786
160.0	80.37	1.0850	1.1248	1.1435	1.1433
180.0	80.52	1.6627	1.7071	1.7365	1.7362
200.0	80.69	2.3927	2.4299	2.4724	2.4720
220.0	80.88	3.2989	3.3083	3.3665	3.3661

Table 10.1: Top decay width Γ^{tWb} parametrized by α and $\bar{\Gamma}^{tWb}$ by G_F in lowest order and including electroweak corrections. All values are given in GeV.

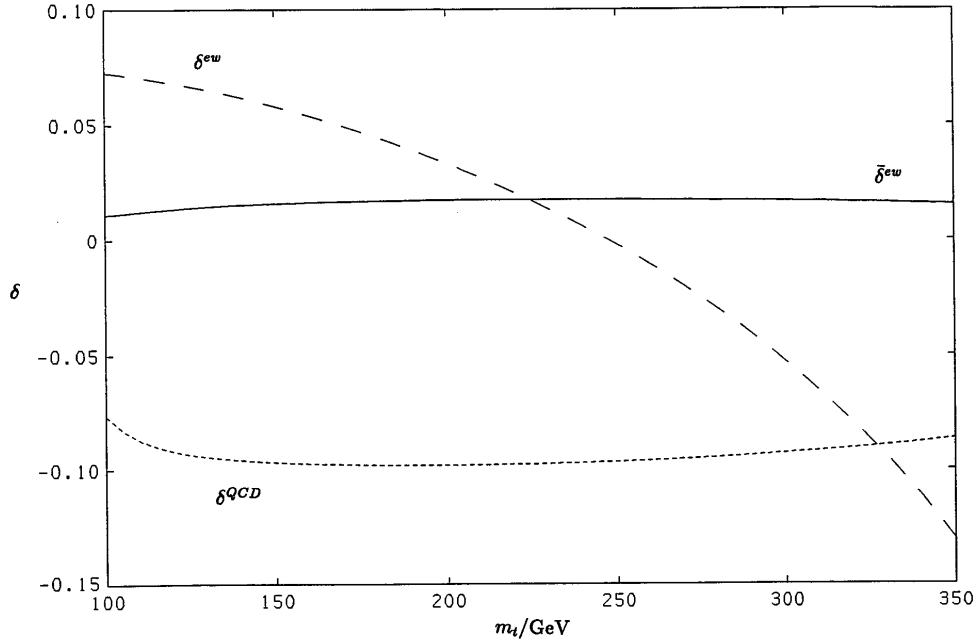


Figure 10.2: Electroweak radiative corrections δ^{ew} and $\bar{\delta}^{ew}$ and QCD corrections δ^{QCD} to the top decay width versus the top mass.

m_t/GeV	200	300	500	1000
leading term	0.023	0.036	0.051	-0.070
next to leading term	-0.043	-0.065	-0.108	-0.217

Table 10.2: The two leading terms of the expansion in eq. (10.10) for various values of the top quark mass.

at $m_t = 350$ GeV. The large variation arises from terms $\propto \alpha m_t^2/M_W^2$ in the first order corrections. Contrarily in the parametrization with G_F the corrections are only $\approx +1\%$ for $m_t = 100$ GeV and remain almost constant at $\approx +1.7\%$ for $m_t \geq 160$ GeV. This feature is independent of the Higgs boson mass. However, we expected large corrections $\propto m_t^2$ to arise from the vertex diagrams containing large Yukawa couplings; in the similar case of $Z^0 \rightarrow b\bar{b}$ the corresponding contributions are noticeable. The slow variation of the relative correction in this parametrization indicates that the strong Yukawa couplings have no sizable effect on the top width. In order to demonstrate the absence of large corrections the plot in Fig. 10.2 has been extended up to $m_t = 350$ GeV, although this is well above the present upper limits on the top quark mass.

Some understanding of this surprising feature can be obtained from the expansion of the relative correction factor in the parametrization with G_F and M_W , $\bar{\delta}^{ew}$, for large top quark masses ($m_t \gg M_W, M_Z, M_H$)

$$\bar{\delta}^{ew} = \delta_1^{ew} - \Delta r \sim \frac{\alpha}{4\pi} \frac{1}{2s_W^2} \frac{m_t^2}{M_W^2} \left\{ \left[\frac{17}{4} + \log\left(\frac{M_H^2}{m_t^2}\right) \right] + \left[-\frac{7}{2}\pi \frac{M_H}{m_t} \right] + O\left(\log^2\left(\frac{m_t^2}{M_i^2}\right)\right) \right\} \quad (10.10)$$

with $M_i = M_W, M_Z, M_H$. The two leading terms are evaluated in Tab. 10.2 for a wide range of values of the top quark mass and $M_W = 80$ GeV, $M_H = 100$ GeV. For $m_t < 1$ TeV we find the leading term of the expansion to be smaller than the next to leading term. Consequently the expansion is only asymptotic and the contributions $\propto \alpha m_t^2/M_W^2$ are not dominant unless the top mass has a value of several TeV. In the physically acceptable range of top quark masses, the quadratic terms are numerically compensated by logarithmic contributions. This remains true also for large Higgs masses. The small corrections result from intricate cancellations between leading and nonleading terms.

In Fig. 10.3 we show the lowest order width in both parametrizations $\Gamma_0, \hat{\Gamma}_0$, the electroweak corrections $\delta\Gamma_{ew}$, the QCD corrections $\delta\Gamma_{QCD}$ as well as the fully corrected width Γ as a function of the top quark mass.

The dependence of the total width on the Higgs mass is displayed in Tab. 10.3 where this parameter is varied from 50 to 1000 GeV. Although the influence of M_H becomes stronger for large top masses it never exceeds 1%.

We have compared the pure QCD corrections to those obtained in [58] and found complete agreement. Our results for the electroweak corrections agree with those of [61].

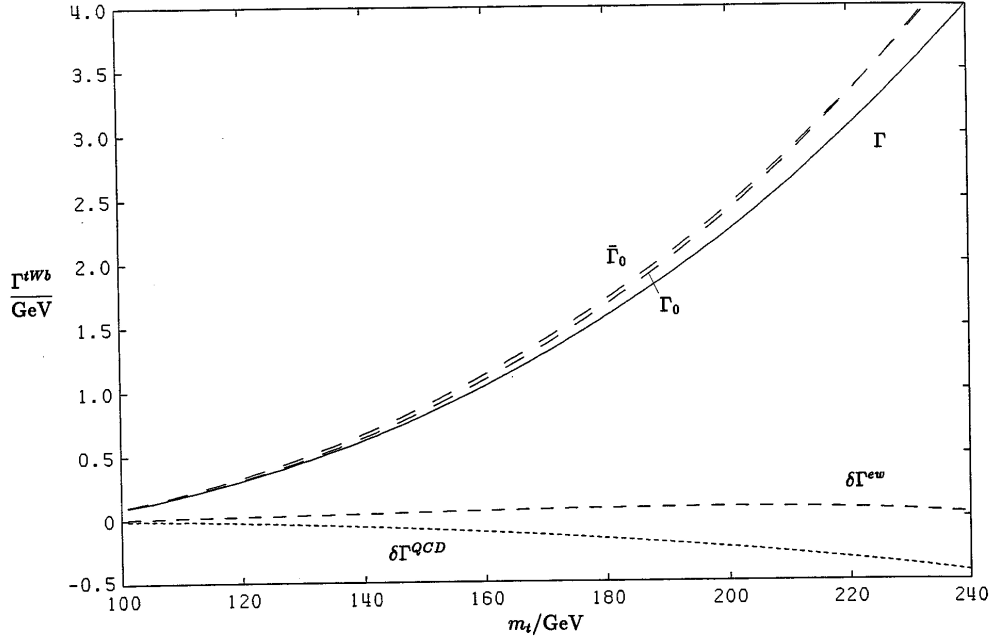


Figure 10.3: Top decay width Γ^{tWb} versus the top mass in lowest order Γ_0 , $\bar{\Gamma}_0$ including all corrections Γ and the contribution of the electroweak $\delta\Gamma_{ew}$ and QCD corrections $\delta\Gamma_{QCD}$.

m_t	$M_H = 50$	$M_H = 100$	$M_H = 300$	$M_H = 1000$
100.0	0.0882	0.0883	0.0886	0.0891
120.0	0.3022	0.3021	0.3020	0.3022
140.0	0.6179	0.6174	0.6165	0.6157
160.0	1.0385	1.0377	1.0356	1.0329
180.0	1.5742	1.5734	1.5697	1.5641
200.0	2.2373	2.2376	2.2321	2.2221
220.0	3.0411	3.0438	3.0369	3.0207

Table 10.3: Top decay width Γ^{tWb} including first order QCD and electroweak corrections for different values of the Higgs mass. All values are given in GeV.

11 W -pair production

One of the predominant aims of LEP200 is the high precision investigation of the properties of the W -boson, i.e. its mass, its total and partial widths and its couplings. Probably the most interesting aspect will be the study of the nonabelian gauge interaction which has no direct experimental evidence so far.

The general properties of W -pair production at LEP200 have been studied in [62, 63]. While the total cross section of $e^+e^- \rightarrow W^+W^-$ is extremely sensitive to deviations from the triple gauge boson couplings of the SM at energies high above the production threshold, the sensitivity to variations of this coupling in the LEP200 energy range is only at the percent level. Consequently theoretical predictions should be better than 1% to obtain reasonable limits on the structure of the gauge boson self interaction.

The W -pair production process allows an independent direct measurement of the W -boson mass with an expected accuracy of about 100 MeV [47]. Again this requires the knowledge of the total cross section with a precision better than 1%.

Much effort has been made in recent years to obtain such precise theoretical predictions for W -pair production. The virtual electroweak and soft photonic corrections were calculated by several authors [64, 65, 66, 67]. The complete analytical results for arbitrary polarizations of the external particles were published in [66]. These will be used for our evaluations. For the unpolarized case they numerically agree with those of [67] better than 0.3% and essentially also with [64]. The hard photon bremsstrahlung corrections have been evaluated by [68, 14, 69, 70] for definite initial and final state polarizations. The effects arising from the finite width of the W -bosons have been studied in the Born approximation in [71] and including the leading weak corrections in [72]. Recently also the hard bremsstrahlung to the process $e^+e^- \rightarrow W^+W^- \rightarrow 4$ fermions has been evaluated [73].

In the following we will review and update existing results for the virtual and real electroweak corrections and the finite width effects. We will add some new results on approximate formulae for the W -pair production cross section.

11.1 Notation and amplitudes

We discuss the process

$$e^+(p_1, \sigma_1) + e^-(p_2, \sigma_2) \rightarrow W^+(k_1, \lambda_1) + W^-(k_2, \lambda_2). \quad (11.1)$$

The arguments indicate the momenta and helicities of the incoming fermions and outgoing bosons ($\sigma_i = \pm\frac{1}{2}$, $\lambda_i = 1, 0, -1$). We introduce the usual Mandelstam variables

$$\begin{aligned} s &= (p_1 + p_2)^2 = (k_1 + k_2)^2 = 4E^2, \\ t &= (p_1 - k_1)^2 = (p_2 - k_2)^2 = M_W^2 - 2E^2 + 2E^2\beta \cos \vartheta. \end{aligned} \quad (11.2)$$

Here E is the beam energy, ϑ the scattering angle between the e^- and the W^- and $\beta = \sqrt{1 - M_W^2/E^2}$ the velocity of the W -bosons in the center of mass frame. The electron mass has been consistently neglected.

In the approximation of zero electron mass the invariant matrix element vanishes due to chiral symmetry for equal helicities of the e^+ and e^- . Consequently we can write

$$\mathcal{M}(\sigma_1, \sigma_2, \lambda_1, \lambda_2, s, t) = \mathcal{M}(\sigma, \lambda_1, \lambda_2, s, t) \quad (11.3)$$

with $\sigma = \sigma_2 = -\sigma_1$. If we neglect the CP-violating phase in the quark mixing matrix, CP is a symmetry of the process leading to the relation

$$\mathcal{M}(\sigma, \lambda_1, \lambda_2, s, t) = \mathcal{M}(\sigma, -\lambda_2, -\lambda_1, s, t). \quad (11.4)$$

Consequently there are only 12 independent helicity matrix elements instead of 36.

As discussed in Chap. 5 the general matrix element

$$\mathcal{M}(\sigma, \lambda_1, \lambda_2, s, t) = \bar{v}(p_1, -\sigma) \mathcal{M}^{\mu\nu} u(p_2, \sigma) \varepsilon_\mu(k_1, \lambda_1) \varepsilon_\nu(k_2, \lambda_2) \quad (11.5)$$

can be decomposed into formfactors and standard matrix elements. Due to the above-mentioned symmetries we do not need all of the (overcomplete) 40 standard matrix elements given in (5.14) for a general process of vector pair production in fermion-antifermion annihilation, but only seven for each fermion helicity

$$\mathcal{M}(\sigma, \lambda_1, \lambda_2, s, t) = \sum_{i=1}^7 \mathcal{M}_i^\sigma F_i^\sigma(s, t). \quad (11.6)$$

The standard matrix elements \mathcal{M}_i^σ are defined in (5.14) together with

$$\begin{aligned} \mathcal{M}_3^\sigma &= \mathcal{M}_{3,1}^\sigma + \mathcal{M}_{3,2}^\sigma, \\ \mathcal{M}_4^\sigma &= \mathcal{M}_{4,1}^\sigma + \mathcal{M}_{4,2}^\sigma, \\ \mathcal{M}_7^\sigma &= \mathcal{M}_{7,1}^\sigma + \mathcal{M}_{7,2}^\sigma. \end{aligned} \quad (11.7)$$

Only six are linear independent. Using (5.15) we can express \mathcal{M}_7 by the others

$$\mathcal{M}_7^\sigma = -\frac{s}{2}(\mathcal{M}_1^\sigma + \mathcal{M}_2^\sigma) + \frac{M_W^2 - t}{2} \mathcal{M}_3^\sigma + \frac{s}{2} \mathcal{M}_4^\sigma + \mathcal{M}_5^\sigma. \quad (11.8)$$

Therefore there are only twelve independent formfactors. The standard matrix elements can be calculated with the methods described in Sect. 5.3. The explicit results can be found in [66, 74].

11.2 Born cross section

At the Born level three diagrams contribute to W -pair production (Fig. 11.1). We omitted a Higgs-exchange diagram, which is suppressed by a factor m_e/M_W and thus completely negligible. The t -channel ν_e -exchange diagram contributes only for left-handed

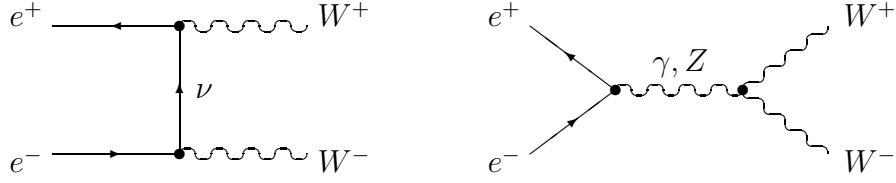


Figure 11.1: Born diagrams for $e^+e^- \rightarrow W^+W^-$.

electrons whereas the s -channel diagrams containing the nonabelian gauge coupling contribute also for right handed electrons. The analytical expressions read

$$\begin{aligned}
\mathcal{M}_0(-, \lambda_1, \lambda_2, s, t) &= \mathcal{M}_1^- \frac{e^2}{2s_W^2} \frac{1}{t} + 2(\mathcal{M}_3^- - \mathcal{M}_2^-) e^2 \left[\frac{1}{s} - \frac{c_W}{s_W} g_e^- \frac{1}{s - M_Z^2} \right] \\
&= \frac{e^2}{2s_W^2} \left[\frac{1}{t} \mathcal{M}_1^- + \frac{2}{s - M_Z^2} (\mathcal{M}_3^- - \mathcal{M}_2^-) \right] \\
&\quad + e^2 \left[\frac{1}{s} - \frac{1}{s - M_Z^2} \right] 2(\mathcal{M}_3^- - \mathcal{M}_2^-), \tag{11.9}
\end{aligned}$$

$$\begin{aligned}
\mathcal{M}_0(+, \lambda_1, \lambda_2, s, t) &= 2(\mathcal{M}_3^+ - \mathcal{M}_2^+) e^2 \left[\frac{1}{s} - \frac{c_W}{s_W} g_e^+ \frac{1}{s - M_Z^2} \right] \\
&= e^2 \left[\frac{1}{s} - \frac{1}{s - M_Z^2} \right] 2(\mathcal{M}_3^+ - \mathcal{M}_2^+),
\end{aligned}$$

where we have inserted the explicit form of the Z -boson fermion couplings g_e^- , g_e^+ (A.14). The corresponding cross section for arbitrary longitudinal polarizations of the leptons and bosons is given by

$$\left(\frac{d\sigma}{d\Omega} \right)_0 = \frac{\beta}{64\pi^2 s} \sum_{\lambda_1, \lambda_2} \frac{1}{4} (1 - 2\sigma P^+) (1 + 2\sigma P^-) |\mathcal{M}_0(\sigma, \lambda_1, \lambda_2, s, t)|^2, \tag{11.10}$$

and P^\pm are the polarization degrees of the leptons ($P^- = \pm 1$ corresponds to purely right- and left-handed electrons, respectively).

The Born cross section determines the main features of W -pair production. We first study the threshold behaviour [75, 76]. For small β the matrix elements behave as

$$\mathcal{M}_2^\sigma, \mathcal{M}_3^\sigma \propto \beta, \quad \mathcal{M}_1^\sigma \propto 1. \tag{11.11}$$

Consequently the s -channel diagrams vanish at threshold and the t -channel graph dominates in the threshold region. For $\beta \ll 1$ the total cross section is given by

$$\sigma_0(s) \approx \frac{\pi\alpha^2}{s} \frac{1}{4s_W^4} 4\beta + O(\beta^3). \tag{11.12}$$

All terms $\propto \beta^2$ which are present in the differential cross section drop out in the total cross section. s -channel diagrams yield contributions $\propto \beta^3$. In the SM the coefficient of the β^3

term in (11.12) is roughly equal to the one of the leading β term. As long as that coefficient is not enhanced drastically the β^3 term is negligible in the threshold region, i.e. for $2M_W < \sqrt{s} < 2M_W + 10$ GeV (for $\sqrt{s} = 2M_W + 10$ GeV we have $\beta = 0.33$ and $\beta^3 = 0.04$). Consequently the shape of the total cross section close to threshold is completely governed by the linear rise in β and hence by kinematics alone. Any change in the couplings will only affect the coefficient of the β term and thus the normalization of the cross section. Moreover many new physics effects such as anomalous gauge couplings contribute to the s -channel only and thus do not affect the leading term. The inclusion of the finite width of the W -boson smears the threshold considerably (see Sect. 11.5). However, since the next to leading β^3 term becomes only sizable several Γ^W above threshold only the leading term is relevant for the cross section in the region of the nominal threshold.

This fact allows a model independent determination of the W -mass from the W -pair production threshold [75]. The measured cross section up to about 10 GeV above threshold is fitted with a three-parameter curve

$$\sigma(s) = \frac{a}{s} + b \sigma_{SM}(M_W, s) \quad (11.13)$$

where a/s accounts for the background, b is a model dependent normalization factor and σ_{SM} the W -pair production cross section in the SM depending on the W -mass. Eq. (11.13) is valid including radiative corrections and finite width effects.

At high energies the W -pair production cross section is subject to large gauge cancellations arising from the contributions of longitudinally polarized W -bosons. For $s \gg M_W^2$ the matrix elements behave as

$$\frac{\mathcal{M}_1^\sigma}{t}, \frac{\mathcal{M}_{2,3}^\sigma}{s} \sim \frac{s}{M_W^2}, \quad (11.14)$$

but

$$\begin{aligned} \frac{1}{t} \mathcal{M}_1^\sigma + \frac{1}{s - M_Z^2} 2(\mathcal{M}_3^\sigma - \mathcal{M}_2^\sigma) &\sim \frac{M_W^2}{t} + O(1), \\ \left(\frac{1}{s} - \frac{1}{s - M_Z^2} \right) 2(\mathcal{M}_3^\sigma - \mathcal{M}_2^\sigma) &\sim O(1). \end{aligned} \quad (11.15)$$

Consequently the Born matrix elements (11.9) have a good high energy behaviour. While the cross sections corresponding to the s -channel or t -channel diagrams alone violate unitarity at high energies

$$\sigma_{0,t}(s) \approx \sigma_{0,s}(s) \approx \frac{\pi\alpha^2}{s} \frac{1}{4s_W^4} \frac{s^2}{24M_W^4}, \quad (11.16)$$

the SM cross section respects it

$$\sigma_0 \approx \frac{\pi\alpha^2}{s} \frac{1}{4s_W^4} \left[2 \left(\log \frac{s}{M_W^2} - 1 \right) - \frac{1}{2} - \frac{1}{3c_W^2} + \frac{5}{24c_W^4} \right]. \quad (11.17)$$

The gauge cancellations are illustrated in Fig. 11.2. They reach one order of magnitude at 400 GeV and two orders at 1 TeV. They only occur for longitudinal W -bosons. After the gauge cancellations the t -channel again dominates the SM cross section. Compared to

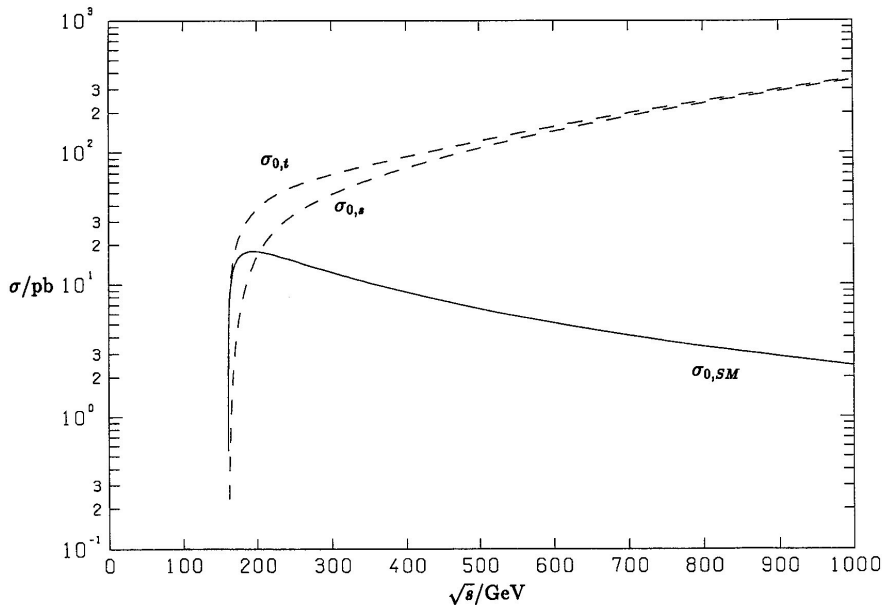


Figure 11.2: Gauge cancellations in the total cross section for W -pair production. Shown are the Born cross sections arising from the s -channel $\sigma_{0,s}$ and t -channel $\sigma_{0,t}$ diagrams alone and the SM cross section σ_0 .

the t -channel contribution all other contributions to the total cross section are suppressed by $\sim 50 \log(s/M_W^2)$. For example the cross section for right handed electrons is

$$\sigma_0(e_R^- e^+ \rightarrow W^+ W^-) \approx \frac{\pi\alpha^2}{s} \frac{1}{12c_W^4}, \quad (11.18)$$

and the cross section for longitudinal W -bosons

$$\sigma_0(e^- e^+ \rightarrow W_L^+ W_L^-) \approx \frac{\pi\alpha^2}{s} \frac{1}{24c_W^4} \left(\frac{1}{4s_W^4} + 1 \right). \quad (11.19)$$

We now consider the complete Born expressions for the W -pair production cross section. The differential cross section for the unpolarized case and for longitudinally polarized W -bosons is shown in Fig. 11.3 and 11.4, respectively. Due to the t -channel pole the unpolarized cross section is strongly peaked in forward direction at high energies and drops smoothly with increasing scattering angle. In contrast the differential cross section for longitudinal W -bosons has a minimum for a certain energy dependent finite scattering angle $\neq \pi$.

In order to show the importance of the separate contributions we give in Tab. 11.1 the integrated cross section for different center of mass energies and different polarizations of the leptons and W -bosons.

The gauge cancellations depend crucially on the values of the SM couplings. Any deviations from these values can lead to sizable effects at higher energies since they are enhanced by a factor $\beta s/M_W^2$. This fact concerns especially anomalous three gauge boson

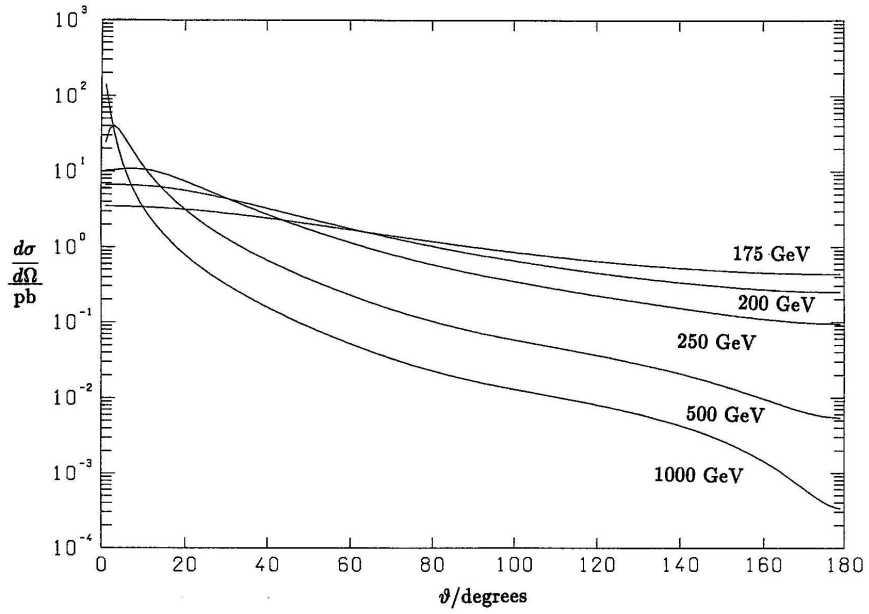


Figure 11.3: Lowest order differential cross section for the production of unpolarized

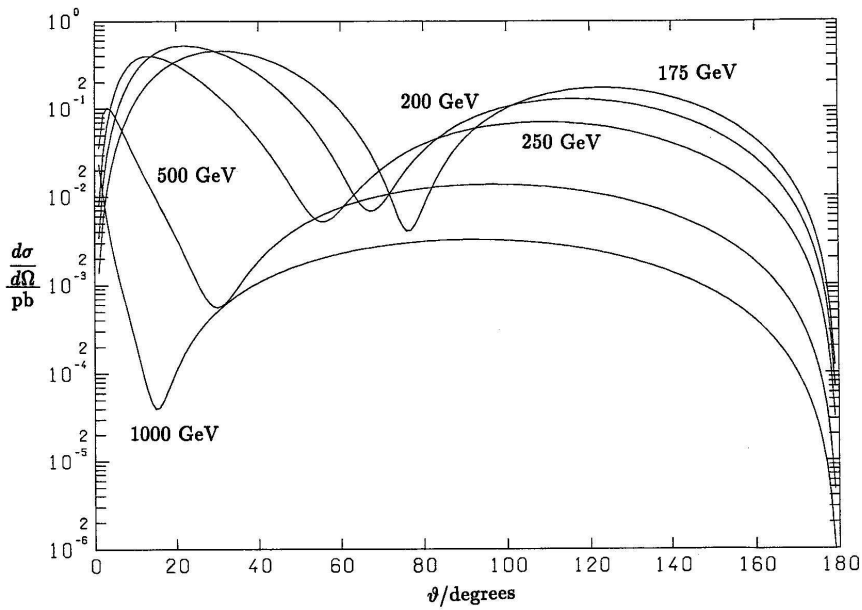


Figure 11.4: Lowest order differential cross section for the production of longitudinal W -pairs at different center of mass energies.

\sqrt{s}/GeV	σ_0/pb					
	unpolarized	e_L^-	e_R^-	$W_T^+W_T^-$	$W_L^+W_L^-$	$W_T^+W_L^- + W_L^+W_T^-$
165.0	10.761	21.466	0.056	5.254	1.349	4.158
180.0	16.928	33.600	0.256	9.397	1.743	5.788
200.0	17.709	35.070	0.348	11.189	1.428	5.092
250.0	15.011	29.745	0.277	11.487	0.731	2.793
500.0	6.534	13.019	0.050	6.178	0.113	0.244
1000.0	2.439	4.867	0.010	2.395	0.027	0.017

Table 11.1: Integrated lowest order cross section for different polarizations and different center of mass energies and $M_W = 80.23$ GeV.

couplings which have been studied by many authors [77]. The sensitivity to these effects is best at high energies and large scattering angles where the t -channel pole is not dominant. Nevertheless one hopes to determine the anomalous couplings up to 20% at LEP200 [6].

Using right-handed electrons one could study a pure triple gauge coupling process, but this would require longitudinally polarized electron beams. Furthermore the right-handed cross section is suppressed by two orders of magnitude compared to the dominant left-handed mode, mainly because there is no t -channel contribution. On the other hand, nonstandard couplings or other new physics can enhance it drastically exactly for this reason.

11.3 Virtual and soft photonic corrections

The radiative corrections can be naturally divided into three classes, the virtual corrections, the soft photonic, and the hard photonic corrections. Since the process $e^+e^- \rightarrow W^+W^-$ involves the charged current, the radiative corrections cannot be separated into electromagnetic and weak ones in a gauge invariant way. We first discuss the virtual and soft photonic corrections.

11.3.1 Virtual corrections

The virtual corrections get contributions from the ν_e -, γ - and Z -self energies, the γ - Z -mixing energy, from the vertex corrections to the $ee\gamma$ -, eeZ -, $e\nu_e W$ -, $WW\gamma$ - and WWZ -vertices and from box diagrams. The necessary counterterms involve in addition the e - and W -self energies. Altogether one has to calculate more than 200 individual diagrams. These can be treated using the methods described in the first part of this review. The number of generic diagrams to be evaluated is about 30. The results can be expressed in terms of the formfactors defined in (11.6)

$$\delta\mathcal{M}_1(\sigma, \lambda_1, \lambda_2, s, t) = \sum_{i=1}^7 \mathcal{M}_i^\sigma \delta F_i^\sigma. \quad (11.20)$$

The formfactors δF_i^σ can be evaluated for every CP-invariant set of diagrams separately. For CP-violating diagrams we need in addition the standard matrix elements $\mathcal{M}_{3,1}^\sigma - \mathcal{M}_{3,2}^\sigma$, $\mathcal{M}_{4,1}^\sigma - \mathcal{M}_{4,2}^\sigma$ and $\mathcal{M}_{7,1}^\sigma - \mathcal{M}_{7,2}^\sigma$. These drop out in CP-invariant combinations. The explicit analytical results for the formfactors are given in terms of the scalar coefficients of tensor integrals in [66, 74]. The reduction to scalar integrals and their evaluation is done numerically using the formulae given in Chap. 4. The contribution of the virtual corrections to the cross section is given by

$$\delta \left(\frac{d\sigma}{d\Omega} \right)_V = \frac{\beta}{64\pi^2 s} \sum_{\lambda_1, \lambda_2} \frac{1}{4} (1 - 2\sigma P^+) (1 + 2\sigma P^-) 2\text{Re} (\mathcal{M}_0^* \delta \mathcal{M}_1). \quad (11.21)$$

The cancellations already present at the Born level occur as well at the level of radiative corrections. These cancellations only work for gauge invariant quantities. Consequently the inclusion of the leading higher order contributions must be done such that gauge invariance is respected. Otherwise one may introduce sizable unphysical corrections. This will be discussed in more detail in Sect. 11.3.3.

The presence of these cancellations enforces very careful tests of the numerical stability of the computer programs. The reliability of the results is founded on agreement between independent calculations [66, 67].

11.3.2 Soft photonic corrections

The soft photonic corrections can be easily obtained using the results of Chap. 7. The soft photon matrix element reads (k is the photon momentum)

$$\mathcal{M}_s = e\mathcal{M}_0 \left[\frac{\varepsilon p_2}{k p_2} - \frac{\varepsilon p_1}{k p_1} + \frac{\varepsilon k_1}{k k_1} - \frac{\varepsilon k_2}{k k_2} \right]. \quad (11.22)$$

This yields the soft photon cross section as

$$\left(\frac{d\sigma}{d\Omega} \right)_s = \left(\frac{d\sigma}{d\Omega} \right)_0 \delta_s \quad (11.23)$$

with

$$\begin{aligned} \delta_s &= -\frac{\alpha}{2\pi^2} \int_{|k| < \Delta E} \frac{d^3 k}{2\omega_k} \left\{ \frac{p_1^2}{(p_1 k)^2} + \frac{p_2^2}{(p_2 k)^2} - \frac{2p_1 p_2}{(p_1 k)(p_2 k)} \right. \\ &\quad + \frac{k_1^2}{(k_1 k)^2} + \frac{k_2^2}{(k_2 k)^2} - \frac{2k_1 k_2}{(k_1 k)(k_2 k)} \\ &\quad \left. - \frac{2p_1 k_1}{(p_1 k)(k_1 k)} - \frac{2p_2 k_2}{(p_2 k)(k_2 k)} + \frac{2p_1 k_2}{(p_1 k)(k_2 k)} + \frac{2p_2 k_1}{(p_2 k)(k_1 k)} \right\} \\ &= -\frac{\alpha}{\pi} \left\{ 4 \log \frac{2\Delta E}{\lambda} - 2 \log \frac{2\Delta E}{\lambda} \log \frac{s}{m_e^2} + 4 \log \frac{2\Delta E}{\lambda} \log \frac{M_W^2 - u}{M_W^2 - t} \right. \\ &\quad \left. + \frac{1 + \beta^2}{\beta} \log \frac{2\Delta E}{\lambda} \log \left(\frac{1 - \beta}{1 + \beta} \right) \right\} \end{aligned}$$

$$\begin{aligned}
& + \log \frac{m_e^2}{s} + \frac{1}{\beta} \log \left(\frac{1-\beta}{1+\beta} \right) + \frac{\pi^2}{3} + \frac{1}{2} \log^2 \frac{m_e^2}{s} \\
& + \frac{1+\beta^2}{\beta} \left[\text{Li}_2 \left(\frac{2\beta}{1+\beta} \right) + \frac{1}{4} \log^2 \left(\frac{1-\beta}{1+\beta} \right) \right] \\
& + 2 \left[\text{Li}_2 \left(1 - \frac{s(1-\beta)}{2(M_W^2 - t)} \right) + \text{Li}_2 \left(1 - \frac{s(1+\beta)}{2(M_W^2 - t)} \right) \right. \\
& \quad \left. - \text{Li}_2 \left(1 - \frac{s(1-\beta)}{2(M_W^2 - u)} \right) - \text{Li}_2 \left(1 - \frac{s(1+\beta)}{2(M_W^2 - u)} \right) \right] \Big\}.
\end{aligned} \tag{11.24}$$

Adding the soft photon cross section to the contribution of the virtual corrections (11.21) the IR-singularities cancel. Moreover also the large Sudakov double logarithms $\log^2(m_e^2/s)$ drop out.

11.3.3 Leading weak corrections

In order to set up improved Born approximations which are often very handy the first step is to extract the leading corrections [78]. The universal corrections involving $\Delta\alpha$ and $\Delta\rho$ can be easily obtained from (8.25) including the leading $O(\alpha^2)$ contributions. There are no nonuniversal corrections $\propto \alpha m_t^2/M_W^2$ to the W -pair production cross section for not too high energies, i.e. as long as the unitarity cancellations are not sizeable. In the LEP200 energy region also terms involving $\log m_t^2$ or $\log M_H^2$ may become important. These have been evaluated in the limit $M_H^2, m_t^2 \gg s$. In addition close to threshold apart from the large bremsstrahlung corrections which will be discussed in the next section there is a sizable effect of the Coulomb singularity. This can be simply obtained from general considerations or to $O(\alpha)$ directly from the loop diagrams involving photons exchanged between the final state W -bosons. Altogether this yields the following approximation

$$\begin{aligned}
\mathcal{M}_a^- &= \frac{e^2}{2s_W^2} \left[\frac{1}{t} \mathcal{M}_1^- + \frac{1}{s - M_Z^2} 2(\mathcal{M}_3^- - \mathcal{M}_2^-) \right] \left[\frac{1}{1 - \Delta\alpha} \frac{1}{1 + \frac{c_W^2}{s_W^2} \Delta\rho} \right. \\
&\quad \left. + \frac{\alpha}{4\pi} \frac{1}{2s_W^2} \left(\frac{1}{3} - \frac{c_W^2}{s_W^2} \right) \log \frac{m_t^2}{M_W^2} + \frac{\alpha}{4\pi} \frac{11}{6} \frac{1}{2s_W^2} \log \frac{M_H^2}{M_W^2} + \frac{\alpha\pi}{4\beta} \right] \\
&\quad + e^2 \left(\frac{1}{s} - \frac{1}{s - M_Z^2} \right) 2(\mathcal{M}_3^- - \mathcal{M}_2^-) \left[\frac{1}{1 - \Delta\alpha} + \frac{\alpha\pi}{4\beta} \right] \\
&\quad + e^2 \frac{\alpha}{4\pi} \frac{1}{s - M_Z^2} 2(\mathcal{M}_3^- - \mathcal{M}_2^-) \left[\frac{4s_W^2 - 3}{12c_W^2 s_W^4} \log \frac{m_t^2}{M_W^2} - \frac{1}{48c_W^2 s_W^4} \log \frac{M_H^2}{M_W^2} \right], \\
\mathcal{M}_a^+ &= e^2 \left(\frac{1}{s} - \frac{1}{s - M_Z^2} \right) 2(\mathcal{M}_3^+ - \mathcal{M}_2^+) \left[\frac{1}{1 - \Delta\alpha} + \frac{\alpha\pi}{4\beta} \right]
\end{aligned} \tag{11.25}$$

$$+ e^2 \frac{\alpha}{4\pi} \frac{1}{s - M_Z^2} 2(\mathcal{M}_3^+ - \mathcal{M}_2^+) \frac{1}{6s_W^2 c_W^2} \left[\log \frac{m_t^2}{M_W^2} - \frac{1}{4} \log \frac{M_H^2}{M_W^2} \right].$$

All terms in (11.25) respect the high energy cancellations apart from those involving $\log m_t^2$ and $\log M_H^2$. However, these were obtained for $M_H^2, m_t^2 \gg s$, whereas the unitarity cancellations work for $s \gg M_H^2, m_t^2$. In this limit the terms containing $\log m_t^2$ and $\log M_H^2$ are absent. These may, however, cause large effects for small energies and large top quark or Higgs boson masses. This phenomenon was called delayed unitarity cancellation in [79]. Introducing G_F instead of e^2/s_W^2 and the running $\alpha(s)$ we obtain

$$\begin{aligned} \mathcal{M}_a^- &= 2\sqrt{2}G_F M_W^2 \left[\frac{1}{t} \mathcal{M}_1^- + \frac{1}{s - M_Z^2} 2(\mathcal{M}_3^- - \mathcal{M}_2^-) \right] \left[1 + \frac{\alpha\pi}{4\beta} + C_1^-(s, t) \right] \\ &+ 4\pi\alpha(s) \left(\frac{1}{s} - \frac{1}{s - M_Z^2} \right) 2(\mathcal{M}_3^- - \mathcal{M}_2^-) \left[1 + \frac{\alpha\pi}{4\beta} + C_2^-(s, t) \right] \\ &+ e^2 \frac{\alpha}{4\pi} \frac{1}{s - M_Z^2} 2(\mathcal{M}_3^- - \mathcal{M}_2^-) \left[\frac{4s_W^2 - 3}{12c_W^2 s_W^4} \log \frac{m_t^2}{M_Z^2} - \frac{1}{48c_W^2 s_W^4} \log \frac{M_H^2}{s} \right], \\ \mathcal{M}_a^+ &= 4\pi\alpha(s) \left(\frac{1}{s} - \frac{1}{s - M_Z^2} \right) 2(\mathcal{M}_3^+ - \mathcal{M}_2^+) \left[1 + \frac{\alpha\pi}{4\beta} + C_2^+(s, t) \right] \\ &+ 2\sqrt{2}G_F M_W^2 \left[\frac{1}{t} \mathcal{M}_1^+ + \frac{1}{s - M_Z^2} 2(\mathcal{M}_3^+ - \mathcal{M}_2^+) \right] C_1^+(s, t) \\ &+ e^2 \frac{\alpha}{4\pi} \frac{1}{s - M_Z^2} 2(\mathcal{M}_3^+ - \mathcal{M}_2^+) \frac{1}{6s_W^2 c_W^2} \left[\log \frac{m_t^2}{M_Z^2} - \frac{1}{4} \log \frac{M_H^2}{s} \right]. \end{aligned} \quad (11.26)$$

We have included four functions $C_i(s, t)$, $i = 1, 2$, $\sigma = \pm$ in this approximation. These are necessary to describe the angular dependence of the differential cross section. The complete one-loop invariant matrix element for W -pair production involves 12 formfactors F_i^σ . It turns out, however, that only four of them namely the C_i^σ are relevant in the LEP200 energy region. For higher energies even C_1^+ can be omitted. The functions C_i^σ have been determined such that they reproduce the corresponding exact one-loop formfactors sufficiently well in the LEP200 energy region [78].

We want to stress that the naive summation of the Dyson series of the self energies may lead to incorrect results, i.e. a wrong high energy behaviour. This happens because the leading corrections are not only contained in the self energies but also in the vertex corrections. The actual place of their appearance depends on the choice of the field renormalization.

11.3.4 Numerical results for the virtual and soft photonic corrections

We now present some numerical results for the radiative corrections in the soft photon approximation. The numerical input parameters are defined in Sect. 8.1. The soft photon cutoff is chosen as $\Delta E/E = 0.1$. Different choices of $\Delta E/E$ uniformly shift the absolute

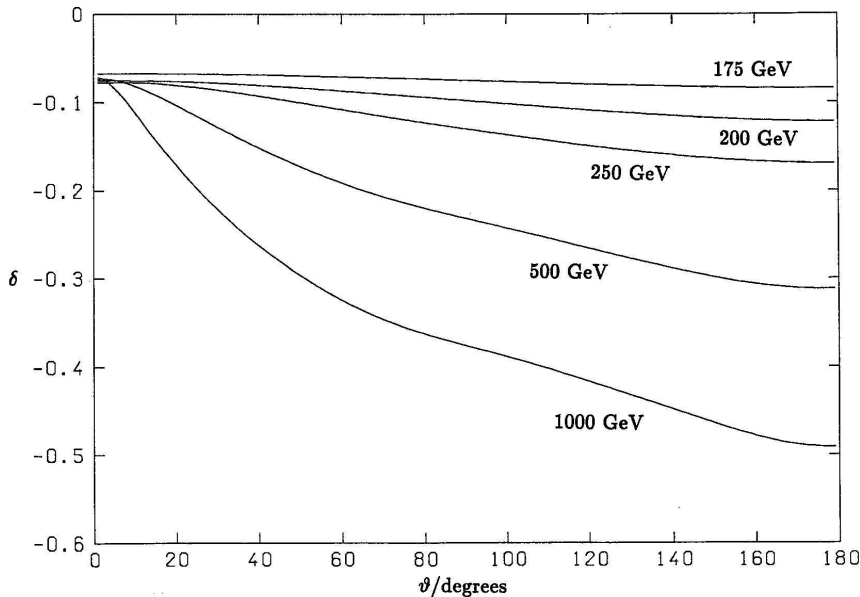


Figure 11.5: Radiative corrections to the differential cross section relative to lowest order for the unpolarized case at various center of mass energies.

value of the corrections but do not influence their angular dependence very much. Fig. 11.5 shows the relative correction factor δ defined through

$$\frac{d\sigma}{d\Omega} = \left(\frac{d\sigma}{d\Omega}\right)_0 (1 + \delta_s) + \delta \left(\frac{d\sigma}{d\Omega}\right)_V = \left(\frac{d\sigma}{d\Omega}\right)_0 (1 + \delta) \quad (11.27)$$

for the unpolarized case. While the variation with the scattering angle is relatively flat for LEP200 energies it becomes stronger with increasing energy. In the forward direction where the Born cross section is dominated by the t -channel pole the energy dependence is very weak. In the backward direction, however, the percentage correction varies strongly with energy and reaches large negative values up to -50% at 1 TeV. Nevertheless since the absolute cross section is small for large scattering angles (see Fig. 11.3), the relative corrections to the integrated cross section stay below 20% up to 1 TeV. Note that the one-loop corrections are large exactly in that region where the sensitivity to new physics is highest.

The behaviour of the corrections for purely transverse W -bosons is similar to the unpolarized case. In contrast to this the corrections for purely longitudinal bosons (Fig. 11.6) exhibit a strong angular dependence arising from the minima in the lowest order cross section (Fig. 11.4).

The sensitivity of the total unpolarized cross section on the unknown masses of the Higgs boson and top quark is illustrated in Tab. 11.2 and 11.3. A change of m_t from 80 to 200 GeV affects the cross section by less than 3% apart from the region very close to threshold. The large effect close to threshold is due to the variation of M_W and thus

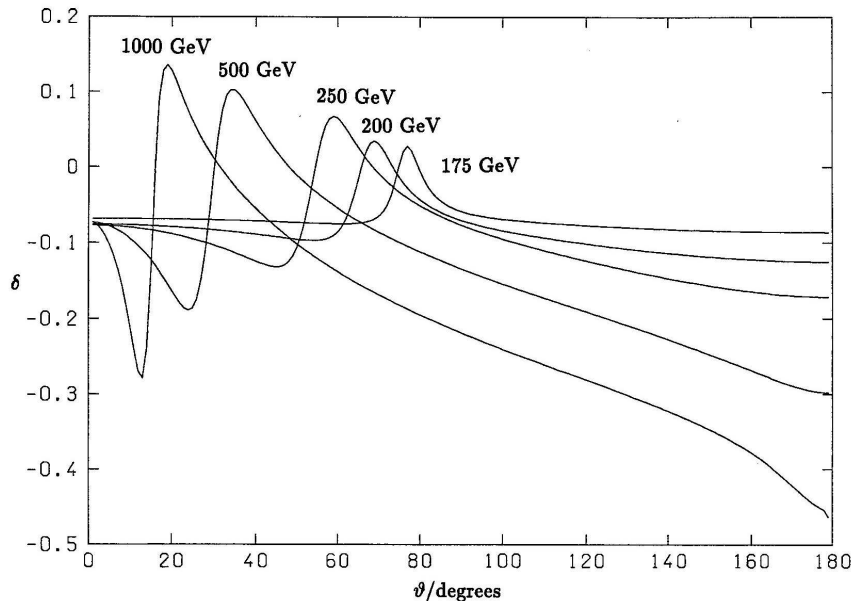


Figure 11.6: Radiative corrections to the differential cross section relative to lowest order for purely longitudinal W -bosons at various center of mass energies.

the variation of the threshold with m_t . A variation of M_H between 50 and 1000 GeV influences the total cross section by less than 0.5%, again with the exception of the threshold region. Note that this is valid for constant α , G_F and M_Z . Fixing instead G_F , M_W and M_Z the dependence on m_t is much weaker. This allows to determine M_W from the cross section practically independently on m_t and M_H as pointed out by Jegerlehner [80]. These results for the top and Higgs mass dependence remain valid if we include hard photonic corrections.

Using the functions C_i^σ given in [78] the improved Born approximation (11.26) agrees with the full one-loop order result within 0.5% for $\sqrt{s} < 220$ GeV and within 1% for $\sqrt{s} < 270$ GeV in the case of the total cross section. For the differential cross section the deviation is at most 1% for $\sqrt{s} < 210$ GeV. The largest difference occurs for large scattering angles, i.e. where the cross section is small.

11.4 Hard photon bremsstrahlung

11.4.1 Complete calculations

The complete hard photonic bremsstrahlung to $e^+e^- \rightarrow W^+W^-$ was determined in [68, 70]. The polarized amplitudes for the process $e^+e^- \rightarrow W^+W^-\gamma$ were calculated using three different methods. The first one, described in detail in [69] uses the Weyl representation for Dirac matrices and spinors and results in expressions for the amplitudes in terms of the components of momentum and polarization vectors in the center of mass frame of the incoming leptons. The second method used in [14] is based on the Weyl-van

$m_t/\text{GeV} =$	80	120	160	200
$M_W/\text{GeV} =$	79.87	80.10	80.37	80.69
\sqrt{s}/GeV	σ/pb			
165.0	10.120	9.743	9.218	8.461
180.0	15.521	15.620	15.646	15.626
200.0	15.944	16.112	16.220	16.301
500.0	5.689	5.760	5.807	5.847
1000.0	2.064	2.088	2.103	2.113

Table 11.2: Total unpolarized cross section for $e^+e^- \rightarrow W^+W^-$ including virtual and soft photonic corrections for different top quark masses at various center of mass energies.

$M_H/\text{GeV} =$	50	100	300	1000
$M_W/\text{GeV} =$	80.26	80.23	80.16	80.06
\sqrt{s}/GeV	σ/pb			
165.0	9.488	9.503	9.614	9.793
180.0	15.654	15.638	15.612	15.598
200.0	16.168	16.168	16.143	16.105
500.0	5.785	5.785	5.776	5.764
1000.0	2.097	2.096	2.093	2.088

Table 11.3: Total unpolarized cross section for $e^+e^- \rightarrow W^+W^-$ including virtual and soft photonic corrections for different Higgs boson masses at various center of mass energies.

der Waerden formalism. It yields concise analytical formulae for the amplitude which are manifestly Lorentz invariant. The relative numerical difference between both results was found to be less than 10^{-6} for the amplitude squared. In [70] the amplitudes were calculated numerically.

From this the total cross section is obtained as

$$\begin{aligned}\sigma(s) &= \frac{1}{(2\pi)^5} \frac{1}{2s} \int \frac{d^3k_1}{2k_{10}} \frac{d^3k_2}{2k_{20}} \frac{d^3k}{2k_0} \frac{1}{4} \sum_{pol} |\mathcal{M}|^2 \delta^{(4)}(p_1 + p_2 - k_1 - k_2 - k) \\ &= \frac{1}{2s} \frac{1}{8(2\pi)^4} \int d\cos\vartheta_2 d\cos\vartheta d\phi dk_0 \left| \frac{k_0 |\mathbf{k}_2|^2}{|\mathbf{k}_2|(\sqrt{s} - k_0) + k_0 k_{20} c_{20}} \right| \frac{1}{4} \sum_{pol} |\mathcal{M}|^2,\end{aligned}\tag{11.28}$$

where ϑ_2, ϑ are the polar angles of the W^- -boson and the photon, ϕ is the azimuthal angle of the photon with respect to the incoming electron and

$$c_{20} = \sin\vartheta_2 \sin\vartheta \cos\phi + \cos\vartheta_2 \cos\vartheta.\tag{11.29}$$

The nontrivial phase space integrations are performed using Monte Carlo routines. Thus experimental cuts can be easily implemented.

Eq. (11.28) contains the soft photon poles. These are eliminated by a cut $k_0 > \Delta E$ on the photon energy. After combining soft and hard photonic corrections the cut dependence drops out. This has been checked numerically for $\Delta E/E$ between 10^{-3} and 10^{-6} .

11.4.2 Leading logarithmic approximation

The leading logarithmic (LL) QED corrections to the W -pair production cross section were already calculated in [43]. The resulting cross section is given by [68]

$$\sigma_{LL}(s) = \int_{4M_W^2/s}^1 dz \phi(z) \hat{\sigma}_0(zs),\tag{11.30}$$

where $\hat{\sigma}_0(zs)$ denotes the (improved) Born cross section at the reduced CMS energy squared zs . The flux $\phi(z)$ reads

$$\begin{aligned}\phi(z) &= \delta(1-z) \\ &+ \frac{\alpha}{\pi} (L-1) \left[\delta(1-z) 2 \log \varepsilon + \theta(1-\varepsilon-z) \frac{2}{1-z} \right] \\ &+ \frac{\alpha}{\pi} L \left[\delta(1-z) \frac{3}{2} - \theta(1-\varepsilon-z) (1+z) \right] \\ &+ \left(\frac{\alpha}{\pi} L \right)^2 \left\{ \delta(1-z) \left(2 \log^2 \varepsilon + 3 \log \varepsilon + \frac{9}{8} - \frac{\pi^2}{3} \right) \right. \\ &\left. + \theta(1-\varepsilon-z) \left[\frac{1+z^2}{1-z} (2 \log(1-z) - \log z + \frac{3}{2}) + \frac{1}{2} (1+z) \log z - (1-z) \right] \right\}\end{aligned}\tag{11.31}$$

where $L = \log(Q^2/m_e^2)$ is the leading logarithm and $\varepsilon = \Delta E/E$ the soft photon cutoff. $\phi(z)$ is given including $O(\alpha^2)$ LL-contributions. Furthermore some nonleading terms are incorporated taking into account the fact that the residue of the soft photon pole

is proportional to $L - 1$ rather than L for the initial state radiation. The scale Q^2 is a free parameter. It can only be determined through higher order calculations. In [68] the integral in (11.30) was performed numerically. Neglecting the $O(\alpha^2)$ leading logarithms and the nonlogarithmic terms it has been evaluated analytically [78].

11.4.3 Numerical results

The results presented in this section were calculated by [68, 81]. The parameters are the same as in Sect. 8.1. In the Born cross section $\hat{\sigma}_0$, entering the LL approximation, α has been replaced by G_F everywhere. Thus the large fermionic corrections are absorbed at least in the dominant t -channel contributions.

The total cross section is plotted in Fig. 11.7 in the LEP200 energy range. Shown are the Born cross section with α replaced by G_F , the cross section including the full $O(\alpha)$ corrections and including in addition the $O(\alpha^2)$ LL corrections. The corresponding numbers are given in Tab. 11.4 for various CMS energies. The uncertainty of the full $O(\alpha)$ result is due to the Monte Carlo integration of the hard bremsstrahlung corrections. This error refers also to the last column of Tab. 11.4. The $O(\alpha)$ LL results were evaluated for two scale choices

$$\begin{aligned} Q^2 &= s \\ Q^2 &= -t_{min} = -M_W^2 + \frac{s}{2}(1 - \beta). \end{aligned} \tag{11.32}$$

The second one is motivated by the fact that the total cross section is dominated by the t -channel pole. It reproduces the exact $O(\alpha)$ results better. The difference is found to be less than 2% for $\sqrt{s} > 165$ GeV. Choosing the scale $Q^2 = s$ the deviation from the exact $O(\alpha)$ result is about 5% at 165 GeV. Also at higher energies the scale choice $Q^2 = -t_{min}$ turns out to be preferable. It reproduces the complete $O(\alpha)$ result including hard photon bremsstrahlung within 1% for $170 \text{ GeV} < \sqrt{s} < 500 \text{ GeV}$. The effect of the $O(\alpha^2)$ LL contribution is demonstrated in the last column of Tab. 11.4. It reaches about 5% at 165 GeV, decreases with increasing energy and is small for $\sqrt{s} > 190$ GeV. A practically identical result is obtained by soft photon exponentiation.

The large deviation between $O(\alpha)$ LL and the exact result close to threshold is due to the Coulomb singularity (see Sect. 11.3.3). It amounts to about 10% at 1 GeV above threshold and is not included in the $O(\alpha)$ LL result. Note also the large $O(\alpha^2)$ correction close to threshold (28% at 161 GeV).

11.5 Finite widths effects

Realistic calculations for W -pair production must include the decays of the W -bosons into fermions. These are especially important around threshold.

In real experiments one observes the reaction

$$e^+e^- \rightarrow W^+W^- \rightarrow \text{final states}. \tag{11.33}$$

The W -bosons give rise to peaks in the invariant mass distributions of the final state particles. Therefore one has to calculate the cross section for $e^+e^- \rightarrow f_1\bar{f}_2f_3\bar{f}_4(\gamma, g)$. This task has been attacked but not completed so far [83]. Above the W -pair production threshold the dominant contributions come from Feynman diagrams containing resonant

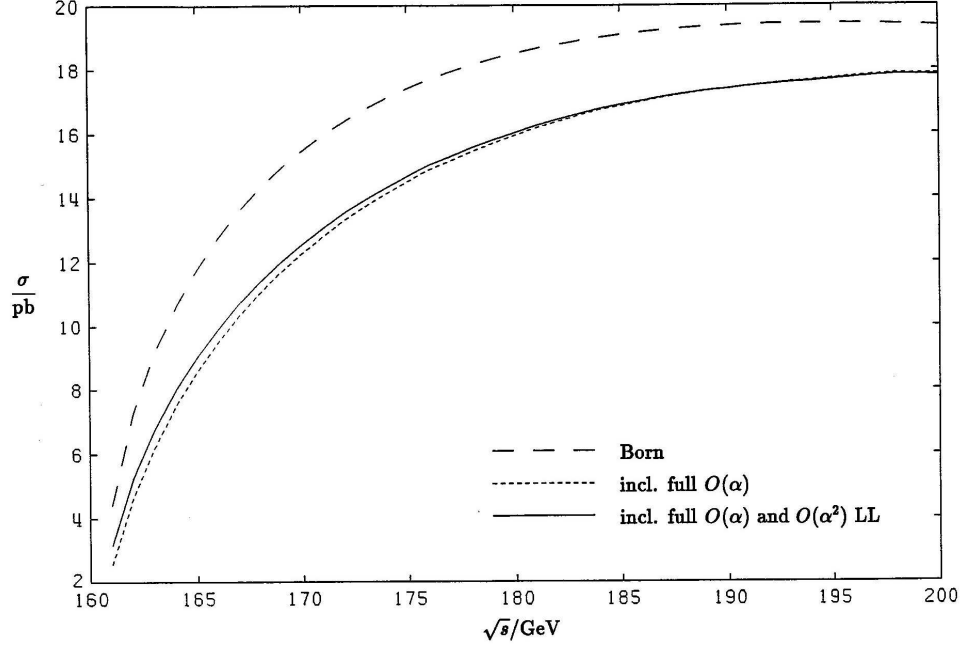


Figure 11.7: Total cross section for W -pair production including hard photonic corrections.

\sqrt{s}/GeV	Born(G_F)	incl. $O(\alpha)$ LL $Q^2 = s$	incl. $O(\alpha)$ LL $Q^2 = -t_{min}$	incl. $O(\alpha)$ exact	incl. $O(\alpha)$ exact $+O(\alpha^2)$ LL
161.0	4.411	2.003	2.158	2.556 ± 0.002	3.255
165.0	11.761	8.141	8.429	8.553 ± 0.006	9.089
170.0	15.465	11.967	12.285	12.264 ± 0.010	12.606
175.0	17.413	14.264	14.578	14.484 ± 0.013	14.690
180.0	18.501	15.730	16.028	15.920 ± 0.014	16.033
190.0	19.361	17.272	17.525	17.373 ± 0.016	17.375
200.0	19.354	17.810	18.015	17.796 ± 0.017	17.742
250.0	16.406	16.223	16.257	16.033 ± 0.023	15.937
300.0	13.473	13.734	13.682	13.543 ± 0.026	13.470
500.0	7.142	7.664	7.519	7.449 ± 0.019	7.430

Table 11.4: Total cross section for $e^+e^- \rightarrow W^+W^-$ in pb including hard photonic corrections.

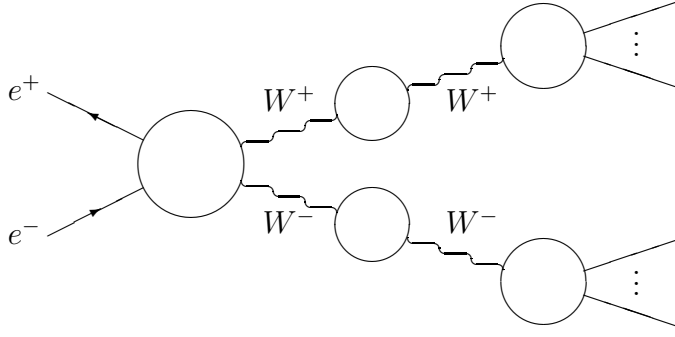


Figure 11.8: General structure of diagrams containing two resonant W -propagators.

W -propagators. The cross section for W -pair production is obtained by calculating all diagrams containing two resonant W -propagators. Diagrams contributing to the same final state but without two resonant propagators are considered as background. They are suppressed by a factor $M_W/\Gamma^W \approx 40$ if the full range of invariant masses $\sqrt{s_i}$ of the final state particles is included. If $\sqrt{s_i}$ is restricted by a cut Δ

$$M_W - \Delta < \sqrt{s_i} < M_W + \Delta, \quad (11.34)$$

the suppression is even $M_W^2/(\Gamma^W \Delta) \approx 300$ for $\Delta \approx 10$ GeV. Explicit calculations show that the background contributions are below 1% for $\sqrt{s} \geq 2M_W$ [83]. It becomes, however, more relevant below the nominal threshold. But even above threshold nonresonant Born contributions to $e^+e^- \rightarrow f_1\bar{f}_2f_3\bar{f}_4(\gamma, g)$ must be taken into account to obtain an accuracy of better than 1%.

There are three types of diagrams which may give resonant contributions. The most important ones are factorizable diagrams with the structure shown in Fig. 11.8 which evidently contain two resonant W -propagators. The corresponding cross section is given by

$$\sigma(s) = \int_{(M_W - \Delta)^2}^{(M_W + \Delta)^2} ds_1 ds_2 \sigma^*(s, s_1, s_2) \rho(s_1) \rho(s_2) \theta(\sqrt{s} - \sqrt{s_1} - \sqrt{s_2}), \quad (11.35)$$

where $\sigma^*(s, s_1, s_2)$ is the 'cross section' for the production of two off-shell W -bosons and

$$\rho(s) = \frac{1}{\pi} \frac{\sqrt{s} \Gamma^W(s)}{(s - M_W^2)^2 + s(\Gamma^W(s))^2}, \quad (11.36)$$

with the 'decay width' $\Gamma^W(s)$ for an off-shell W -boson. Note that

$$\rho(s) \rightarrow \delta(s - M_W^2) \quad \text{for} \quad \Gamma^W \rightarrow 0. \quad (11.37)$$

The off-shell quantities $\sigma^*(s, s_1, s_2)$ and $\Gamma^W(s)$ are not gauge invariant. However, the leading resonant contributions to $\sigma(s)$ are. Eq. (11.35) closely resembles a Breit-Wigner approximation for the unstable W -bosons. In the threshold region $\sigma^*(s, s_1, s_2)$ depends strongly on s_1 and s_2 . Consequently $\sigma(s)$ deviates considerably from $\sigma^*(s, M_W^2, M_W^2)$, the cross section for on-shell stable W 's. Fig. 11.9 [81] shows this effect in lowest order and with the full $O(\alpha)$ corrections to σ^* and $\Gamma^W(s)$ included. This dependence is mainly

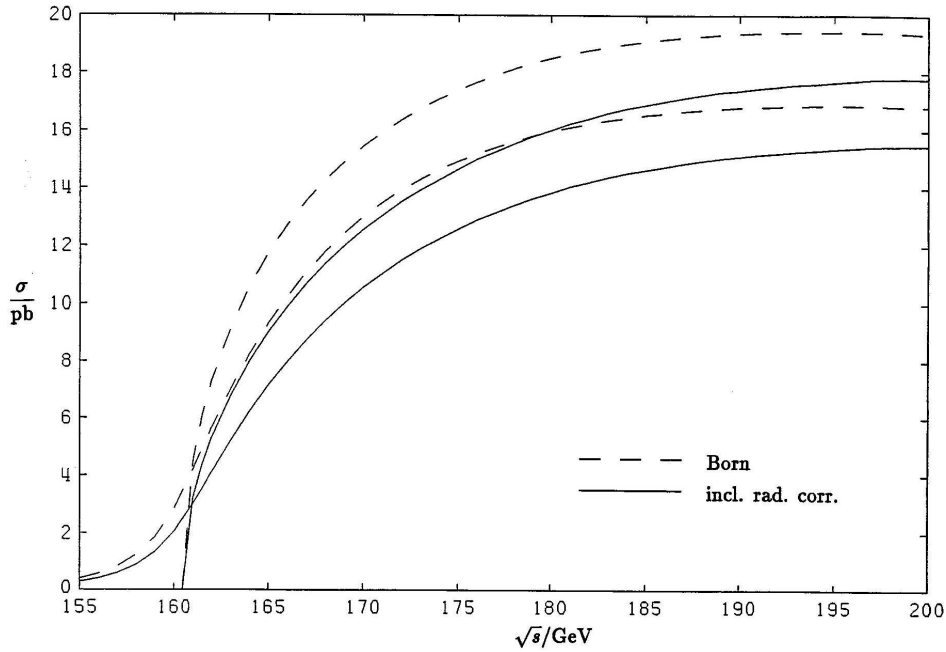


Figure 11.9: Total cross section for W -pair production in lowest order and including the full $O(\alpha)$ corrections with and without finite width effects.

due to the threshold factor $\kappa^{1/2}(s, s_1, s_2)$ contained in $\sigma^*(s, s_1, s_2)$. Extracting this factor, $\sigma^*/\kappa^{1/2}$ depends only weakly on s_1 and s_2 . This is also the case for $\Gamma^W(s)/\sqrt{s}$ with respect to s . Replacing these quantities by their on-shell values we find the following approximation

$$\sigma(s) \approx \frac{\sigma^*(s, M_W^2, M_W^2)}{\kappa^{1/2}(s, M_W^2, M_W^2)} \int_{(M_W - \Delta)^2}^{(M_W + \Delta)^2} ds_1 ds_2 \kappa^{1/2}(s, s_1, s_2) \tilde{\rho}(s_1) \tilde{\rho}(s_2) \theta(\sqrt{s} - \sqrt{s_1} - \sqrt{s_2}) \quad (11.38)$$

with

$$\tilde{\rho}(s) = \frac{1}{\pi} \frac{\frac{s}{M_W} \Gamma^W(M_W^2)}{(s - M_W^2)^2 + \frac{s^2}{M_W^2} (\Gamma^W(M_W^2))^2}. \quad (11.39)$$

This approximation is gauge invariant because $\sigma^*(s, M_W^2, M_W^2)$ and $\Gamma^W(M_W^2)$ are physical on-shell quantities. It is particularly useful above the nominal threshold, whereas it gets worse below threshold because there at least one of the W -bosons has to be off-shell.

For high energies ($s \gg M_W^2$) also $\kappa(s, s_1, s_2)$ varies only weakly with s_1 and s_2 in the resonance region $s_1 \approx s_2 \approx M_W^2$. Replacing it by its on-shell value we can perform the integrations and obtain

$$\sigma(s) \approx \sigma^*(s, M_W^2, M_W^2), \quad \text{for } s \gg M_W \quad \text{and} \quad \Delta \gg \Gamma^W. \quad (11.40)$$

Eq. (11.35) incorporates all resonant lowest order contributions and all one-loop corrections associated either with the production of W -pairs or the decay of the W -bosons (given in Chap. 9). This includes in particular all self energy and vertex corrections and thus all

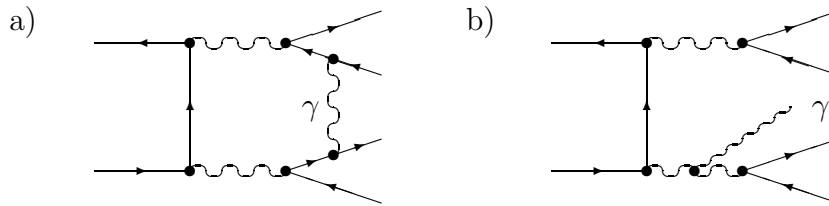


Figure 11.10: Examples for additional diagrams leading to resonant contributions.

leading corrections. A more thorough analysis of this kind has been carried through for the case of Z -pair production [82].

Feynman diagrams which do not fit into the structure shown in Fig. 11.8 give nonresonant contributions and can thus be neglected with the exception of two classes. Both originate from photonic corrections. The first type results from virtual photons exchanged between the external lines connected to different blobs in Fig. 11.8. An example is shown in Fig. 11.10a. These diagrams give rise to resonant contributions coming from photons which are nearly on-shell. From similar cases in μ -pair production we know that these are cancelled by the corresponding bremsstrahlung diagrams if one integrates over the whole photon phase space. For stringent cuts, however, resonant contributions survive.

The second type of diagrams consists of those where a real photon is emitted from the internal W -boson line (Fig. 11.10b). There are three W -propagators in the diagram. If the photon is hard the corresponding resonances appear in three different regions of phase space. Therefore these diagrams seem not to fit into the simple Breit-Wigner-like picture discussed above.

In order to take into account these resonant contributions properly one has to calculate the virtual and real photonic corrections to $e^+e^- \rightarrow 4$ fermions. This has been done for real photon radiation [73]. Evaluation of the virtual photonic corrections is under way [83].

12 Conclusion

With the electroweak standard model (SM) we have a theory that describes all known experimental facts about the electroweak interaction. It has successfully survived all precision experiments at low energies and at LEP100. The upcoming experiments at LEP200, HERA and the planned hadron colliders will allow to investigate sectors of the SM which were not directly accessible so far. For a conclusive confrontation of future experimental results with the SM precise predictions are mandatory.

For the adequate theoretical description of the experiments at LEP100 the calculation of radiative corrections was inevitable. Although experiments outside the Z -region will not profit from the presence of a resonance, the expected experimental accuracy will be such that radiative corrections will be indispensable. Moreover radiative corrections allow to obtain information on otherwise not accessible quantities such as the mass of the top quark or the Higgs boson.

One of the next important classes of experiments will be the investigation of the W -boson and its nonabelian couplings at LEP200. We have presented the relevant formulae necessary for the corresponding higher order calculations. Together with [66, 14] these cover the complete analytical expressions for processes with on-shell W -bosons. The one-loop virtual corrections are settled for the polarized differential and total cross section. Also hard bremsstrahlung has been calculated by several authors. We have given an improved Born approximation including the leading two-loop contributions for the total and differential cross section. The effects of the finite width of the W -bosons have been discussed for the lowest order cross section and the cross section including radiative corrections. While the inclusion of the non-photon corrections is simple the correct simultaneous treatment of photonic corrections and finite width effects involves nonfactorizable box diagrams. These contributions are under consideration.

We have discussed the total and partial W -decay widths including all one-loop and leading two-loop corrections. Because the W -boson decays only into light fermions the widths can be described by a very simple expression with an accuracy better than 0.6%.

Furthermore we have given results on the t -quark decay width. Also in this case the electroweak corrections can be incorporated into a simple approximation valid for a top mass below 250 GeV with an accuracy of about 1.7%.

Apart from giving these explicit results we have discussed many techniques needed for the calculation of one-loop corrections. We have compiled a comprehensive set of formulae which are relevant for the calculation of one-loop radiative corrections within and outside the standard model. We have listed the complete set of Feynman rules for the electroweak standard model including the counter terms. These were expressed by the self energies of the physical particles in terms of two-point functions. We have given explicit results for the scalar N -point functions for $N = 1, \dots, 4$ and the relevant formulae for the reduction of the higher scalar functions and the tensor functions to those. Furthermore we have outlined a general strategy for the calculation of one-loop diagrams. Finally we have given the general expressions for the soft photonic corrections.

If the SM will prove to describe the upcoming experimental results successfully, further precision checks will become necessary and a lot more calculations of radiative corrections will be required. These calculations will be even more involved than the existing ones because the structure of the corresponding physical processes will in general be more

complicated. The techniques and formulae presented in this review are general enough to serve as a basis for the evaluation of radiative corrections to reactions which will be studied at future colliders such as gauge boson scattering processes ($W^+W^- \rightarrow W^+W^-$), electron photon reactions ($e\gamma \rightarrow \nu_e W$), reactions with three or more final state particles and so on.

The methods described here have been implemented in the computer algebra package *FEYN CALC*. Many of the quoted formulae are included in this package. We hope that this compilation together with the packages *FEYN CALC* and *FEYN ARTS* can serve as a useful tool, facilitating future calculations of radiative corrections.

Acknowledgements

I would like to thank M. Böhm for his support and permanent encouragement during the past years. Many of the results presented here were calculated together with T. Sack who also provided some of the figures and tables. The results on W -pair-production were obtained in a fruitful collaboration with W. Beenakker, F. A. Berends, H. Kuijf, M. Böhm and T. Sack. I have profited from many stimulating and clarifying discussions with the people mentioned above and H. Spiesberger, W. Hollik, J. H. Kühn, F. Jegerlehner and W. L. van Neerven. I am grateful to R. Mertig, J. Küblbeck, R. Guth, H. Eck, R. Scharf, U. Nierste and S. Dittmaier for their assistance. I am indebted to my wife R. Denner for typing parts of the manuscript and in particular for her patience.

A Feynman rules

In this appendix we list the Feynman rules of the SM in the 't Hooft-Feynman gauge including the counter terms in a way appropriate for the concept of generic diagrams. I.e. we write down generic Feynman rules and give the possible actual insertions. We omit any field renormalization constants for the unphysical fields. For brevity we introduce the shorthand notation

$$c = c_W, \quad s = s_W. \quad (\text{A.1})$$

In the vertices all momenta are considered as incoming.

Propagators:

for gauge bosons $V = \gamma, Z, W$ in the 't Hooft Feynman gauge ($\xi_i = 1$)

$$\boxed{V_\mu \text{---}^k \text{---} V_\nu} = \frac{-ig_{\mu\nu}}{k^2 - M_V^2},$$

for Faddeev-Popov ghosts $G = u^\gamma, u^Z, u^W$

$$\boxed{G \text{---}^k \text{---} \bar{G}} = \frac{i}{k^2 - M_G^2},$$

for scalar fields $S = H, \chi, \phi$

$$\boxed{S \text{---}^k \text{---} S} = \frac{i}{k^2 - M_S^2},$$

and for fermion fields $F = f_i$

$$\boxed{F \text{---}^p \text{---} \bar{F}} = \frac{i(\not{p} + m_F)}{p^2 - m_F^2}.$$

In the 't Hooft-Feynman gauge we have the following relations:

$$M_{u^\gamma} = 0, \quad M_{u^Z} = M_\chi = M_Z, \quad M_{u^\pm} = M_\phi = M_W. \quad (\text{A.2})$$

Tadpole:

$$\boxed{\text{X} \text{---}^S} = i\delta t.$$

VV-counterterm:

$$\boxed{V_{1,\mu} \text{---}^k \text{---} V_{2,\nu}} = -ig_{\mu\nu} [C_1 k^2 - C_2]$$

with the actual values of V_1, V_2 and C_1, C_2

$$\begin{aligned} W^+W^- &: C_1 = \delta Z_W, & C_2 &= M_W^2 \delta Z_W + \delta M_W^2, \\ ZZ &: C_1 = \delta Z_{ZZ}, & C_2 &= M_Z^2 \delta Z_{ZZ} + \delta M_Z^2, \\ AZ &: C_1 = \frac{1}{2} \delta Z_{AZ} + \frac{1}{2} \delta Z_{ZA}, & C_2 &= M_Z^2 \frac{1}{2} \delta Z_{ZA}, \\ AA &: C_1 = \delta Z_{AA}, & C_2 &= 0. \end{aligned} \quad (\text{A.3})$$

SS-counterterm:

$$\boxed{S_1, k \text{ --- } \times \text{ --- } S_2} = i[C_1 k^2 - C_2]$$

with the actual values of S_1 , S_2 and C_1 , C_2

$$\begin{aligned} HH & : C_1 = \delta Z_H, & C_2 &= M_H^2 \delta Z_H + \delta M_H^2, \\ \chi\chi & : C_1 = 0, & C_2 &= -\frac{e}{2s} \frac{\delta t}{M_W} + \delta M_Z^2, \\ \phi^+ \phi^- & : C_1 = 0, & C_2 &= -\frac{e}{2s} \frac{\delta t}{M_W} + \delta M_W^2. \end{aligned} \quad (\text{A.4})$$

FF-counterterm:

$$\boxed{F_1, p \text{ --- } \times \text{ --- } \bar{F}_2} = i[C_L \not{p} \omega_- + C_R \not{p} \omega_+ - C_S^- \omega_- - C_S^+ \omega_+]$$

with the actual values of F_1 , \bar{F}_2 and C_L , C_R , C_S^- , C_S^+

$$f_j \bar{f}_i : \begin{cases} C_L = \frac{1}{2} (\delta Z_{ij}^{f,L} + \delta Z_{ij}^{f,L^\dagger}), & C_R = \frac{1}{2} (\delta Z_{ij}^{f,R} + \delta Z_{ij}^{f,R^\dagger}), \\ C_S^- = m_{f,i} \frac{1}{2} \delta Z_{ij}^{f,L} + m_{f,j} \frac{1}{2} \delta Z_{ij}^{f,R^\dagger} + \delta_{ij} \delta m_{f,i}, \\ C_S^+ = m_{f,i} \frac{1}{2} \delta Z_{ij}^{f,R} + m_{f,j} \frac{1}{2} \delta Z_{ij}^{f,L^\dagger} + \delta_{ij} \delta m_{f,i}. \end{cases} \quad (\text{A.5})$$

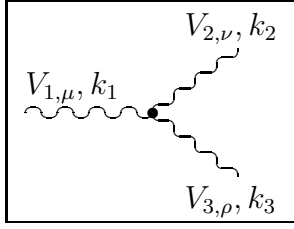
VVVV-coupling:

$$\boxed{\begin{array}{cc} V_{1,\mu} & V_{3,\rho} \\ \diagdown & \diagup \\ & \bullet \\ \diagup & \diagdown \\ V_{2,\nu} & V_{4,\sigma} \end{array}} = ie^2 C [2g_{\mu\nu} g_{\sigma\rho} - g_{\nu\rho} g_{\mu\sigma} - g_{\rho\mu} g_{\nu\sigma}]$$

with the actual values of V_1 , V_2 , V_3 , V_4 and C

$$\begin{aligned} W^+ W^+ W^- W^- & : C = \frac{1}{s^2} [1 + 2\delta Z_e - 2\frac{\delta s}{s} + 2\delta Z_W], \\ W^+ W^- Z Z & : C = -\frac{c^2}{s^2} [1 + 2\delta Z_e - 2\frac{1}{c^2} \frac{\delta s}{s} + \delta Z_W + \delta Z_{ZZ}] + \frac{c}{s} \delta Z_{AZ}, \\ W^+ W^- AZ & : \begin{cases} C = \frac{c}{s} [1 + 2\delta Z_e - \frac{1}{c^2} \frac{\delta s}{s} + \delta Z_W + \frac{1}{2} \delta Z_{ZZ} + \frac{1}{2} \delta Z_{AA}] \\ \quad - \frac{1}{2} \delta Z_{AZ} - \frac{1}{2} \frac{c^2}{s^2} \delta Z_{ZA}, \end{cases} \\ W^+ W^- AA & : C = -[1 + 2\delta Z_e + \delta Z_W + \delta Z_{AA}] + \frac{c}{s} \delta Z_{ZA}. \end{aligned} \quad (\text{A.6})$$

VVV-coupling:

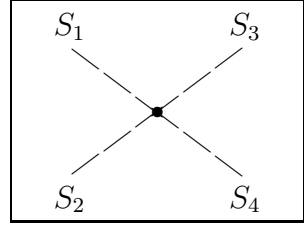


$$= -ieC \left[g_{\mu\nu}(k_2 - k_1)_\rho + g_{\nu\rho}(k_3 - k_2)_\mu + g_{\rho\mu}(k_1 - k_3)_\nu \right]$$

with the actual values of V_1 , V_2 , V_3 and C

$$\begin{aligned} AW^+W^- & : C = 1 + \delta Z_e + \delta Z_W + \frac{1}{2}\delta Z_{AA} - \frac{1}{2}\frac{c}{s}\delta Z_{ZA}, \\ ZW^+W^- & : C = -\frac{c}{s}(1 + \delta Z_e - \frac{1}{c^2}\frac{\delta s}{s} + \delta Z_W + \frac{1}{2}\delta Z_{ZZ}) + \frac{1}{2}\delta Z_{AZ}. \end{aligned} \quad (\text{A.7})$$

SSSS-coupling:

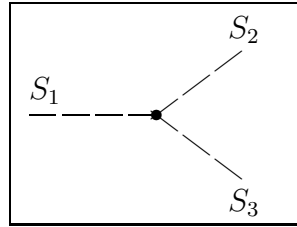


$$= ie^2C$$

with the actual values of S_1 , S_2 , S_3 , S_4 and C

$$\begin{aligned} HHHH & : C = -\frac{3}{4s^2}\frac{M_H^2}{M_W^2} \left[1 + 2\delta Z_e - 2\frac{\delta s}{s} + \frac{\delta M_H^2}{M_H^2} + \frac{e}{2s}\frac{\delta t}{M_W M_H^2} - \frac{\delta M_W^2}{M_W^2} + 2\delta Z_H \right], \\ \left. \begin{aligned} HH\chi\chi \\ HH\phi\phi \end{aligned} \right\} & : C = -\frac{1}{4s^2}\frac{M_H^2}{M_W^2} \left[1 + 2\delta Z_e - 2\frac{\delta s}{s} + \frac{\delta M_H^2}{M_H^2} + \frac{e}{2s}\frac{\delta t}{M_W M_H^2} - \frac{\delta M_W^2}{M_W^2} + \delta Z_H \right], \\ XXXX & : C = -\frac{3}{4s^2}\frac{M_H^2}{M_W^2} \left[1 + 2\delta Z_e - 2\frac{\delta s}{s} + \frac{\delta M_H^2}{M_H^2} + \frac{e}{2s}\frac{\delta t}{M_W M_H^2} - \frac{\delta M_W^2}{M_W^2} \right], \\ \chi\chi\phi\phi & : C = -\frac{1}{4s^2}\frac{M_H^2}{M_W^2} \left[1 + 2\delta Z_e - 2\frac{\delta s}{s} + \frac{\delta M_H^2}{M_H^2} + \frac{e}{2s}\frac{\delta t}{M_W M_H^2} - \frac{\delta M_W^2}{M_W^2} \right], \\ \phi\phi\phi\phi & : C = -\frac{1}{2s^2}\frac{M_H^2}{M_W^2} \left[1 + 2\delta Z_e - 2\frac{\delta s}{s} + \frac{\delta M_H^2}{M_H^2} + \frac{e}{2s}\frac{\delta t}{M_W M_H^2} - \frac{\delta M_W^2}{M_W^2} \right]. \end{aligned} \quad (\text{A.8})$$

SSS-coupling:

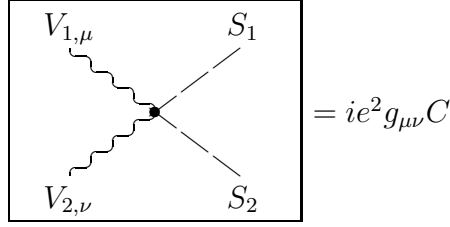


$$= ieC$$

with the actual values of S_1 , S_2 , S_3 and C

$$\begin{aligned} HHH & : C = -\frac{3}{2s}\frac{M_H^2}{M_W} \left[1 + \delta Z_e - \frac{\delta s}{s} + \frac{\delta M_H^2}{M_H^2} + \frac{e}{2s}\frac{\delta t}{M_W M_H^2} - \frac{1}{2}\frac{\delta M_W^2}{M_W^2} + \frac{3}{2}\delta Z_H \right], \\ \left. \begin{aligned} H\chi\chi \\ H\phi\phi \end{aligned} \right\} & : C = -\frac{1}{2s}\frac{M_H^2}{M_W} \left[1 + \delta Z_e - \frac{\delta s}{s} + \frac{\delta M_H^2}{M_H^2} + \frac{e}{2s}\frac{\delta t}{M_W M_H^2} - \frac{1}{2}\frac{\delta M_W^2}{M_W^2} + \frac{1}{2}\delta Z_H \right]. \end{aligned} \quad (\text{A.9})$$

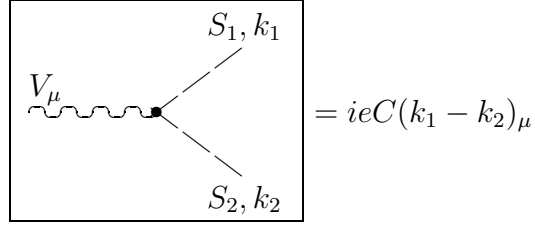
VVSS-coupling:



with the actual values of V_1 , V_2 , S_1 , S_2 and C

$$\begin{aligned}
W^+W^-HH & : C = \frac{1}{2s^2} \left[1 + 2\delta Z_e - 2\frac{\delta s}{s} + \delta Z_W + \delta Z_H \right], \\
\left. \begin{aligned} W^+W^-\chi\chi \\ W^+W^-\phi^+\phi^- \end{aligned} \right\} & : C = \frac{1}{2s^2} \left[1 + 2\delta Z_e - 2\frac{\delta s}{s} + \delta Z_W \right], \\
ZZ\phi^+\phi^- & : C = \frac{(s^2-c^2)^2}{2s^2c^2} \left[1 + 2\delta Z_e + \frac{2}{(s^2-c^2)c^2} \frac{\delta s}{s} + \delta Z_{ZZ} \right] + \frac{s^2-c^2}{sc} \delta Z_{AZ}, \\
ZA\phi^+\phi^- & : \left\{ \begin{aligned} C &= \frac{s^2-c^2}{sc} \left[1 + 2\delta Z_e + \frac{1}{(s^2-c^2)c^2} \frac{\delta s}{s} + \frac{1}{2}\delta Z_{ZZ} + \frac{1}{2}\delta Z_{AA} \right] \\ &+ \frac{(s^2-c^2)^2}{2s^2c^2} \frac{1}{2}\delta Z_{ZA} + \delta Z_{AZ}, \end{aligned} \right. \\
AA\phi^+\phi^- & : C = 2 \left[1 + 2\delta Z_e + \delta Z_{AA} \right] + \frac{s^2-c^2}{sc} \delta Z_{ZA}, \\
ZZHH & : C = \frac{1}{2s^2c^2} \left[1 + 2\delta Z_e + 2\frac{s^2-c^2}{c^2} \frac{\delta s}{s} + \delta Z_{ZZ} + \delta Z_H \right], \\
ZZ\chi\chi & : C = \frac{1}{2s^2c^2} \left[1 + 2\delta Z_e + 2\frac{s^2-c^2}{c^2} \frac{\delta s}{s} + \delta Z_{ZZ} \right], \\
\left. \begin{aligned} ZAHH \\ ZA\chi\chi \end{aligned} \right\} & : C = \frac{1}{2s^2c^2} \frac{1}{2} \delta Z_{ZA}, \\
W^\pm Z\phi^\mp H & : C = -\frac{1}{2c} \left[1 + 2\delta Z_e - \frac{\delta c}{c} + \frac{1}{2}\delta Z_W + \frac{1}{2}\delta Z_H + \frac{1}{2}\delta Z_{ZZ} \right] - \frac{1}{2s} \frac{1}{2} \delta Z_{AZ}, \\
W^\pm A\phi^\mp H & : C = -\frac{1}{2s} \left[1 + 2\delta Z_e - \frac{\delta s}{s} + \frac{1}{2}\delta Z_W + \frac{1}{2}\delta Z_H + \frac{1}{2}\delta Z_{AA} \right] - \frac{1}{2c} \frac{1}{2} \delta Z_{ZA}, \\
W^\pm Z\phi^\mp \chi & : C = \mp \frac{i}{2c} \left[1 + 2\delta Z_e - \frac{\delta c}{c} + \frac{1}{2}\delta Z_W + \frac{1}{2}\delta Z_{ZZ} \right] \mp \frac{i}{2s} \frac{1}{2} \delta Z_{AZ}, \\
W^\pm A\phi^\mp \chi & : C = \mp \frac{i}{2s} \left[1 + 2\delta Z_e - \frac{\delta s}{s} + \frac{1}{2}\delta Z_W + \frac{1}{2}\delta Z_{AA} \right] \mp \frac{i}{2c} \frac{1}{2} \delta Z_{ZA}.
\end{aligned} \tag{A.10}$$

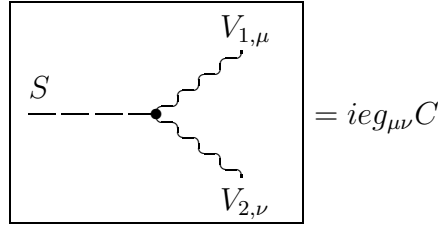
VSS-coupling:



with the actual values of V , S_1 , S_2 and C

$$\begin{aligned}
A\chi H & : C = -\frac{i}{2cs}\frac{1}{2}\delta Z_{ZA}, \\
Z\chi H & : C = -\frac{i}{2cs}\left[1 + \delta Z_e + \frac{s^2-c^2}{c^2}\frac{\delta s}{s} + \frac{1}{2}\delta Z_H + \frac{1}{2}\delta Z_{ZZ}\right], \\
A\phi^+\phi^- & : C = -\left[1 + \delta Z_e + \frac{1}{2}\delta Z_{AA} + \frac{s^2-c^2}{2sc}\frac{1}{2}\delta Z_{ZA}\right], \\
Z\phi^+\phi^- & : C = -\frac{s^2-c^2}{2sc}\left[1 + \delta Z_e + \frac{1}{(s^2-c^2)c^2}\frac{\delta s}{s} + \frac{1}{2}\delta Z_{ZZ}\right] - \frac{1}{2}\delta Z_{AZ}, \\
W^\pm\phi^\mp H & : C = \mp\frac{1}{2s}\left[1 + \delta Z_e - \frac{\delta s}{s} + \frac{1}{2}\delta Z_W + \frac{1}{2}\delta Z_H\right], \\
W^\pm\phi^\mp\chi & : C = -\frac{i}{2s}\left[1 + \delta Z_e - \frac{\delta s}{s} + \frac{1}{2}\delta Z_W\right].
\end{aligned} \tag{A.11}$$

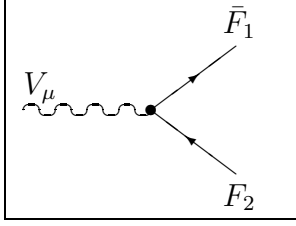
SVV-coupling:



with the actual values of S , V_1 , V_2 and C

$$\begin{aligned}
HW^+W^- & : C = M_W\frac{1}{s}\left[1 + \delta Z_e - \frac{\delta s}{s} + \frac{1}{2}\frac{\delta M_W^2}{M_W^2} + \frac{1}{2}\delta Z_H + \delta Z_W\right], \\
HZZ & : C = M_W\frac{1}{sc^2}\left[1 + \delta Z_e + \frac{2s^2-c^2}{c^2}\frac{\delta s}{s} + \frac{1}{2}\frac{\delta M_W^2}{M_W^2} + \frac{1}{2}\delta Z_H + \delta Z_{ZZ}\right], \\
HZA & : C = M_W\frac{1}{sc^2}\frac{1}{2}\delta Z_{ZA}, \\
\phi^\pm W^\mp Z & : C = -M_W\frac{s}{c}\left[1 + \delta Z_e + \frac{1}{c^2}\frac{\delta s}{s} + \frac{1}{2}\frac{\delta M_W^2}{M_W^2} + \frac{1}{2}\delta Z_W + \frac{1}{2}\delta Z_{ZZ}\right] - M_W\frac{1}{2}\delta Z_{AZ}, \\
\phi^\pm W^\mp A & : C = -M_W\left[1 + \delta Z_e + \frac{1}{2}\frac{\delta M_W^2}{M_W^2} + \frac{1}{2}\delta Z_W + \frac{1}{2}\delta Z_{AA}\right] - M_W\frac{s}{c}\frac{1}{2}\delta Z_{ZA}.
\end{aligned} \tag{A.12}$$

VFF-coupling:



$$= ie\gamma_\mu(C^-\omega_- + C^+\omega_+)$$

with the actual values of V , \bar{F}_1 , F_2 and C^+ , C^-

$$\begin{aligned}
\gamma \bar{f}_i f_j &: \begin{cases} C^+ = -Q_f \left[\delta_{ij} \left(1 + \delta Z_e + \frac{1}{2} \delta Z_{AA} \right) + \frac{1}{2} (\delta Z_{ij}^{f,R} + \delta Z_{ij}^{f,R\dagger}) \right] + \delta_{ij} g_f^+ \frac{1}{2} \delta Z_{ZA}, \\ C^- = -Q_f \left[\delta_{ij} \left(1 + \delta Z_e + \frac{1}{2} \delta Z_{AA} \right) + \frac{1}{2} (\delta Z_{ij}^{f,L} + \delta Z_{ij}^{f,L\dagger}) \right] + \delta_{ij} g_f^- \frac{1}{2} \delta Z_{ZA}, \end{cases} \\
Z \bar{f}_i f_j &: \begin{cases} C^+ = g_f^+ \left[\delta_{ij} \left(1 + \frac{\delta g_f^+}{g_f^+} + \frac{1}{2} \delta Z_{ZZ} \right) + \frac{1}{2} (\delta Z_{ij}^{f,R} + \delta Z_{ij}^{f,R\dagger}) \right] - \delta_{ij} Q_f \frac{1}{2} \delta Z_{AZ}, \\ C^- = g_f^- \left[\delta_{ij} \left(1 + \frac{\delta g_f^-}{g_f^-} + \frac{1}{2} \delta Z_{ZZ} \right) + \frac{1}{2} (\delta Z_{ij}^{f,L} + \delta Z_{ij}^{f,L\dagger}) \right] - \delta_{ij} Q_f \frac{1}{2} \delta Z_{AZ}, \end{cases} \\
W^+ \bar{u}_i d_j &: \begin{cases} C^+ = 0, & C^- = \frac{1}{\sqrt{2}s} \left[V_{ij} \left(1 + \delta Z_e - \frac{\delta s}{s} + \frac{1}{2} \delta Z_W \right) + \delta V_{ij} \right. \\ & \left. + \frac{1}{2} \sum_k (\delta Z_{ik}^{u,L\dagger} V_{kj} + V_{ik} \delta Z_{kj}^{d,L}) \right], \end{cases} \\
W^- \bar{d}_j u_i &: \begin{cases} C^+ = 0, & C^- = \frac{1}{\sqrt{2}s} \left[V_{ji}^\dagger \left(1 + \delta Z_e - \frac{\delta s}{s} + \frac{1}{2} \delta Z_W \right) + \delta V_{ji}^\dagger \right. \\ & \left. + \frac{1}{2} \sum_k (\delta Z_{jk}^{d,L\dagger} V_{ki}^\dagger + V_{jk}^\dagger \delta Z_{ki}^{u,L}) \right], \end{cases} \\
W^+ \bar{\nu}_i l_j &: C^+ = 0, \quad C^- = \frac{1}{\sqrt{2}s} \delta_{ij} \left[1 + \delta Z_e - \frac{\delta s}{s} + \frac{1}{2} \delta Z_W + \frac{1}{2} (\delta Z_{ii}^{\nu,L\dagger} + \delta Z_{ii}^{L,L}) \right], \\
W^- \bar{l}_j \nu_i &: C^+ = 0, \quad C^- = \frac{1}{\sqrt{2}s} \delta_{ij} \left[1 + \delta Z_e - \frac{\delta s}{s} + \frac{1}{2} \delta Z_W + \frac{1}{2} (\delta Z_{ii}^{l,L\dagger} + \delta Z_{ii}^{\nu,L}) \right], \end{aligned} \tag{A.13}$$

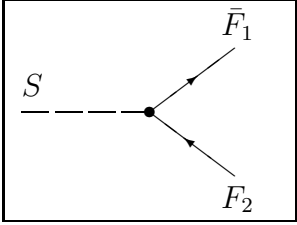
where

$$\begin{aligned}
g_f^+ &= -\frac{s}{c} Q_f, & \delta g_f^+ &= -\frac{s}{c} Q_f \left[\delta Z_e + \frac{1}{c^2} \frac{\delta s}{s} \right], \\
g_f^- &= \frac{I_{W,f}^3 - s^2 Q_f}{sc}, & \delta g_f^- &= \frac{I_{W,f}^3}{sc} \left[\delta Z_e + \frac{s^2 - c^2}{c^2} \frac{\delta s}{s} \right] + \delta g_f^+. \end{aligned} \tag{A.14}$$

The vector and axial vector couplings of the Z -boson are given by

$$v_f = \frac{1}{2} (g_f^- + g_f^+) = \frac{I_{W,f}^3 - 2s^2 Q_f}{2sc}, \quad a_f = \frac{1}{2} (g_f^- - g_f^+) = \frac{I_{W,f}^3}{2sc}. \tag{A.15}$$

SFF-coupling:



$$= ie(C^-\omega_- + C^+\omega_+)$$

with the actual values of S , \bar{F}_1 , F_2 and C^+ , C^-

$$\begin{aligned}
H\bar{f}_i f_j &: \begin{cases} C^+ = -\frac{1}{2s} \frac{1}{M_W} \left[\delta_{ij} m_{f,i} \left(1 + \delta Z_e - \frac{\delta s}{s} + \frac{\delta m_{f,i}}{m_{f,i}} - \frac{\delta M_W}{M_W} + \frac{1}{2} \delta Z_H \right) \right. \\ \quad \left. + \frac{1}{2} (m_{f,i} \delta Z_{ij}^{f,R} + \delta Z_{ij}^{f,L\dagger} m_{f,j}) \right], \\ C^- = -\frac{1}{2s} \frac{1}{M_W} \left[\delta_{ij} m_{f,i} \left(1 + \delta Z_e - \frac{\delta s}{s} + \frac{\delta m_{f,i}}{m_{f,i}} - \frac{\delta M_W}{M_W} + \frac{1}{2} \delta Z_H \right) \right. \\ \quad \left. + \frac{1}{2} (m_{f,i} \delta Z_{ij}^{f,L} + \delta Z_{ij}^{f,R\dagger} m_{f,j}) \right], \end{cases} \\
\chi\bar{f}_i f_j &: \begin{cases} C^+ = i \frac{1}{2s} 2I_{W,f}^3 \frac{1}{M_W} \left[\delta_{ij} m_{f,i} \left(1 + \delta Z_e - \frac{\delta s}{s} + \frac{\delta m_{f,i}}{m_{f,i}} - \frac{\delta M_W}{M_W} \right) \right. \\ \quad \left. + \frac{1}{2} (m_{f,i} \delta Z_{ij}^{f,R} + \delta Z_{ij}^{f,L\dagger} m_{f,j}) \right], \\ C^- = -i \frac{1}{2s} 2I_{W,f}^3 \frac{1}{M_W} \left[\delta_{ij} m_{f,i} \left(1 + \delta Z_e - \frac{\delta s}{s} + \frac{\delta m_{f,i}}{m_{f,i}} - \frac{\delta M_W}{M_W} \right) \right. \\ \quad \left. + \frac{1}{2} (m_{f,i} \delta Z_{ij}^{f,L} + \delta Z_{ij}^{f,R\dagger} m_{f,j}) \right], \end{cases} \\
\phi^+ \bar{u}_i d_j &: \begin{cases} C^+ = -\frac{1}{\sqrt{2}s} \frac{1}{M_W} \left[V_{ij} m_{d,j} \left(1 + \delta Z_e - \frac{\delta s}{s} + \frac{\delta m_{d,j}}{m_{d,j}} - \frac{\delta M_W}{M_W} \right) + \delta V_{ij} m_{d,j} \right. \\ \quad \left. + \frac{1}{2} \sum_k (\delta Z_{ik}^{u,L\dagger} V_{kj} m_{d,j} + V_{ik} m_{d,k} \delta Z_{kj}^{d,R}) \right], \\ C^- = \frac{1}{\sqrt{2}s} \frac{1}{M_W} \left[m_{u,i} V_{ij} \left(1 + \delta Z_e - \frac{\delta s}{s} + \frac{\delta m_{u,i}}{m_{u,i}} - \frac{\delta M_W}{M_W} \right) + m_{u,i} \delta V_{ij} \right. \\ \quad \left. + \frac{1}{2} \sum_k (\delta Z_{ik}^{u,R\dagger} m_{u,k} V_{kj} + m_{u,i} V_{ik} \delta Z_{kj}^{d,L}) \right], \end{cases} \\
\phi^- \bar{d}_j u_i &: \begin{cases} C^+ = \frac{1}{\sqrt{2}s} \frac{1}{M_W} \left[V_{ji}^\dagger m_{u,i} \left(1 + \delta Z_e - \frac{\delta s}{s} + \frac{\delta m_{u,i}}{m_{u,i}} - \frac{\delta M_W}{M_W} \right) + \delta V_{ji}^\dagger m_{u,i} \right. \\ \quad \left. + \frac{1}{2} \sum_k (\delta Z_{jk}^{d,L\dagger} V_{ki}^\dagger m_{u,i} + V_{jk}^\dagger m_{u,k} \delta Z_{ki}^{u,R}) \right], \\ C^- = -\frac{1}{\sqrt{2}s} \frac{1}{M_W} \left[m_{d,j} V_{ji}^\dagger \left(1 + \delta Z_e - \frac{\delta s}{s} + \frac{\delta m_{d,j}}{m_{d,j}} - \frac{\delta M_W}{M_W} \right) + m_{d,j} \delta V_{ji}^\dagger \right. \\ \quad \left. + \frac{1}{2} \sum_k (\delta Z_{jk}^{d,R\dagger} m_{d,k} V_{ki}^\dagger + m_{d,j} V_{jk}^\dagger \delta Z_{ki}^{u,L}) \right], \end{cases} \\
\phi^+ \bar{\nu}_i l_j &: \begin{cases} C^+ = -\frac{1}{\sqrt{2}s} \frac{m_{l,i}}{M_W} \delta_{ij} \left[1 + \delta Z_e - \frac{\delta s}{s} + \frac{\delta m_{l,i}}{m_{l,i}} - \frac{\delta M_W}{M_W} + \frac{1}{2} (\delta Z_{ii}^{\nu,L\dagger} + \delta Z_{ii}^{l,R}) \right], \\ C^- = 0, \end{cases} \\
\phi^- \bar{l}_j \nu_i &: \begin{cases} C^+ = 0, \\ C^- = -\frac{1}{\sqrt{2}s} \frac{m_{l,i}}{M_W} \delta_{ij} \left[1 + \delta Z_e - \frac{\delta s}{s} + \frac{\delta m_{l,i}}{m_{l,i}} - \frac{\delta M_W}{M_W} + \frac{1}{2} (\delta Z_{ii}^{l,R\dagger} + \delta Z_{ii}^{\nu,L}) \right]. \end{cases}
\end{aligned} \tag{A.16}$$

VGG-coupling:

with the actual values of V , \bar{G}_1 , G_2 and C

$$\begin{aligned}
A\bar{u}^\pm u^\pm & : C = \pm \left[1 + \delta Z_e + \frac{1}{2} \delta Z_{AA} \right] \mp \frac{c}{s} \delta Z_{ZA}, \\
Z\bar{u}^\pm u^\pm & : C = \mp \frac{c}{s} \left[1 + \delta Z_e - \frac{1}{c^2} \frac{\delta s}{s} + \frac{1}{2} \delta Z_{ZZ} \right] \pm \frac{1}{2} \delta Z_{AZ}, \\
W^\pm \bar{u}^\pm u^Z & : C = \pm \frac{c}{s} \left[1 + \delta Z_e - \frac{1}{c^2} \frac{\delta s}{s} + \frac{1}{2} \delta Z_W \right], \\
W^\pm \bar{u}^Z u^\mp & : C = \mp \frac{c}{s} \left[1 + \delta Z_e - \frac{1}{c^2} \frac{\delta s}{s} + \frac{1}{2} \delta Z_W \right], \\
W^\pm \bar{u}^\pm u^\gamma & : C = \mp \left[1 + \delta Z_e + \frac{1}{2} \delta Z_W \right], \\
W^\pm \bar{u}^\gamma u^\mp & : C = \pm \left[1 + \delta Z_e + \frac{1}{2} \delta Z_W \right].
\end{aligned} \tag{A.17}$$

SGG-coupling:

with the actual values of S , \bar{G}_1 , G_2 and C

$$\begin{aligned}
H\bar{u}^Z u^Z & : C = -\frac{1}{2sc^2} M_W \left[1 + \delta Z_e + \frac{2s^2 - c^2}{c^2} \frac{\delta s}{s} + \frac{1}{2} \frac{\delta M_W^2}{M_W^2} + \frac{1}{2} \delta Z_H \right], \\
H\bar{u}^\pm u^\pm & : C = -\frac{1}{2s} M_W \left[1 + \delta Z_e - \frac{\delta s}{s} + \frac{1}{2} \frac{\delta M_W^2}{M_W^2} + \frac{1}{2} \delta Z_H \right], \\
\chi\bar{u}^\pm u^\pm & : C = \mp i \frac{1}{2s} M_W \left[1 + \delta Z_e - \frac{\delta s}{s} + \frac{1}{2} \frac{\delta M_W^2}{M_W^2} \right], \\
\phi^\pm \bar{u}^Z u^\pm & : C = \frac{1}{2sc} M_W \left[1 + \delta Z_e + \frac{s^2 - c^2}{c^2} \frac{\delta s}{s} + \frac{1}{2} \frac{\delta M_W^2}{M_W^2} \right], \\
\phi^\pm \bar{u}^\pm u^Z & : C = \frac{s^2 - c^2}{2sc} M_W \left[1 + \delta Z_e + \frac{1}{(s^2 - c^2)c^2} \frac{\delta s}{s} + \frac{1}{2} \frac{\delta M_W^2}{M_W^2} \right], \\
\phi^\pm \bar{u}^\pm u^\gamma & : C = M_W \left[1 + \delta Z_e + \frac{1}{2} \frac{\delta M_W^2}{M_W^2} \right].
\end{aligned} \tag{A.18}$$

B Self energies

In this appendix we list all self energies of the physical fields.

The gauge boson self energies read

$$\begin{aligned} \Sigma_T^{AA}(k^2) = & -\frac{\alpha}{4\pi} \left\{ \frac{2}{3} \sum_{f,i} N_C^f 2Q_f^2 \left[-(k^2 + 2m_{f,i}^2) B_0(k^2, m_{f,i}, m_{f,i}) \right. \right. \\ & \left. \left. + 2m_{f,i}^2 B_0(0, m_{f,i}, m_{f,i}) + \frac{1}{3}k^2 \right] \right. \\ & \left. + \left\{ [3k^2 + 4M_W^2] B_0(k^2, M_W, M_W) - 4M_W^2 B_0(0, M_W, M_W) \right\} \right\}, \end{aligned} \quad (\text{B.1})$$

$$\begin{aligned} \Sigma_T^{AZ}(k^2) = & -\frac{\alpha}{4\pi} \left\{ \frac{2}{3} \sum_{f,i} N_C^f (-Q_f) (g_f^+ + g_f^-) \left[-(k^2 + 2m_{f,i}^2) B_0(k^2, m_{f,i}, m_{f,i}) \right. \right. \\ & \left. \left. + 2m_{f,i}^2 B_0(0, m_{f,i}, m_{f,i}) + \frac{1}{3}k^2 \right] \right. \\ & \left. - \frac{1}{3s_W c_W} \left\{ \left[(9c_W^2 + \frac{1}{2})k^2 + (12c_W^2 + 4)M_W^2 \right] B_0(k^2, M_W, M_W) \right. \right. \\ & \left. \left. - (12c_W^2 - 2)M_W^2 B_0(0, M_W, M_W) + \frac{1}{3}k^2 \right\} \right\}, \end{aligned} \quad (\text{B.2})$$

$$\begin{aligned} \Sigma_T^{ZZ}(k^2) = & -\frac{\alpha}{4\pi} \left\{ \frac{2}{3} \sum_{f,i} N_C^f \left\{ ((g_f^+)^2 + (g_f^-)^2) \left[-(k^2 + 2m_{f,i}^2) B_0(k^2, m_{f,i}, m_{f,i}) \right. \right. \right. \\ & \left. \left. + 2m_{f,i}^2 B_0(0, m_{f,i}, m_{f,i}) + \frac{1}{3}k^2 \right] + \frac{3}{4s_W^2 c_W^2} m_{f,i}^2 B_0(k^2, m_{f,i}, m_{f,i}) \right\} \\ & + \frac{1}{6s_W^2 c_W^2} \left\{ \left[(18c_W^4 + 2c_W^2 - \frac{1}{2})k^2 + (24c_W^4 + 16c_W^2 - 10)M_W^2 \right] B_0(k^2, M_W, M_W) \right. \\ & \left. - (24c_W^4 - 8c_W^2 + 2)M_W^2 B_0(0, M_W, M_W) + (4c_W^2 - 1)\frac{1}{3}k^2 \right\} \\ & + \frac{1}{12s_W^2 c_W^2} \left\{ (2M_H^2 - 10M_Z^2 - k^2) B_0(k^2, M_Z, M_H) \right. \\ & \left. - 2M_Z^2 B_0(0, M_Z, M_Z) - 2M_H^2 B_0(0, M_H, M_H) \right. \\ & \left. - \frac{(M_Z^2 - M_H^2)^2}{k^2} (B_0(k^2, M_Z, M_H) - B_0(0, M_Z, M_H)) - \frac{2}{3}k^2 \right\}, \end{aligned} \quad (\text{B.3})$$

$$\begin{aligned}
\Sigma_T^W(k^2) = & -\frac{\alpha}{4\pi} \left\{ \frac{2}{3} \frac{1}{2s_W^2} \sum_i \left[-\left(k^2 - \frac{m_{l,i}^2}{2}\right) B_0(k^2, 0, m_{l,i}) + \frac{1}{3} k^2 \right. \right. \\
& \left. \left. + m_{l,i}^2 B_0(0, m_{l,i}, m_{l,i}) + \frac{m_{l,i}^4}{2k^2} \left(B_0(k^2, 0, m_{l,i}) - B_0(0, 0, m_{l,i}) \right) \right] \right. \\
& + \frac{2}{3} \frac{1}{2s_W^2} 3 \sum_{i,j} |V_{ij}|^2 \left[-\left(k^2 - \frac{m_{u,i}^2 + m_{d,j}^2}{2}\right) B_0(k^2, m_{u,i}, m_{d,j}) + \frac{1}{3} k^2 \right. \\
& \left. + m_{u,i}^2 B_0(0, m_{u,i}, m_{u,i}) + m_{d,j}^2 B_0(0, m_{d,j}, m_{d,j}) \right. \\
& \left. + \frac{(m_{u,i}^2 - m_{d,j}^2)^2}{2k^2} \left(B_0(k^2, m_{u,i}, m_{d,j}) - B_0(0, m_{u,i}, m_{d,j}) \right) \right] \\
& + \frac{2}{3} \left\{ \left(2M_W^2 + 5k^2 \right) B_0(k^2, M_W, \lambda) - 2M_W^2 B_0(0, M_W, M_W) \right. \\
& \left. - \frac{M_W^4}{k^2} \left(B_0(k^2, M_W, \lambda) - B_0(0, M_W, \lambda) \right) + \frac{1}{3} k^2 \right\} \\
& + \frac{1}{12s_W^2} \left\{ \left[(40c_W^2 - 1)k^2 + (16c_W^2 + 54 - 10c_W^{-2})M_W^2 \right] B_0(k^2, M_W, M_Z) \right. \\
& - (16c_W^2 + 2) \left[M_W^2 B_0(0, M_W, M_W) + M_Z^2 B_0(0, M_Z, M_Z) \right] + (4c_W^2 - 1) \frac{2}{3} k^2 \\
& \left. - (8c_W^2 + 1) \frac{(M_W^2 - M_Z^2)^2}{k^2} \left(B_0(k^2, M_W, M_Z) - B_0(0, M_W, M_Z) \right) \right\} \\
& + \frac{1}{12s_W^2} \left\{ \left(2M_H^2 - 10M_W^2 - k^2 \right) B_0(k^2, M_W, M_H) \right. \\
& - 2M_W^2 B_0(0, M_W, M_W) - 2M_H^2 B_0(0, M_H, M_H) \\
& \left. - \frac{(M_W^2 - M_H^2)^2}{k^2} \left(B_0(k^2, M_W, M_H) - B_0(0, M_W, M_H) \right) - \frac{2}{3} k^2 \right\}. \tag{B.4}
\end{aligned}$$

For the self energy of the physical Higgs boson we obtain

$$\begin{aligned}
\Sigma_T^H(k^2) = & -\frac{\alpha}{4\pi} \left\{ \sum_{f,i} N_C^f \frac{m_{f,i}^2}{2s_W^2 M_W^2} \left[2A_0(m_{f,i}) + (4m_{f,i}^2 - k^2) B_0(k^2, m_{f,i}, m_{f,i}) \right] \right. \\
& - \frac{1}{2s_W^2} \left[\left(6M_W^2 - 2k^2 + \frac{M_H^4}{2M_W^2} \right) B_0(k^2, M_W, M_W) + \left(3 + \frac{M_H^2}{2M_W^2} \right) A_0(M_W) - 6M_W^2 \right] \\
& \left. - \frac{1}{4s_W^2 c_W^2} \left[\left(6M_Z^2 - 2k^2 + \frac{M_H^4}{2M_Z^2} \right) B_0(k^2, M_Z, M_Z) + \left(3 + \frac{M_H^2}{2M_Z^2} \right) A_0(M_Z) - 6M_Z^2 \right] \right\}
\end{aligned}$$

$$- \frac{3}{8s_W^2} \left[3 \frac{M_H^4}{M_W^2} B_0(k^2, M_H, M_H) + \frac{M_H^2}{M_W^2} A_0(M_H) \right] \}. \quad (\text{B.5})$$

The fermion self energies are given by

$$\begin{aligned} \Sigma_{ij}^{f,L}(p^2) = & -\frac{\alpha}{4\pi} \left\{ \delta_{ij} Q_f^2 \left[2B_1(p^2, m_{f,i}, \lambda) + 1 \right] \right. \\ & + \delta_{ij} (g_f^-)^2 \left[2B_1(p^2, m_{f,i}, M_Z) + 1 \right] \\ & + \delta_{ij} \frac{1}{2s_W^2} \frac{1}{2} \frac{m_{f,i}^2}{M_W^2} \left[B_1(p^2, m_{f,i}, M_Z) + B_1(p^2, m_{f,i}, M_H) \right] \\ & \left. + \frac{1}{2s_W^2} \sum_k V_{ik} V_{kj}^\dagger \left[\left(2 + \frac{m_{f',k}^2}{M_W^2} \right) B_1(p^2, m_{f',k}, M_W) + 1 \right] \right\}, \quad (\text{B.6}) \end{aligned}$$

$$\begin{aligned} \Sigma_{ij}^{f,R}(p^2) = & -\frac{\alpha}{4\pi} \left\{ \delta_{ij} Q_f^2 \left[2B_1(p^2, m_{f,i}, \lambda) + 1 \right] \right. \\ & + \delta_{ij} (g_f^+)^2 \left[2B_1(p^2, m_{f,i}, M_Z) + 1 \right] \\ & + \delta_{ij} \frac{1}{2s_W^2} \frac{1}{2} \frac{m_{f,i}^2}{M_W^2} \left[B_1(p^2, m_{f,i}, M_Z) + B_1(p^2, m_{f,i}, M_H) \right] \\ & \left. + \frac{1}{2s_W^2} \frac{m_{f,i} m_{f,j}}{M_W^2} \sum_k V_{ik} V_{kj}^\dagger B_1(p^2, m_{f',k}, M_W) \right\}, \quad (\text{B.7}) \end{aligned}$$

$$\begin{aligned} \Sigma_{ij}^{f,S}(p^2) = & -\frac{\alpha}{4\pi} \left\{ \delta_{ij} Q_f^2 \left[4B_0(p^2, m_{f,i}, \lambda) - 2 \right] \right. \\ & + \delta_{ij} g_f^+ g_f^- \left[4B_0(p^2, m_{f,i}, M_Z) - 2 \right] \\ & + \delta_{ij} \frac{1}{2s_W^2} \frac{1}{2} \frac{m_{f,i}^2}{M_W^2} \left[B_0(p^2, m_{f,i}, M_Z) - B_0(p^2, m_{f,i}, M_H) \right] \\ & \left. + \frac{1}{2s_W^2} \sum_k V_{ik} V_{kj}^\dagger \frac{m_{f',k}^2}{M_W^2} B_0(p^2, m_{f',k}, M_W) \right\}. \quad (\text{B.8}) \end{aligned}$$

f' is the isospin partner of the fermion f and N_C^f the colour factor. i, j, k run over the fermion generations. For down-type quarks $V_{ik} V_{kj}^\dagger$ has to be replaced by $V_{ik}^\dagger V_{kj}$.

The two-point function B_0 was given in Sect. 4.3. For B_1 we find

$$B_1(p^2, m_0, m_1) = \frac{m_1^2 - m_0^2}{2p^2} \left(B_0(p^2, m_0, m_1) - B_0(0, m_0, m_1) \right) - \frac{1}{2} B_0(p^2, m_0, m_1). \quad (\text{B.9})$$

For the field renormalization constants one needs in addition the derivatives of the self energies with respect to k^2 or p^2 , respectively. These are easily obtained from the expressions above. $\frac{\partial B_0}{\partial p^2}$ was given in Sect. 4.3, $\frac{\partial B_1}{\partial p^2}$ can be calculated from (B.9) as

$$\begin{aligned} \frac{\partial}{\partial p^2} B_1(p^2, m_0, m_1) &= -\frac{m_1^2 - m_0^2}{2p^4} \left(B_0(p^2, m_0, m_1) - B_0(0, m_0, m_1) \right) \\ &+ \frac{m_1^2 - m_0^2 - p^2}{2p^2} \frac{\partial}{\partial p^2} B_0(p^2, m_0, m_1). \end{aligned} \quad (\text{B.10})$$

These derivatives become IR-singular for $m_0^2 = p^2$ and $m_1^2 = 0$ or vice versa. This leads to IR-singular contributions in the field renormalization constants of charged particles arising from photonic corrections to the corresponding self energies. Because these reduce to very simple expressions we give the photonic contributions to the field renormalization constants of the W -boson and the charged fermions explicitly

$$\delta Z_W|_{\text{photonic}} = -\frac{\alpha}{\pi} \log \frac{\lambda}{M_W} + \frac{\alpha}{6\pi} \left(\frac{1}{3} + 5 \left(\Delta + 1 - \log \frac{M_W^2}{\mu^2} \right) \right), \quad (\text{B.11})$$

$$\begin{aligned} \delta Z_{ii}^{f,L}|_{\text{photonic}} &= \delta Z_{ii}^{f,R}|_{\text{photonic}} \\ &= -\frac{\alpha}{4\pi} Q_f^2 \left[\Delta - \log \frac{m_{f,i}^2}{\mu^2} + 4 + 4 \log \frac{\lambda}{m_{f,i}} \right]. \end{aligned} \quad (\text{B.12})$$

C Vertex formfactors

The vertex formfactors \mathcal{V} , \mathcal{W} , \mathcal{X} , can be expressed by the scalar one-loop integrals $B_0(m_0^2, M_1, M_2)$, $C_0(m_1^2, m_0^2, m_2^2, M_0, M_1, M_2)$ and the scalar coefficients of the vector and tensor integrals $B_1(m_0^2, M_1, M_2)$, $C_{i(j)}(m_1^2, m_0^2, m_2^2, M_0, M_1, M_2)$

$$\begin{aligned} \mathcal{V}_a(m_1^2, m_0^2, m_2^2, M_0, M_1, M_2) &= B_0(m_0^2, M_1, M_2) - 2 - (M_0^2 - m_1^2 - M_1^2)C_1 \\ &\quad - (M_0^2 - m_2^2 - M_2^2)C_2 - 2(m_0^2 - m_1^2 - m_2^2)(C_1 + C_2 + C_0), \end{aligned} \quad (\text{C.1})$$

$$\begin{aligned} \mathcal{V}_b^-(m_1^2, m_0^2, m_2^2, M_0, M_1, M_2) &= 3B_0(m_0^2, M_1, M_2) + 4M_0^2C_0 \\ &\quad + (4m_1^2 + 2m_2^2 - 2m_0^2 + M_0^2 - M_1^2)C_1 \\ &\quad + (4m_2^2 + 2m_1^2 - 2m_0^2 + M_0^2 - M_2^2)C_2, \end{aligned} \quad (\text{C.2})$$

$$\mathcal{V}_b^+(m_1^2, m_0^2, m_2^2, M_0, M_1, M_2) = 3m_1^2C_0, \quad (\text{C.3})$$

$$\mathcal{V}_c(m_1^2, m_0^2, m_2^2, M_0, M_1, M_2) = -2\frac{m_1^2m_2^2}{M_W^2}(C_1 + C_2 + 2C_0), \quad (\text{C.4})$$

$$\mathcal{V}_d(m_1^2, m_0^2, m_2^2, M_0, M_1, M_2) = m_1^2(C_1 - C_0), \quad (\text{C.5})$$

$$\mathcal{V}_e(m_1^2, m_0^2, m_2^2, M_0, M_1, M_2) = \frac{m_1^2}{M_W^2}C_{00}, \quad (\text{C.6})$$

$$\mathcal{V}_f^-(m_1^2, m_0^2, m_2^2, M_0, M_1, M_2) = m_1^2C_0 + m_2^2C_2, \quad (\text{C.7})$$

$$\mathcal{V}_f^+(m_1^2, m_0^2, m_2^2, M_0, M_1, M_2) = m_1^2C_1, \quad (\text{C.8})$$

$$\mathcal{W}_a^-(m_1^2, m_0^2, m_2^2, M_0, M_1, M_2) = 2(C_1 + C_2 + C_0), \quad (\text{C.9})$$

$$\mathcal{W}_a^+(m_1^2, m_0^2, m_2^2, M_0, M_1, M_2) = -2C_0, \quad (\text{C.10})$$

$$\mathcal{W}_b^-(m_1^2, m_0^2, m_2^2, M_0, M_1, M_2) = 3(C_1 + C_2), \quad (\text{C.11})$$

$$\mathcal{W}_b^+(m_1^2, m_0^2, m_2^2, M_0, M_1, M_2) = 3C_0, \quad (\text{C.12})$$

$$\mathcal{W}_c^-(m_1^2, m_0^2, m_2^2, M_0, M_1, M_2) = \frac{1}{2M_W^2} \left[B_0(m_0^2, M_1, M_2) - 1 - M_0^2(C_1 + C_2) \right], \quad (\text{C.13})$$

$$\mathcal{W}_c^+(m_1^2, m_0^2, m_2^2, M_0, M_1, M_2) = \frac{2}{M_W^2} \left[m_1^2C_1 + m_2^2C_2 \right], \quad (\text{C.14})$$

$$\mathcal{W}_d(m_1^2, m_0^2, m_2^2, M_0, M_1, M_2) = -C_2, \quad (\text{C.15})$$

$$\mathcal{W}_e(m_1^2, m_0^2, m_2^2, M_0, M_1, M_2) = \frac{-1}{M_W^2} C_{00}, \quad (\text{C.16})$$

$$\mathcal{W}_f^-(m_1^2, m_0^2, m_2^2, M_0, M_1, M_2) = -C_1, \quad (\text{C.17})$$

$$\mathcal{W}_f^+(m_1^2, m_0^2, m_2^2, M_0, M_1, M_2) = -C_2 - C_0, \quad (\text{C.18})$$

$$\mathcal{X}_a^-(m_1^2, m_0^2, m_2^2, M_0, M_1, M_2) = -4[C_{11} + C_{12} + 2C_1 + C_2 + C_0], \quad (\text{C.19})$$

$$\mathcal{X}_a^+(m_1^2, m_0^2, m_2^2, M_0, M_1, M_2) = 4[C_1 + C_2 + C_0], \quad (\text{C.20})$$

$$\mathcal{X}_b^-(m_1^2, m_0^2, m_2^2, M_0, M_1, M_2) = 2[2C_{11} + 2C_{12} - C_2], \quad (\text{C.21})$$

$$\mathcal{X}_b^+(m_1^2, m_0^2, m_2^2, M_0, M_1, M_2) = 6[C_1 + C_2], \quad (\text{C.22})$$

$$\mathcal{X}_c^-(m_1^2, m_0^2, m_2^2, M_0, M_1, M_2) = -2\frac{m_2^2}{M_W^2}[C_{22} + C_{12}], \quad (\text{C.23})$$

$$\mathcal{X}_c^+(m_1^2, m_0^2, m_2^2, M_0, M_1, M_2) = -4\frac{m_2^2}{M_W^2}C_2, \quad (\text{C.24})$$

$$\mathcal{X}_d(m_1^2, m_0^2, m_2^2, M_0, M_1, M_2) = 2C_2, \quad (\text{C.25})$$

$$\mathcal{X}_e^-(m_1^2, m_0^2, m_2^2, M_0, M_1, M_2) = \frac{m_1^2}{M_W^2}[C_{11} + C_{12} + C_1], \quad (\text{C.26})$$

$$\mathcal{X}_e^0(m_1^2, m_0^2, m_2^2, M_0, M_1, M_2) = [C_{22} + C_{12} + C_2], \quad (\text{C.27})$$

$$\mathcal{X}_e^+(m_1^2, m_0^2, m_2^2, M_0, M_1, M_2) = \frac{m_1^2}{M_W^2}[C_1 + C_2 + C_0], \quad (\text{C.28})$$

$$\mathcal{X}_f(m_1^2, m_0^2, m_2^2, M_0, M_1, M_2) = -2C_1. \quad (\text{C.29})$$

Using the reduction methods described in Chap. 4 the vector and tensor coefficients can be expressed by scalar integrals. For illustration we give the explicit reduction formulae. The vertex function is defined as

$$\begin{aligned} C_{\dots} &= C_{\dots}(p_1, p_2, M_0, M_1, M_2) = C_{\dots}(m_1^2, m_0^2, m_2^2, M_0, M_1, M_2) \\ &= \frac{(2\pi\mu)^{4-D}}{i\pi^2} \int d^D q \frac{\dots}{[q^2 - M_0^2][(q + p_1)^2 - M_1^2][(q + p_2)^2 - M_2^2]} \end{aligned} \quad (\text{C.30})$$

with

$$p_1^2 = m_1^2, \quad p_2^2 = m_2^2, \quad p_1 p_2 = -\frac{1}{2}(m_0^2 - m_1^2 - m_2^2). \quad (\text{C.31})$$

For the three-point vector functions (4.18) yields ($P = 1$, $M = N - 1 = 2$)

$$C_k = T_k^3 = (X_2^{-1})_{kk'} R^{3,k'} \quad (\text{C.32})$$

with $k, k' = 1, 2$ and

$$X_2 = \begin{pmatrix} m_1^2 & \frac{1}{2}(m_1^2 + m_2^2 - m_0^2) \\ \frac{1}{2}(m_1^2 + m_2^2 - m_0^2) & m_2^2 \end{pmatrix}. \quad (\text{C.33})$$

Evaluating X_2^{-1} this gives

$$\begin{aligned} C_1 &= -\frac{4}{\kappa^2} \left[m_2^2 R^{3,1} + \frac{1}{2} (m_0^2 - m_1^2 - m_2^2) R^{3,2} \right], \\ C_2 &= -\frac{4}{\kappa^2} \left[\frac{1}{2} (m_0^2 - m_1^2 - m_2^2) R^{3,1} + m_1^2 R^{3,2} \right], \end{aligned} \quad (\text{C.34})$$

where

$$\kappa = \kappa(m_0^2, m_1^2, m_2^2), \quad (\text{C.35})$$

from (4.28). The R 's are obtained from (4.19) as

$$\begin{aligned} R^{3,1} &= \frac{1}{2} \left[B_0(m_2^2, M_0, M_2) - (m_1^2 - M_1^2 + M_0^2) C_0 - B_0(m_0^2, M_2, M_1) \right], \\ R^{3,2} &= \frac{1}{2} \left[B_0(m_1^2, M_0, M_1) - (m_2^2 - M_2^2 + M_0^2) C_0 - B_0(m_0^2, M_2, M_1) \right]. \end{aligned} \quad (\text{C.36})$$

The tensor coefficients are evaluated analogously as ($P = 2$, $M = 2$)

$$\begin{aligned} C_{00} &= \frac{1}{D-2} \left[R^{3,00} - R_1^{3,1} - R_2^{3,2} \right] \\ C_{ki} &= T_{ki}^3 = (X_2^{-1})_{kk'} [R_i^{3,k'} - \delta_i^{k'} C_{00}] \end{aligned} \quad (\text{C.37})$$

or more explicitly

$$\begin{aligned} C_{00} &= \frac{1}{4} \left[B_0(m_0^2, M_2, M_1) + (M_0^2 - M_1^2 + m_1^2) C_1 \right. \\ &\quad \left. + (M_0^2 - M_2^2 + m_2^2) C_2 + 1 + 2M_0^2 C_0 \right], \\ C_{11} &= -\frac{4}{\kappa^2} \left[m_2^2 (R_1^{3,1} - C_{00}) + \frac{1}{2} (m_0^2 - m_1^2 - m_2^2) R_1^{3,2} \right], \\ C_{21} &= -\frac{4}{\kappa^2} \left[\frac{1}{2} (m_0^2 - m_1^2 - m_2^2) (R_1^{3,1} - C_{00}) + m_1^2 R_1^{3,2} \right] = \\ C_{12} &= -\frac{4}{\kappa^2} \left[m_2^2 R_2^{3,1} + \frac{1}{2} (m_0^2 - m_1^2 - m_2^2) (R_2^{3,2} - C_{00}) \right], \\ C_{22} &= -\frac{4}{\kappa^2} \left[\frac{1}{2} (m_0^2 - m_1^2 - m_2^2) R_2^{3,1} + m_1^2 (R_2^{3,2} - C_{00}) \right] \end{aligned} \quad (\text{C.38})$$

with

$$\begin{aligned}
R^{3,00} &= M_0^2 C_0 + B_0(m_0^2, M_2, M_1), \\
R_1^{3,1} &= \frac{1}{2} \left[- (m_1^2 - M_1^2 + M_0^2) C_1 - B_1(m_0^2, M_2, M_1) \right], \\
R_2^{3,1} &= \frac{1}{2} \left[B_1(m_2^2, M_0, M_2) - (m_1^2 - M_1^2 + M_0^2) C_2 + (B_0 + B_1)(m_0^2, M_2, M_1) \right], \\
R_1^{3,2} &= \frac{1}{2} \left[B_1(m_1^2, M_0, M_1) - (m_2^2 - M_2^2 + M_0^2) C_1 - B_1(m_0^2, M_2, M_1) \right], \\
R_2^{3,2} &= \frac{1}{2} \left[- (m_2^2 - M_2^2 + M_0^2) C_2 + (B_0 + B_1)(m_0^2, M_2, M_1) \right]. \quad (\text{C.39})
\end{aligned}$$

Note that $C_{12} = C_{21}$ can be calculated in two different ways. In the evaluation of C_{00} we used (4.55)

B_1 was given in (B.9). The results for the scalar integrals can again be found in Sect. 4.3.

D Bremsstrahlung integrals

For the decay width of a massive particle with momentum p_0 and mass m_0 into two massive particles with momenta p_1, p_2 and masses m_1, m_2 and a photon with momentum q and mass λ we need the following phase space integrals

$$I_{i_1, \dots, i_n}^{j_1, \dots, j_m}(m_0, m_1, m_2) = \frac{1}{\pi^2} \int \frac{d^3 p_1}{2p_{10}} \frac{d^3 p_2}{2p_{20}} \frac{d^3 q}{2q_0} \delta(p_0 - p_1 - p_2 - q) \frac{(\pm 2q p_{j_1}) \cdots (\pm 2q p_{j_m})}{(\pm 2q p_{i_1}) \cdots (\pm 2q p_{i_n})}. \quad (\text{D.1})$$

Here $j_k, i_l = 0, 1, 2$ and the plus signs belong to p_1, p_2 , the minus signs to p_0 .

Introducing the abbreviations

$$\kappa = \kappa(m_0^2, m_1^2, m_2^2), \quad (\text{D.2})$$

as defined in (4.28) and

$$\begin{aligned} \beta_0 &= \frac{m_0^2 - m_1^2 - m_2^2 + \kappa}{2m_1 m_2}, \\ \beta_1 &= \frac{m_0^2 - m_1^2 + m_2^2 - \kappa}{2m_0 m_2}, \quad \beta_2 = \frac{m_0^2 + m_1^2 - m_2^2 - \kappa}{2m_0 m_1}, \end{aligned} \quad (\text{D.3})$$

with

$$\beta_0 \beta_1 \beta_2 = 1, \quad (\text{D.4})$$

we get compact expressions for the final results. From (D.1) it is evident that the integrals with the indices 1 and 2 interchanged are obtained by interchanging m_1 and m_2 . We list only the independent integrals. The IR-singular ones are given by

$$I_{00} = \frac{1}{4m_0^4} \left[\kappa \log\left(\frac{\kappa^2}{\lambda m_0 m_1 m_2}\right) - \kappa - (m_1^2 - m_2^2) \log\left(\frac{\beta_1}{\beta_2}\right) - m_0^2 \log(\beta_0) \right], \quad (\text{D.5})$$

$$I_{11} = \frac{1}{4m_1^2 m_0^2} \left[\kappa \log\left(\frac{\kappa^2}{\lambda m_0 m_1 m_2}\right) - \kappa - (m_0^2 - m_2^2) \log\left(\frac{\beta_0}{\beta_2}\right) - m_1^2 \log(\beta_1) \right], \quad (\text{D.6})$$

$$\begin{aligned} I_{01} &= \frac{1}{4m_0^2} \left[-2 \log\left(\frac{\lambda m_0 m_1 m_2}{\kappa^2}\right) \log(\beta_2) + 2 \log^2(\beta_2) - \log^2(\beta_0) - \log^2(\beta_1) \right. \\ &\quad \left. + 2Sp(1 - \beta_2^2) - Sp(1 - \beta_0^2) - Sp(1 - \beta_1^2) \right], \end{aligned} \quad (\text{D.7})$$

$$\begin{aligned} I_{12} &= -I_{01} - I_{02} \\ &= \frac{1}{4m_0^2} \left[-2 \log\left(\frac{\lambda m_0 m_1 m_2}{\kappa^2}\right) \log(\beta_0) + 2 \log^2(\beta_0) - \log^2(\beta_1) - \log^2(\beta_2) \right. \\ &\quad \left. + 2Sp(1 - \beta_0^2) - Sp(1 - \beta_1^2) - Sp(1 - \beta_2^2) \right]. \end{aligned} \quad (\text{D.8})$$

For the IR finite integrals we obtain

$$I = \frac{1}{4m_0^2} \left[\frac{\kappa}{2} (m_0^2 + m_1^2 + m_2^2) + 2m_0^2 m_1^2 \log(\beta_2) + 2m_0^2 m_2^2 \log(\beta_1) + 2m_1^2 m_2^2 \log(\beta_0) \right],$$

$$I_0 = \frac{1}{4m_0^2} \left[-2m_1^2 \log(\beta_2) - 2m_2^2 \log(\beta_1) - \kappa \right], \quad (\text{D.9})$$

$$I_1 = \frac{1}{4m_0^2} \left[-2m_0^2 \log(\beta_2) - 2m_2^2 \log(\beta_0) - \kappa \right], \quad (\text{D.10})$$

$$I_0^1 = \frac{1}{4m_0^2} \left[m_1^4 \log(\beta_2) - m_2^2(2m_0^2 - 2m_1^2 + m_2^2) \log(\beta_1) - \frac{\kappa}{4}(m_0^2 - 3m_1^2 + 5m_2^2) \right], \quad (\text{D.11})$$

$$I_1^0 = \frac{1}{4m_0^2} \left[m_0^4 \log(\beta_2) - m_2^2(2m_1^2 - 2m_0^2 + m_2^2) \log(\beta_0) - \frac{\kappa}{4}(m_1^2 - 3m_0^2 + 5m_2^2) \right], \quad (\text{D.12})$$

$$\begin{aligned} I_2^1 &= -I - I_2^0 \\ &= \frac{1}{4m_0^2} \left[m_1^4 \log(\beta_0) - m_0^2(2m_2^2 - 2m_1^2 + m_0^2) \log(\beta_1) - \frac{\kappa}{4}(m_2^2 - 3m_1^2 + 5m_0^2) \right], \end{aligned} \quad (\text{D.13})$$

$$I_{00}^{12} = -\frac{1}{4m_0^2} \left[m_1^4 \log(\beta_2) + m_2^4 \log(\beta_1) + \frac{\kappa^3}{6m_0^2} + \frac{\kappa}{4}(3m_1^2 + 3m_2^2 - m_0^2) \right], \quad (\text{D.14})$$

$$I_{11}^{02} = -\frac{1}{4m_0^2} \left[m_0^4 \log(\beta_2) + m_2^4 \log(\beta_0) + \frac{\kappa^3}{6m_1^2} + \frac{\kappa}{4}(3m_0^2 + 3m_2^2 - m_1^2) \right], \quad (\text{D.15})$$

$$I_{11}^{00} = -I_1^0 - I_{11}^{02} = \frac{1}{4m_0^2} \left[2m_2^2(m_1^2 + m_2^2 - m_0^2) \log(\beta_0) + \frac{\kappa^3}{6m_1^2} + 2\kappa m_2^2 \right], \quad (\text{D.16})$$

$$I_{00}^{11} = -I_0^1 - I_{00}^{12} = \frac{1}{4m_0^2} \left[2m_2^2(m_0^2 + m_2^2 - m_1^2) \log(\beta_1) + \frac{\kappa^3}{6m_0^2} + 2\kappa m_2^2 \right], \quad (\text{D.17})$$

$$I_{11}^{22} = -I_1^2 - I_{11}^{02} = \frac{1}{4m_0^2} \left[2m_0^2(m_0^2 + m_1^2 - m_2^2) \log(\beta_2) + \frac{\kappa^3}{6m_1^2} + 2\kappa m_0^2 \right]. \quad (\text{D.18})$$

Note the symmetries in $0 \leftrightarrow 1$ and $0 \leftrightarrow 2$.

References

- [1] S.L. Glashow, *Nucl. Phys.* **22** (1961) 579.
- [2] S. Weinberg, *Phys. Rev. Lett.* **19** (1967) 1264.
- [3] A. Salam, in *Elementary Particle Theory*, ed. N. Svartholm (Almqvist and Wiksell, Stockholm, 1968), p. 367.
- [4] S.L. Glashow, J. Illiopoulos, L. Maiani, *Phys. Rev.* **D2** (1970) 1285.
- [5] F. Dydak, in 'Proceedings of the 25th International Conference on High Energy Physics', eds. K. K. Phua and Y. Yamaguchi, World Scientific, Singapore (1991), Vol. 1 p. 3.
- [6] M. Davier et al., in [63] p. 120. Vol. 1.
- [7] M. Veltman, *Nucl. Phys.* **B123** (1977) 89.
- [8] J. Ellis and G. L. Fogli, *Phys. Lett.* **249B** (1990) 543.
- [9] A. C. K. Hsieh and E. Yehudai, SLAC-PUB-5576 (1991).
- [10] E. E. Boos et al.; in 'New computing techniques in physics research', eds. D. Perret-Gallix and W. Wojcik, Paris (1990), p. 573; Moscow State University preprint MGU-89-63/140.
- [11] J. Küblbeck, M. Böhm and A. Denner, *Comp. Phys. Comm.* **60** (1990) 165.
- [12] R. Mertig, M. Böhm and A. Denner, *Comp. Phys. Comm.* **64** (1991) 345.
- [13] 'Z-physics at LEP', CERN-89-08 eds. G. Altarelli, R. Kleiss and C. Verzegnassi, Vol. 1-3 and references therein.
- [14] W. Beenakker, F. A. Berends and T. Sack, *Nucl. Phys.* **B367** (1991) 287.
- [15] R. Kleiss, in [13], Vol. 3, p. 1 and references therein.
- [16] P. W. Higgs, *Phys. Lett.* **12** (1964) 132; *Phys. Rev. Lett.* **13** (1964) 508; *Phys. Rev.* **145** (1966) 1156;
R. Brout and F. Englert, *Phys. Rev. Lett.* **13** (1964) 321;
T. W. B. Kibble, *Phys. Rev.* **155** (1967) 1554.
- [17] G. 't Hooft, *Nucl. Phys.* **B33** (1971) 173; **B35** (1971) 167.
- [18] G. Passarino and M. Veltman, *Nucl. Phys.* **B160** (1979) 151;
M. Consoli, *Nucl. Phys.* **B160** (1979) 208;
M. Veltman, *Phys. Lett* **91B** (1980) 95;
M. Green and M. Veltman, *Nucl. Phys.* **B169** (1980) 137; *E: Nucl. Phys.* **B175** (1980) 547.
- [19] D. C. Kennedy and B. W. Lynn, *Nucl. Phys.* **B322** (1989) 1;
B. W. Lynn, SLAC-PUB 5077 (1989) and SU-ITP-867(1989);
D. C. Kennedy, *Nucl. Phys.* **B351** (1991) 81;
M. Kuroda, G. Moutaka and D. Schildknecht, *Nucl. Phys.* **B350** (1991) 25.

- [20] D. A. Ross and J. C. Taylor, *Nucl. Phys.* **B51** (1979) 25.
- [21] D. Yu. Bardin, P. Ch. Christova and O. M. Federenko, *Nucl. Phys.* **175** (1980) 435; *Nucl. Phys.* **197** (1982) 1.
- [22] J. Fleischer and F. Jegerlehner, *Phys. Rev.* **D23** (1981) 2001.
- [23] S. Sakakibara, *Phys. Rev.* **D24** (1981) 1149.
- [24] K. I. Aoki, Z. Hioki, R. Kawabe, M. Konuma and T. Muta, *Prog. Theo. Phys.* **64** (1980) 707; **65** (1981) 1001; *Suppl. Prog. Theo. Phys.* **73** (1982) 1.
- [25] M. Böhm, W. Hollik and H. Spiesberger, *Fortschr. Phys.* **34** (1986) 687.
- [26] A. Sirlin, *Phys. Rev.* **D22** (1980) 971;
W. J. Marciano and A. Sirlin, *Phys. Rev.* **D22** (1980) 2695;
A. Sirlin and W. J. Marciano, *Nucl. Phys.* **B189** (1981) 442.
- [27] A. Denner and T. Sack, *Nucl. Phys.* **B347** (1990) 203.
- [28] G. 't Hooft and M. Veltman, *Nucl. Phys.* **B153** (1979) 365.
- [29] D. B. Melrose, *Nuovo Cimento* **XL A** (1965) 181.
- [30] R. G. Stuart, *Comp. Phys. Comm.* **48** (1988) 367 and 56 (1990) 337.
- [31] G. J. van Oldenborgh and J. A. M. Vermaseren, *Z. Phys.* **C46** (1990) 425,
G. J. van Oldenborgh, Ph.D Thesis, Amsterdam 1990,
G. J. van Oldenborgh, *Comp. Phys. Comm.* **B66** (1991) 1.
- [32] A. Denner, U. Nierste and R. Scharf, *Nucl. Phys.* **B367** (1991) 637.
- [33] B. Grzadkowski, P. Krawczyk, J. H. Kühn and R. G. Stuart, *Nucl. Phys.* **B281** (1987) 18;
R. J. Guth and J. H. Kühn, *Nucl. Phys.* **B368** (1992) 38.
- [34] H. Eck, Diploma thesis, Würzburg (1990).
- [35] *SCHOONSHIP* by M. Veltman, see H. Strubbe, *Comp. Phys. Comm.* **8** (1974) 1;
REDUCE by A. C. Hearn, see *REDUCE* User's Manual, Rand Corporation, 1985;
FORM by J. A. M. Vermaseren, see *FORM* User's guide, Amsterdam (1990).
- [36] F. Bloch and A. Nordsieck, *Phys. Rev.* **52** (1937) 54.
- [37] M. Greco, G. Pancheri and Y. Srivastava, *Nucl. Phys.* **B171** (1980) 118;
E: *Nucl. Phys.* **B197** (1982) 543.
- [38] M. Böhm and W. Hollik, *Nucl. Phys.* **B204** (1982) 45.
- [39] Particle Data Group, *Phys. Lett.* **239B** (1990) 1.
- [40] H. Harari and M. Leurer, *Phys. Lett.* **B181** (1986) 123.
- [41] H. Burkhardt, F. Jegerlehner, G. Penso and C. Verzegnassi, *Z. Phys.* **C43** (1989) 497;
G. Burgers and F. Jegerlehner, in [13], Vol. 1, p. 55.

- [42] W. J. Marciano, *Phys. Rev.* **D20** (1979) 274;
A. Sirlin, *Phys. Rev.* **D29** (1984) 89.
- [43] W. Beenakker, F. A. Berends and W. L. van Neerven, in 'Radiative Corrections for e^+e^- -collisions', ed. J. H. Kühn, Springer, Berlin Heidelberg (1989).
- [44] M. Consoli, W. Hollik and F. Jegerlehner, *Phys. Lett.* **227B** (1989) 167;
M. Consoli and W. Hollik, in [13], Vol. 1, p. 7.
- [45] J. J. van der Bij and F. Hoogeveen, *Nucl. Phys.* **B283** (1987) 477.
- [46] E. Longo et al., in [63], p. 85.
- [47] P. Roudeau et al., in [63], p. 49.
- [48] D. Albert, W. J. Marciano, D. Wyler and Z. Parsa, *Nucl. Phys.* **B166** (1980) 460;
K. Inoue, A. Kakuto, H. Komatsu and S. Takeshita, *Prog. Theo. Phys.* **64** (1980) 1008;
T. H. Chang, K. J. F. Gaemers and W. L. van Neerven, *Nucl. Phys.* **B202** (1982) 407.
- [49] D. Yu. Bardin, S. Riemann and T. Riemann, *Z. Phys.* **C32** (1986) 121.
- [50] F. Jegerlehner, *Z. Phys.* **C32** (1986) 425 and in [51].
- [51] Proc. of the 11th International School of Theoretical Physics "Testing of the Standard Model", Szczyrk-Bila (Poland) 1987; eds. M. Zralek and R. Manka, World Scientific, Singapore (1988).
- [52] F. A. Berends and R. Kleiss, *Z. Phys.* **C27** (1985) 365.
- [53] J. Fleischer and F. Jegerlehner, *Z. Phys.* **C26** (1985) 629.
- [54] T. Alvarez, A. Leites and J. Terron, *Nucl. Phys.* **B301** (1988) 1.
- [55] A. Denner and T. Sack, *Z. Phys.* **C46** (1990) 653.
- [56] T. Kinoshita, *J. Math. Phys.* **3** (1962) 650;
T. D. Lee and M. Nauenberg, *Phys. Rev.* **133** (1964) 1549.
- [57] CDF collaboration, K. Sliwa, in Proceedings of the XXV Rencontres de Moriond, Electroweak and Unified Theories, Les Arcs, March 1990.
- [58] M. Jezabek and J.H. Kühn, *Nucl. Phys.* **B314** (1989) 1.
- [59] J. Liu and Y.-P. Yao, *Int. J. Mod. Phys.* **A6** (1991) 4925.
- [60] A. Denner and T. Sack, *Nucl. Phys.* **B358** (1991) 46.
- [61] G. Eilam, R. R. Mendel, R. Migneron and A. Soni, *Phys. Rev. Lett.* **66** (1991) 3105.
- [62] 'Physics at LEP', CERN-86-02, eds. J. Ellis and R. Peccei, Vol. 2.
- [63] 'ECFA Workshop on LEP200', CERN-87-08, eds. A. Böhm and W. Hoogland, Vol. 1.
- [64] M. Lemoine and M. Veltman, *Nucl. Phys.* **B164** (1980)445.

- [65] R. Philippe, *Phys. Rev.* **D26** (1982) 1588.
- [66] M. Böhm, A. Denner, T. Sack, W. Beenakker, F. A. Berends and H. Kuijf, *Nucl. Phys.* **B304** (1988) 463.
- [67] J. Fleischer, F. Jegerlehner and M. Zralek, *Z. Phys.* **C42** (1989) 409 and in [51].
- [68] W. Beenakker, K. Kołodziej and T. Sack, *Phys. Lett.* **258B** (1991) 469.
- [69] K. Kołodziej and M. Zralek, *Phys. Rev.* **D43** (1991) 3619.
- [70] H. Tanaka, T. Kaneko and Y. Shimizu, *Comp. Phys. Comm.* **64** (1991) 149.
- [71] T. Muta, R. Najima and S. Wakaizumi, *Mod. Phys. Lett.* **A1** (1986) 203; G. Barbiellini et al. in [62].
- [72] B. Grzadkowski and Z. Hioki, *Phys. Lett.* **B197** (1987) 213.
- [73] A. Aeppli and D. Wyler, *Phys. Lett.* **B262** (1991) 125.
- [74] T. Sack, Ph. D. Thesis, Würzburg (1987).
- [75] K. Hagiwara and D. Zeppenfeld, *Phys. Lett.* **B196** (1987) 97.
- [76] B. Grzadkowski, Z. Hioki and J. H. Kühn, *Phys. Lett.* **B205** (1988) 388; Z. Hioki, *Nucl. Phys.* **B316** (1989) 1.
- [77] H. Neufeld, J. D. Stroughair and D. Schildknecht, *Phys. Lett.* **B198** (1987) 563; K. Hagiwara, R. D. Peccei, D. Zeppenfeld and K. Hikasa, *Nucl. Phys.* **B282** (1987) 253; P. Mery, M. Perottet and F. Renard, *Z. Phys.* **C36** (1987) 249.
- [78] S. Dittmaier, M. Böhm and A. Denner, CERN-TH.6306/91, to appear in *Nucl. Phys.* **B**.
- [79] C. Ahn, B. W. Lynn, M. Pescin and S. Selipsky, *Nucl. Phys.* **B309** (1988) 221.
- [80] F. Jegerlehner, in 'Radiative Corrections for e^+e^- -collisions', ed. J. H. Kühn, Springer, Berlin Heidelberg (1989).
- [81] T. Sack, private communication.
- [82] A. Denner and T. Sack, *Z. Phys.* **C45** (1990) 439.
- [83] A. Aeppli, private communication.